

The Long-term Chemical Fate of Crude Oil Released in the Arctic during the Baffin Island Oil

Spill (BIOS) Project

By

Blake Hunnie

A thesis submitted to the Faculty of Graduate Studies of

The University of Manitoba

In partial fulfilment of the requirements of the degree of

MASTER OF SCIENCE

Department of Environment and Geography

University of Manitoba

Winnipeg

Copyright © 2023 by Blake Hunnie

Abstract

The risks of crude oil spills occurring within the Arctic heighten as ongoing impacts of climate change have given rise to ever increasing amounts of ship traffic. The Baffin Island Oil Spill (BIOS) project was designed in 1979 to further the collective understanding regarding the fate and behaviour of crude oil within the Arctic marine environment. A series of experimentally controlled oil releases occurred in Cape Hatt, Baffin Island, NU between 1980-1982 and were left subject to natural weathering processes. The sites of the BIOS project were revisited on numerous occasions to observe the long-term fate of crude oil spilled in an otherwise pristine, remote Arctic setting; most recently during the 2019 CCGS Amundsen expedition. Bulk surface (0-2cm) and subsurface (5-10cm) sediment samples were collected from oiled backshore plots from Crude Oil Point and Bay 106 within the Z-lagoon, and from the intertidal sediments of Bay 11 within the Ragged Channel, where a surface oil slick was left to encroach onto the beach. Collected samples were analyzed for a total of 99 petroleum hydrocarbons including Polycyclic Aromatic Hydrocarbons (PAHs), n-alkanes, branched alkanes, alkylcycloalkanes, hopane and sterane biomarkers, and alkylbenzenes using Gas Chromatography Mass Spectrometry. These hydrocarbon groups were detected in concentrations ranging from 0.0486 – 14.0, 1.15 - 1170, 0.224 – 51.7, 0.0643 – 16.9, 0.213 – 11.7, and 0.0171 – 8.60 mg/kg, respectively. The oiled sediments were generally observed to contain the highest concentrations of each hydrocarbon group at Crude Oil Point, followed by Bay 106, then finally Bay 11; suggesting that tidal and wave action were significant contributors to the removal of petroleum. Fourteen of the 16 US EPA priority PAHs were detected in concentrations exceeding the marine sediment quality guideline limits established by the Canadian Council of Ministers of the Environment, individually ranging from 7.00 – 640 µg/kg. The Toxic Equivalency Quotient values from these

PAHs ranged from 1.40 – 270 and 1.70 – 350 µg/kg within the surface and subsurface sediments, respectively. Comparisons with available data from the 2001 BIOS revisitation indicate losses in dimethylphenanthrene and chrysene from 240000 – 1000 and 8500 – 640 µg/kg, respectively, suggesting extensive PAH weathering over the past 18 years.

Acknowledgments

I would first like to thank my advisor, Dr. Gary Stern. His support, patience, and trust in me have been unwavering throughout my experience as a researcher. I know that I can always count on him for helpful feedback and advice as it pertains to my work, and life in general. It is also through him that I was able to travel to the Canadian Arctic during the 2019 Amundsen expedition, which was a truly once-in-a-lifetime experience. I would also like to thank Dr. Lars Schrieber, who led the 2019 revisitation to the BIOS site. His scrupulous revisions of my manuscripts have helped shape them into works of high caliber. I have tremendous respect for his work ethic and accomplishments as a young researcher. Additionally, I would like to express my gratitude towards the efforts of my committee members Dr. Mark Hanson and Dr. Eric Collins.

People I am thankful to have had the opportunity to work alongside, collaborate with, and learn from include Durell Desmond, Kasia Polcwiartek, Lisa Oswald, Shiva Lashkari, Nasima Chorfa, Misuk Yun, Fernanda De Matos Ferraz, Diana Saltymakova, Stephen Ciastek, Teresinha Wolfe, Cathrin Venaas, and Jake Ritchie. Thank you to Patrick Lambert and Ben Fieldhouse of ECCC for the sample of Lagomedio crude oil. I would also like to give a special thanks to those who assisted with sample collection at the BIOS site, including Esteban Gongora Bernoske, Ianina Altshuler, Madison Ellis, and Margaret Cramm.

This research was carried out with the financial contributions from the Multi-Partner Research Initiative's (MPRI) Department of Fisheries and Oceans (DFO), GENICE, ArcticNet, the CCGS Amundsen Science Programme and the Natural Science and Engineering Research Council (NSERC) discovery grant (Gary Stern). My position as a graduate student was funded by the NSERC Canadian Graduate Scholarship – Masters (CGS-M).

Dedication

“I’ll always have more time to work on my thesis, but I’ll never have another chance to watch tonight’s sunset.”

I dedicate this work to my family and friends whom I cherish deeply. I would not be here today if it were not for the love and support that they have imparted on me.

Table of Contents

ABSTRACT	II
ACKNOWLEDGMENTS	IV
DEDICATION.....	V
TABLE OF CONTENTS.....	VI
CONTRIBUTIONS OF AUTHORS	VIII
LIST OF TABLES	IX
LIST OF FIGURES	XI
CHAPTER 1: BACKGROUND & INTRODUCTION	13
THE ARCTIC.....	13
CRUDE OIL.....	19
<i>Persian Gulf oil spill</i>	21
<i>Exxon Valdez oil spill</i>	21
<i>Deepwater Horizon oil spill</i>	22
<i>Crude oil composition</i>	23
<i>Degradation of crude oil</i>	32
ANALYSIS USING GAS CHROMATOGRAPHY MASS SPECTROMETRY (GCMS)	36
<i>Full Scan</i>	38
<i>Single Ion Monitoring</i>	39
<i>Multiple Reaction Monitoring</i>	40
<i>Time of Flight</i>	41
THE BAFFIN ISLAND OIL SPILL (BIOS) PROJECT	42
THESIS TOPIC, OBJECTIVES, AND HYPOTHESES	47
REFERENCES	49
CHAPTER 2: THE RECALCITRANCE AND POTENTIAL TOXICITY OF POLYCYCLIC AROMATIC HYDROCARBON RESIDUES WITHIN BEACH SEDIMENTS AT THE BAFFIN ISLAND OIL SPILL (BIOS) SITE, NEARLY FORTY YEARS LATER	68
ABSTRACT	69
INTRODUCTION	70
MATERIALS AND METHODS	76
<i>Sample collection</i>	76
<i>Sample preparation</i>	78
<i>PAH Analysis</i>	79
<i>Toxic Equivalency Quotients</i>	80
<i>Total Carbon and Total Inorganic Carbon Analysis</i>	80
<i>Principal Component Analysis</i>	81
RESULTS AND DISCUSSION	81
<i>Σ16PAH and Σ36PAH concentrations</i>	81
<i>Oil Composition and Weathering</i>	85
<i>Comparison to Previous Data</i>	92
<i>PCA</i>	93
<i>Potential Toxicity</i>	96
CONCLUSION.....	102
REFERENCES	104
SUPPLEMENTARY INFORMATION (SI).....	113

CHAPTER 3: THE LONG-TERM FATE OF SATURATES AND BIOMARKERS WITHIN CRUDE OIL SPILLED DURING THE BAFFIN ISLAND OIL SPILL (BIOS) PROJECT	122
ABSTRACT	123
INTRODUCTION	124
MATERIALS AND METHODS	130
<i>Sample Collection</i>	<i>130</i>
<i>Sample Processing</i>	<i>131</i>
<i>n-Alkane analysis</i>	<i>132</i>
<i>Alkylbenzene and alkylcycloalkane analysis</i>	<i>133</i>
<i>Hopane and sterane analysis</i>	<i>134</i>
<i>Principal Components Analysis (PCA).....</i>	<i>135</i>
RESULTS AND DISCUSSION	136
<i>General compound group comparison</i>	<i>136</i>
<i>Total mean concentrations of each compound group.....</i>	<i>137</i>
<i>n-Alkane composition.....</i>	<i>142</i>
<i>Principal component analysis of n-alkanes.....</i>	<i>144</i>
<i>Percent Residual Comparison between 2001 and 2019 data</i>	<i>146</i>
<i>Weathering ratios</i>	<i>150</i>
CONCLUSION	155
REFERENCES	157
SUPPLEMENTAL INFORMATION	168
CHAPTER 4: CONCLUSION.....	194
SYNTHESIS.....	194
REFLECTION	195
<i>Research process.....</i>	<i>195</i>
<i>Expectations and Outcomes</i>	<i>197</i>
RECOMMENDATIONS FOR FUTURE WORK.....	198
CONTRIBUTIONS AND WRAP-UP	199
REFERENCES	201

Contributions of Authors

Hunnie, B. E., Schreiber, L., Greer, C. W., & Stern, G. A. (2023). The recalcitrance and potential toxicity of polycyclic aromatic hydrocarbons within crude oil residues in beach sediments at the BIOS site, nearly forty years later. *Environmental Research*, 222, 115329.
<https://doi.org/10.1016/j.envres.2023.115329>

Blake Hunnie: Methodology, Validation, Formal Analysis, Investigation, Resources, Data Curation, Writing – Original Draft, Writing – Review & Editing, Visualization, Project Administration

Lars Schreiber: Conceptualization, Methodology, Investigation, Resources, Data Curation, Visualization, Supervision, Project Administration

Charles Greer: Funding acquisition, Writing – Review & Editing, Conceptualization, Methodology, Resources,

Gary Stern: Conceptualization, Methodology, Formal Analysis, Resources, Writing – Original Draft, Supervision, Project Administration

Hunnie, B. E., Schreiber, L., Greer, C. W., & Stern, G. A. (In preparation). The long-term fate of saturates and biomarkers within crude oil spilled during the BIOS project. *Marine Pollution Bulletin*.

Blake Hunnie: Methodology, Validation, Formal Analysis, Investigation, Resources, Data Curation, Writing – Original Draft, Writing – Review & Editing, Visualization, Project Administration

Lars Schreiber: Conceptualization, Methodology, Investigation, Resources, Data Curation, Visualization, Supervision, Project Administration

Charles Greer: Funding acquisition, Writing – Review & Editing, Conceptualization, Methodology, Resources,

Gary Stern: Conceptualization, Methodology, Formal Analysis, Resources, Writing – Original Draft, Supervision, Project Administration

List of Tables

Table 2.1 Total PAH concentrations of oiled samples at the BIOS site and the technical mixture.....	84
Table 2.2 Percent (%) loss of Dimethylphenanthrene and Chrysene in BIOS samples collected during 2001 (Prince et al., 2002), and associated concentrations between 2001 and 2019.....	93
Table 2.3 Coefficient of determination (R^2) values between percent Organic Carbon (OC) and Toxic Equivalency Quotients (TEQs) for light (2 and 3-ringed), medium (4-ringed), and heavy (5 and 6-ringed) MW PAHs in surface and subsurface sediments from the BIOS site.....	97
Table 2.4 Interim Marine Sediment Quality Guidelines (ISQGs) (Canadian Council of Ministers of the Environment, 2001) and TEQs for the 16 EPA Priority PAHs. SQG values are provided on a dry weight, threshold effect level (TEL) basis. The TEQ values are derived from TEFs provided in Nisbet and LaGoy (1992), unless otherwise specified. The lightly highlighted values represent concentrations that exceed the proposed SQGs.....	100
Table 2.S1 List of intertidal and supratidal sediment sample types acquired at respective stations and coordinates from the BIOS site during the 2019 CCGS Amundsen expedition. A surface (0-2cm) and subsurface (5-10cm) sample was collected for each entry.....	115
Table 2.S2 PAH Surrogates Standard Mixture (D, 98%) (ES-5164).....	116
Table 2.S3 A list of the PAHs analyzed, and their attributed abbreviations.....	117
Table 2.S4 GCMS Parameters for analyses using the Agilent 7010B Triple Quadrupole GCMS (QQQ-MS). The column was trimmed on occasion for maintenance purposes.....	117
Table 2.S5 Ion transitions of all PAHs, alkylated PAHs, and deuterated PAHs included in the analyses.....	118
Table 2.S6 Low-end limits of quantitation for all PAHs included in the analysis conducted on the Agilent 7010B Triple Quadrupole GCMS (QQQ-MS).....	120
Table 3.1 Locations and nomenclature of oiled surface (0-2cm) and subsurface (5-10cm) beach sediment samples collected from the BIOS site during the 2019 CCGS Amundsen Expedition.....	131
Table 3.2 Total mean concentrations of detected PAHs, n-alkanes, hopanes and steranes, alkylbenzenes, and alkylcycloalkanes within oiled sediments from the BIOS site revisited in 2019, and the technical mixture.....	139
Table 3.3 Total mean concentrations of alkane subcategories nC11-nC15, nC16-nC26, nC27-nC35, and pristane & phytane within oiled sediments from the BIOS site revisited in 2019, and the technical mixture.....	141

Table 3.4 Diagnostic ratios of n-alkane weathering in crude oil.....	155
Table 3.S1 List of intertidal and supratidal sediment sample types acquired at respective stations and coordinates from the BIOS site during the 2019 CCGS Amundsen expedition. A surface (0-2cm) and subsurface (5-10cm) sample was collected for each entry.....	168
Table 3.S2 Perdeuterated n-alkane standard solution, acquired from Chiron AS (Aslund, 2019b).....	169
Table 3.S3 GCMS Parameters for n-alkane analyses using the LECO Pegasus multidimensional gas chromatography high-resolution time of flight mass spectrometry (GCxGC-HR-TOF-MS, LECO) instrument.....	170
Table 3.S4 List of all analyzed n-alkanes and branched alkanes, along with their associated limits of quantitation.....	171
Table 3.S5 List of all analyzed alkylbenzenes and alkylcycloalkanes, their respective limits of quantitation, and MRM ion transitions.....	172
Table 3.S6 GCMS Parameters for biomarker analyses using the Agilent 7010B Triple Quadrupole GCMS (QQQ-MS).....	173
Table 3.S7 List of all analyzed biomarkers, their respective limits of quantitation, and MRM ion transitions.....	173
Table 3.S8 List of all analyzed polycyclic aromatic hydrocarbons, their respective limits of quantitation, and MRM ion transitions.....	174
Table 3.S9 Mean concentrations (mg/kg) of individual, analyzed n-alkanes and branched alkanes within the technical mixture, oiled sediments, and control sediments from the 2019 revisitation of BIOS site.....	176
Table 3.S10 Mean concentrations (mg/kg) of individual, analyzed alkylbenzenes within the technical mixture, oiled sediments, and control sediments from the 2019 revisitation of BIOS site.....	185
Table 3.S11 Mean concentrations (mg/kg) of individual, analyzed alkylcycloalkanes within the technical mixture, oiled sediments, and control sediments from the 2019 revisitation of BIOS site.....	189

List of Figures

Figure 1.1 Chemical structures of the 16 USEPA priority PAHs, produced in ChemDraw Professional (ver. 22.0).....	26
Figure 1.2 Chemical structures of representative linear n-alkanes, branched alkanes, and cycloalkanes, produced in ChemDraw Professional (ver. 22.0).....	28
Figure 1.3 Chemical structures of representative alkylbenzenes, produced in ChemDraw Professional (ver. 22.0).....	30
Figure 1.4 Chemical structures of the conserved biomarker, 17 α (H)21 β (H)hopane, and a general cholestane molecule, produced in ChemDraw Professional (ver. 22.0).....	31
Figure 1.5 The geographical location of the Baffin Island Oil Spill (BIOS) project. Light blue pinpoints represent oiled sites, and red pinpoints denote field blank stations which were sampled from during the most recent revisitation of the BIOS site during the 2019 CCGS Amundsen expedition.....	44
Figure 2.1 Location of the BIOS site in Cape Hatt, Baffin Island, NU. Sites visited during the 2019 sampling regime are shown. Oiled sampling stations include Crude Oil Point and Bay 106 within Z-lagoon, and Bay 11 in the Ragged Channel. Field blanks were collected from Bay 102 and Milne Inlet within Z-lagoon and Ragged Island, respectively.....	73
Figure 2.2 PAH profiles shown as percentages of each analyzed PAH relative to their total abundance for (A) the technical mixture, (B) the field blanks, (C) the intertidal Bay 11 sediments, and (D) the backshore Bay 11 samples.....	87
Figure 2.3 PAH profiles shown as percentages of each analyzed PAH relative to their total abundance for (A) the technical mixture, (B) the field blanks, (C) the weathered crude oil plot from Crude Oil Point, and (D) the emulsified oil plot from Crude Oil Point.....	89
Figure 2.4 PAH profiles shown as percentages of each analyzed PAH relative to their total abundance for (A) the technical mixture, (B) the field blanks, (C) the tilled crude plot from Bay 106, (D) the tilled emulsion plot from Bay 106, (E) the control crude plot from Bay 106, and (F) the control emulsion plot from Bay 106.....	91
Figure 2.5 PCA, demonstrated by PC1 and PC2, of the weathered PAH concentrations for the oiled samples from the BIOS site. Plot a represents the component loading vectors, and plot b represents the component scores.....	95
Figure 3.1 Locations of the sampling stations from the 2019 revisitation of the BIOS site during the CCGS Amundsen expedition, created in Ocean Data View (Schlitzer, 2023). For the purposes of this study, Bay 102 and Milne Inlet were considered as control sites.....	129

Figure 3.2 Relative proportions of PAHs, alkanes (which are divided into subcategories nC11-nC15, nC16-nC26, nC27-nC35, and pristane-phytane), hopanes and steranes, alkylbenzenes, and alkylcycloalkanes measured within the oil residues from the samples collected during the 2019 revisit of the BIOS site. In this figure, “Tech. Mix” refers to the technical mixture.....137

Figure 3.3 Composition of n-alkanes, represented by the percentage (%) towards the total measured concentration of alkanes present within each sample. (A) = technical mixture, (B) = mean surface and subsurface control sample values, (C) = Bay 11 surface sediments, (D) = Bay 11 subsurface sediments, (E) = Crude Oil Point surface sediments, (F) = Crude Oil Point subsurface sediments, (G) = Bay 106 surface sediments, (H) = Bay 106 subsurface sediments.....143

Figure 3.4 Principal Components Analysis (PCA) made up of component loadings (labelled vectors) and component scores (labelled dots) of the n-alkanes present within the oiled sediments from the BIOS site, separated by sampling stations.....146

Figure 3.5 Percent residual of n-alkanes octadecane (nC18) and triacontane (nC30), and the isoprenoid alkane phytane within oiled samples collected during the 2001 and 2019 revisitations of the BIOS site. The 2001 data is adapted from Prince et al. (2002), and is included for direct comparison purposes.....149

Figure 3.S1 Composition of alkylbenzenes, represented by the percentage (%) towards the total measured concentration of alkylbenzenes present within each sample. (A) = technical mixture, (B) = mean surface and subsurface control sample values, (C) = Bay 11 surface sediments, (D) = Bay 11 subsurface sediments, (E) = Crude Oil Point surface sediments, (F) = Crude Oil Point subsurface sediments, (G) = Bay 106 surface sediments, (H) = Bay 106 subsurface sediments.....183

Figure 3.S2 Composition of alkylcycloalkanes, represented by the percentage (%) towards the total measured concentration of alkylcycloalkanes present within each sample. (A) = technical mixture, (B) = mean surface and subsurface control sample values, (C) = Bay 11 surface sediments, (D) = Bay 11 subsurface sediments, (E) = Crude Oil Point surface sediments, (F) = Crude Oil Point subsurface sediments, (G) = Bay 106 surface sediments, (H) = Bay 106 subsurface sediments.....184

Figure 3.S3 Principal Components Analysis (PCA) made up of principal components (PCs) one and two, accounting for 65.4 and 16.7 % of the cumulative variance, respectively, of the alkylbenzenes present within the oiled sediments from the BIOS site, separated by sampling stations. The ellipses represent the 95 % confidence intervals for each respective site.....192

Figure 3.S4 Principal Components Analysis (PCA) made up of principal components (PCs) one and two, accounting for 64.9 and 13.1 % of the cumulative variance, respectively, of the alkylcycloalkanes present within the oiled sediments from the BIOS site, separated by sampling stations. The ellipses represent the 95 % confidence intervals for each respective site.....193

Chapter 1: Background & Introduction

The Arctic

The Arctic is one of the most unique settings on Earth, encompassing eight countries across North America, Europe, and Asia (Murray et al., 1998). Geographically, the Arctic is sometimes described as the area north of $66^{\circ}32'N$, which denotes the limit of the “Arctic Circle,” where twenty-four hour darkness and sunlight occur throughout different periods of time each year (Murray et al., 1998). This designation of the Arctic is limiting, as are many other definitions of the Arctic proposed by different groups of researchers. Some boundaries are set based on climatology, vegetation, permafrost, politics, or oceanographic parameters (Murray et al., 1998). Due to conflicting perspectives, a broader characterization of the Arctic designated by the Arctic Monitoring and Assessment Programme (AMAP) is defined as “the terrestrial and marine areas north of the Arctic Circle ($66^{\circ}32'N$), and north of $62^{\circ}N$ in Asia and $60^{\circ}N$ in North America, modified to include the marine areas north of the Aleutian chain, Hudson Bay, and parts of the North Atlantic Ocean including the Labrador Sea (Murray et al., 1998).” When making mention of the Arctic within this thesis, refer to the above definition. The total area of the Arctic spans roughly 13.4×10^6 km². The terrestrial component of the Arctic includes ice sheets, tundra plains, valleys, mountainous regions, volcanic islands, archipelagos, marshes, bogs, and forests (Murray et al., 1998). The Arctic is a remote, relatively untouched ecosystem that plays host to some of the most harsh environmental conditions on Earth such as freezing temperatures, fog, ice cover for roughly three quarters of the year, nearly complete darkness for nearly three months per year, and high seas (Pew Charitable Trusts, 2013). The Arctic is also an extremely fragile environment. The many key components that make the Arctic so unique are mostly vulnerable to heat. As such, numerous physical, biological, and chemical processes are sensitive to changes in

temperature (Arctic Monitoring and Assessment Programme, 2017; Yamanouchi & Takata, 2020).

The Arctic has been experiencing an observed warming effect, as the overall temperature anomaly continues to increase with time (Chapin et al., 2005). Both shallow and deep sea water temperatures within the Arctic Ocean have been rising (Arctic Monitoring and Assessment Programme, 2017). Atmospheric concentrations of greenhouse gases (GHGs) have been and continue to rise over time (Arctic Monitoring and Assessment Programme, 2017). The GHG most commonly attributed to impacts of climate change is carbon dioxide, CO₂ (Yamanouchi & Takata, 2020). Natural variability plays a role in measured temperature increases within the Arctic over time; however, it is largely impacted by the continually-increasing concentrations of GHGs, in addition to atmospheric and oceanic forcing processes (Serreze et al., 2007; Stroeve et al., 2012). Along with the myriad of ongoing warming processes, the Arctic, in particular, is becoming an increasingly variable environment. The frequency of extreme weather events is also rising (Arctic Monitoring and Assessment Programme, 2017). Warming trends are anticipated to continue as a result of GHGs already emitted, the heat storage of the Arctic Ocean, and melting permafrost. Even if the release of GHGs are brought to a firm halt, the Arctic will continue to warm (Arctic Monitoring and Assessment Programme, 2017).

The Arctic has been warming more than twice as fast as the global average, over the past 50 years. The heat being trapped within the atmosphere due to increasing GHG concentrations gives rise to a number of positive feedback mechanisms which amplify the rate of warming in the Arctic, in a process called “Arctic Amplification (AA)” (Arctic Monitoring and Assessment Programme, 2017; Jeffries et al., 2013; Stroeve et al., 2012; Yamanouchi & Takata, 2020). Many of these affected systems are dependent on sea ice albedo, or the reflectivity of a surface.

Atmospheric heat transport towards the North Pole, and higher local air temperatures hinder the growth of winter sea ice. Thinner sea ice produced over the winter is more susceptible to melting in the spring, which is exacerbated by increasing areas of open water, which are low in albedo, and thus absorb solar radiation, leading to more warming and later periods of freezing in autumn (Jeffries et al., 2013; Serreze et al., 2007; Stroeve et al., 2012). This effect also occurs in meltwater ponds that form on top of sea ice during the summer (Jeffries et al., 2013) and is exacerbated by earlier onsets of the melting season (Markus et al., 2009). Outcomes of AA contribute towards increased riverine discharge and later sea ice freeze-up (Markus et al., 2009; Neff et al., 2014; X. Zhang et al., 2013). Ongoing melting of numerous non-sea ice types such as glaciers and ice caps within the Arctic is contributing an estimated 35 % of global meltwater contributing towards sea-level rise, which spells additional risks for many coastal ecosystems and human populations (Arctic Monitoring and Assessment Programme, 2017).

Sea ice plays an integral role in diminishing the amount of warming experienced by the Arctic (Markus et al., 2009; Serreze et al., 2007; Stroeve et al., 2012). Due to its high albedo, a large component of solar radiation is reflected back into space, rather than being absorbed within the minimally-reflective waters of the Arctic Ocean (Arctic Monitoring and Assessment Programme, 2017). Long-term observations denote a continual decrease in the thickness and extent of sea ice over time. The measured sea ice thickness from 1975-2012 has demonstrated a 65 % decline (Arctic Monitoring and Assessment Programme, 2017). There has been roughly a 9 % decrease in total sea ice area each decade since records began in 1979 (Serreze et al., 2007). More recent observations indicate the loss of multi-year sea ice during summer months, whereas most of the sea ice produced during the freeze-up season within the Arctic now being characterized as “first year ice” (Arctic Monitoring and Assessment Programme, 2017; Stroeve

et al., 2012). In most regions of the Arctic Ocean (apart from some of the most northern areas), the average number of ice-free days has increased by 10-20 per decade since 1979 (Arctic Monitoring and Assessment Programme, 2017). There have been estimates that the Arctic Ocean could be mostly sea ice-free during the summer by the late 2030's (Arctic Monitoring and Assessment Programme, 2017).

Arctic Amplification has also contributed towards a process called "Arctic Greening." Arctic greening refers to the increased extent of vegetal growth during the summer months within the Arctic, and is being widely noted in response to observed effects of Arctic warming (Box et al., 2019). Increased greenery is observed as a result of exacerbated high latitudinal warming, as the extent of shrubs in areas such as northern Alaska has increased with each passing decade (Sturm et al., 2001). Previous investigations examining the effects of increased temperatures in the Arctic by 1 or 2°C denote an observable increase in shrub growth, which is also in agreement with paleo-climate studies that focused on similar vegetation from pollen records in northern Alaska, specifically (Brubaker et al., 1995; Chapin et al., 2005; Sturm et al., 2001). The underlying concern with Arctic greening is that the low albedo of vegetation that has been replacing areas of ice and snow will hinder the Arctic's ability to combat AA. Although the expected warming effects from the ongoing increase of vegetation within Arctic settings are minimal, they play a role in the myriad of processes contributing towards AA and by further extension, global climate change (Chapin et al., 2005).

In addition to the several outcomes of warming described above, near-surface permafrost has been observed to be warming in the arctic over time as well (Arctic Monitoring and Assessment Programme, 2017). Freeze-up of active permafrost layer in northern Alaska in the 2010s has been recorded at two months later than during the 1980s (Box et al., 2019). There has also been a

noticeable deepening of this active layer, which incurs yearly melting and freezing patterns (Arctic Monitoring and Assessment Programme, 2017). Permafrost is important due to its ability to sequester methane (CH₄) and carbon dioxide (CO₂) from being released into the open atmosphere. By observing the continual warming of Arctic permafrost, there is increased risk of these GHG sinks to become sources, exacerbating the effects of climate change (Box et al., 2019). These effects are currently still relatively small, but are still a cause for concern (Arctic Monitoring and Assessment Programme, 2017).

As warming trends continue, increases in Arctic shipping are guaranteed (Wenning et al., 2018). The opportunities for increased shipping traffic within the Arctic are largely brought about due to the ongoing loss of sea ice (Pew Charitable Trusts, 2013; Pizzolato et al., 2016). Monitoring of shipping traffic within the Arctic has highlighted a measured increase over the past few decades (Pizzolato et al., 2014). Observations denote up to a 250 % increase in total annual distance travelled by ships within the Arctic between 1990 – 2015 (Dawson et al., 2018). Certain areas greatly impacted by warming within the Arctic that allow for shipping traffic to pass through have recently been designated as “Arctic sea routes (Yamanouchi & Takata, 2020).” Along with increased Arctic shipping traffic, the exploration and extraction of oil and gas within the Arctic is becoming an increasingly attractive opportunity (Pew Charitable Trusts, 2013; Wenning et al., 2018). Luckily, certain countries such as Canada have enacted moratoriums to prohibit oil exploration and off-shore drilling within the Arctic (Government of Canada, 2022). However, this is not the case in all Arctic-encompassing nations. Much work has gone into the implementation of safety and pollution mitigation protocols for both Arctic shipping and oil-related activity, but this ultimately does not guarantee that oil spills will not occur (Wenning et al., 2018). Growing concerns are being raised across the world regarding

Arctic oil exploration (Pew Charitable Trusts, 2013), as there is a distinct lack of appropriate infrastructure in place within the Arctic to respond to, and handle oil spills (Knol & Arbo, 2014; Wenning et al., 2018). The main forms of human intervention as responses to oil spills within the Arctic such as mechanical recovery with/without ice management, and in-situ burning are generally hindered or outright ineffective under unfavourable ice coverage, wind, wave height, and visibility conditions (Pew Charitable Trusts, 2013). Since these are common conditions experienced within the Arctic, anthropogenic means of remediating oil spills in this setting are met with regular challenges. Also, there is work needed to be done in terms of reaching a unanimous agreement towards the potential response and remediation of an oil spill affecting more than one country within the Arctic (Knol & Arbo, 2014). An additional series of concerns are raised if the fallout of an oil spill were to reach the Arctic coastlines. In many Arctic terrestrial settings, there is little to no access for cleaning equipment to reach the site of a spill by land, and it is largely impractical to transport the necessary machinery to manually remove oiled coastal sediments (Knol & Arbo, 2014). This is a widespread concern across most areas encompassed within the Arctic (Knol & Arbo, 2014).

Arctic oil exploration is already underway, and has been for a number of years (Knol & Arbo, 2014; Pew Charitable Trusts, 2013). Generally, experience and research regarding oil spills within the Arctic is more limited than in temperate and tropical environments (Wenning et al., 2018). Direct extrapolation of results obtained from oil spill-related laboratory studies may or may not accurately reflect what occurs in a true Arctic setting (Kristensen et al., 2015). In situ testing will assist with direct knowledge and understanding of Arctic systems as it pertains to various components of oil spill research (Box et al., 2019). The Arctic is particularly susceptible to the deleterious impacts of oil spills, as lower temperatures (among other factors) contribute to

the increased recalcitrance of oil residues. (Knol & Arbo, 2014; Kristensen et al., 2015). Despite the remoteness of the Arctic, there are still many communities of people living in this environment. Whether they are in agreement or not with the action being taken towards Arctic oil exploration, the outcomes of those activities directly impact these people (Pew Charitable Trusts, 2013). It is important to protect the marine organisms for both ecological and subsistence purposes (Pew Charitable Trusts, 2013). As such, it is crucial to understand the behaviour and fate of oil spills within an Arctic setting in order to implement tight legislation and protocols to minimize potential damages to the ecosystem.

Crude Oil

Crude oil, also known as petroleum, is a non-renewable resource produced by extensive decay of various creatures over time (National Geographic Society, 2022). It is generally a dark brown liquid, but can vary slightly in colour (Demirbas & Taylan, 2016; National Geographic Society, 2022). Organisms such as algae, plants, and bacteria that existed millions of years ago within ancient seas sank to the bottom of the water body they inhabited when they died. The remains fell to the bottom sediments, and were subsequently buried (National Geographic Society, 2022). Over time, the exposure to extreme heat and pressure from the sediments compacted above is what produced fossil fuels such as petroleum from the remains of these organisms (McCarthy & Calvin, 1967; National Geographic Society, 2022). For the purposes of this work, the terms crude oil and petroleum will be used interchangeably. Petroleum serves as the predominant raw material for the production of gasoline, diesel, and plastics (Harayama et al., 1999; Masnadi et al., 2018). Crude oil can be emulsified when combined with a solvent such as water (Lim et al., 2015; Wong et al., 2015). Emulsions are used in several different industrial

sectors such as pharmacy (Salager, 2000), cosmetics (J.-S. Lee et al., 2004), and food production (Garti, 1997). The global production of crude oil averages roughly four billion tonnes annually, and about 40 % of this is transported overseas (Clarksons, 2016 in Jia, 2018).

It is well understood that either accidental or intentional release of crude oil in significant quantities into the natural environment leads to serious ecological issues (Medić et al., 2020; Tamizhdurai et al., 2022). Petroleum pollution within the marine environment occurs as a result of numerous anthropogenic activities. Some of the main sources of crude oil release include cargo ship ballast water discharge, tanker accidents, off-shore drilling, and runoff from the land (Harayama et al., 1999). However, not all crude oil found within the marine environment comes from anthropogenic sources. There are many natural seeps that slowly release petroleum into the water column (Boehm et al., 2001). Generally, spilled crude oil forms a film on the water surface, but disperses as well (Pashaei et al., 2015). Wind, waves, and currents cause lateral movement of crude oil when it is released into the marine environment. Since crude oil typically has a lower density than seawater, vertical motion also occurs as oil droplets form (M. Reed et al., 1999). Oil spills can kill a plethora of organisms, and/or render their surrounding environments uninhabitable for years or decades, depending on the severity (M. Blumer & Sass, 1972; Mostafawi, 2001; Pashaei et al., 2015).

In this next section, brief descriptions of a subset of disastrous oil spills are discussed, in order to raise awareness of the potential for crude oil to cause harm within various ecosystems. In particular, three different geographical locations, along with differing environmental conditions are explored.

Persian Gulf oil spill

Many consequences arose from the 1991 Gulf War in Kuwait (Mostafawi, 2001). Apart from the typical devastations of war, a significant negative outcome of this event was the 1991 Persian Gulf oil spill, where approximately 1.8×10^6 m³ (10.8 million barrels) of oil was released, with an additional 1.3×10^6 m³ of petroleum fallout from oil well fires and blowouts (Pashaei et al., 2015). This event was deemed as one of the most catastrophic crude oil-related disasters (Mostafawi, 2001; Pashaei et al., 2015). Entire food webs were completely decimated by the air and water pollution, as a result of crude oil release (Pashaei et al., 2015). In more recent times, the vast majority of the exposed, contaminated sediments and oil lakes still impose risks for the biological and environmental health of the organisms and ecosystem (Syal, 2021). Additionally, investigations highlighted that crude oil residues were found leaching into groundwater aquifers, greatly increasing the extent of pollution into adjacent areas (Syal, 2021). In terms of atmospheric contamination, it was reported that it took months to combat the ongoing crude oil spillage and fires (Syal, 2021). As a result, smoke and soot decreased the overall air quality, and led to exacerbated warming effects, as soot readily absorbs solar radiation (Bakan et al., 1991).

Exxon Valdez oil spill

Within the Prince William Sound (PWS), Alaska, a catastrophic oil spill event happened in 1989 when an Exxon Valdez tanker crashed and released approximately 4.2×10^4 m³ crude oil (Galt et al., 1991; Harwell & Gentile, 2006). At its time, this was the largest oil tanker spill in the United States (Wiens et al., 2006). One of the most visible ecological impacts of the oil spill were the mortality rates of seabirds (Galt et al., 1991). Hundreds of thousands of seabirds were

estimated to have died due to acute impacts from the Exxon Valdez Oil Spill (EVOS) (Piatt & Ford, 1996). The loss of organisms that make up a large component of a trophic level leads to heavy changes and imbalances in lower and higher trophic levels, as there is a decreased level of predation on certain prey species, which in turn experience a sudden increase in population densities. The population abundances of various species were also impacted for years post-spill (Wiens et al., 2006).

Deepwater Horizon oil spill

In late April of 2010, an explosion occurred on the offshore drilling rig, the Deepwater Horizon (DWH). An unprecedented crude oil and gas blowout ensued as a result of the explosion roughly 1500m below the sea surface, which took 87 days to cap (Beyer et al., 2016; Kleindienst et al., 2016). An estimated 5.0×10^5 m³ of crude oil was released as a consequence of the blowout (Beyer et al., 2016). A response measure taken at the DWH was the use of chemical dispersants, in attempt to reduce the size of individual oil droplets, which facilitates their capacity to be degraded (Bejarano et al., 2013; Fiocco & Lewis, 1999). This happens as the smaller droplets are more easily dispersed throughout the water column due to their lowered interfacial tension at the sea surface, as opposed to remaining at the surface. As the droplets spread both horizontally and vertically, their concentrations in one particular area dilute significantly (Bejarano et al., 2013; Prince et al., 2016; Prince & Butler, 2014). Prince and Butler (2014) highlight the drastic difference in time taken to degrade crude oil when under the effects of dispersants versus without. After 40 days, they observed an 84 % loss of total oil-related hydrocarbons in the dispersed samples, whereas only a 33 % loss was noted for the undispersed samples from the DWH oil spill. The use of the chemical dispersants were incredibly effective at stimulating the

degradation of the crude oil (Prince et al., 2016). It is important to note that the rapid response to, and degradation of crude oil spills within seawater is crucial to prevent the encroachment of petroleum onto the coastlines, where the crude oil residues can remain for months to years, as opposed to days to weeks within seawater (Prince et al., 2016). Despite the efficacy of dispersants in diluting and remediating the crude oil released from the DWH oil spill, the use of dispersants did in fact cause rapid spread of oil within the deeper layers of the Gulf of Mexico (>1000m), endangering many deep water biological communities (Beyer et al., 2016). Many aquatic species are vulnerable to the toxic effects of crude oil. In the case of the DWH oil spill, one major concern was regarding sea turtle populations, as most species present within the Gulf of Mexico were listed as threatened or endangered (Beyer et al., 2016). In many cases, special recovery programs were implemented to protect vulnerable populations of wildlife. These efforts present logistical and economical challenges, but ultimately outweigh the possibility of species extinctions as a result of crude oil spills (Beyer et al., 2016; Inkley et al., 2013).

To better understand the hazardous effects that oil spills incur on their surroundings, it is crucial to distinguish the different types of chemical compounds that make up crude oil. This is equally important when attempting to design a countermeasure or remediation plan to oil spills (M. Reed et al., 1999; Tamizhdurai et al., 2022).

Crude oil composition

Crude oil is a complex mixture composed of thousands upon thousands of different compounds (Bartle & Myers, 2002; Demirbas & Taylan, 2016; Harayama et al., 1999; Z. Wang et al., 1999). The predominant fraction of crude oil is composed of aliphatic and aromatic hydrocarbons, which are chemical species made up almost entirely of the elements carbon and

hydrogen (Abbasian et al., 2015; Atlas & Hazen, 2011; Moreda et al., 1998). Hydrocarbons are widespread organic compounds, classified as high priority pollutants (Abbasian et al., 2015). The hydrocarbon component of crude oil can be separated into four distinct categories: saturates (aliphatics), aromatics, resins, and asphaltenes (SARA) (Ashoori et al., 2017; Demirbas & Taylan, 2016; Harayama et al., 1999). Some of these compounds are known to contain trace amounts of various metals such as nickel, iron, and copper (Akmaz et al., 2011). The resin and asphaltene fractions of crude oil are generally constituted of high molecular weight (MW) compounds, with largely unknown chemical structures (Harayama et al., 1999). Extensive work has been done to propose hypothetical structures of asphaltenes, based on methods involving elemental composition, molecular mass, and nuclear magnetic resonance (Acevedo et al., 2007). However, given the complexity of these compounds, it is incredibly difficult to be certain about their structures. Oppositely, the structures of many saturates and aromatic hydrocarbons are well-known and relatively easily identifiable (Saltymakova et al., 2020). Asphaltenes as a whole are rather classified based on their solubilities in solvents such as n-heptane and toluene, or their propensity to precipitate within n-hexane or n-pentane (Groenzin & Mullins, 1999). In essence, compounds such as asphaltenes cannot be individually identified. Slightly more is known about the general structure of resins. They are comprised of fused, aromatic rings substituted with branched paraffins and polar compounds (Demirbas & Taylan, 2016). They are expected to be similar in structure to asphaltenes but have lower MWs. As with the asphaltenes, the exact structures of resins are mainly hypothesized, rather than known and identified (Akmaz et al., 2011; Demirbas & Taylan, 2016). Additionally, the asphaltenes and resins typically constitute the two proportionally smallest components of SARA (Ashoori et al., 2017). In some cases, together they can account for up to ~46 %, or as low as 1.3 % of the SARA composition

(Demirbas & Taylan, 2016). As such, a heavier emphasis has been placed on examining the fate of the saturates and aromatics, due to their relative abundances and the ease of their identification.

Polycyclic Aromatic Hydrocarbons (PAHs) are organic contaminants found in nearly all environmental compartments (Jesus et al., 2022; Yuan et al., 2001). PAHs make up a large proportion of the aromatic fraction of crude oil, and consist of two or more benzene rings, arranged in linear or clustered forms (Haritash & Kaushik, 2009; Jesus et al., 2022) (Figure 1.1). Despite their presence in most environmental compartments, they tend to settle disproportionately high in sediments (Haritash & Kaushik, 2009; Yuan et al., 2001). They are typically measured in higher concentrations both within sediment porewater and sorbed to particles, compared to overlying waters (Y. Zhang et al., 2011). PAHs either exist solely as unsubstituted, parent PAHs; or can be found with substituted alkyl groups (Jesus et al., 2022) (Figure 1.1). PAHs are a very recalcitrant group of hydrocarbons, owing mainly to the high stability and aromaticity of benzene rings (Haritash & Kaushik, 2009). PAHs can be toxic, mutagenic, and carcinogenic, therefore it is crucial to understand the fate and behaviour of PAHs within various environmental compartments (Head et al., 2006; Medić et al., 2020; Moreda et al., 1998; Saha et al., 2009; Southworth, 1979; Yuan et al., 2001). A list of 16 parent PAHs of grave health and environmental concern was developed in the late 1970s by the US Environmental Protection Agency (USEPA) (Keith, 2015). The 16 PAHs included in this list are Naphthalene, Acenaphthylene, Acenaphthene, Fluorene, Phenanthrene, Anthracene, Fluoranthene, Pyrene, Benzo[a]anthracene, Chrysene, Benzo[b]fluoranthene, Benzo[k]fluoranthene, Benzo[a]pyrene, Benzo[g,h,i]perylene, Indeno[1,2,3-c,d]pyrene, and Dibenz[a,h]anthracene (Jesus et al., 2022). The molecular structures of these 16 priority pollutants can be found in Figure 1.1. More

recently, there has been debate on revising this list to account for additional PAHs of high concern (Andersson & Achten, 2015; Keith, 2015).

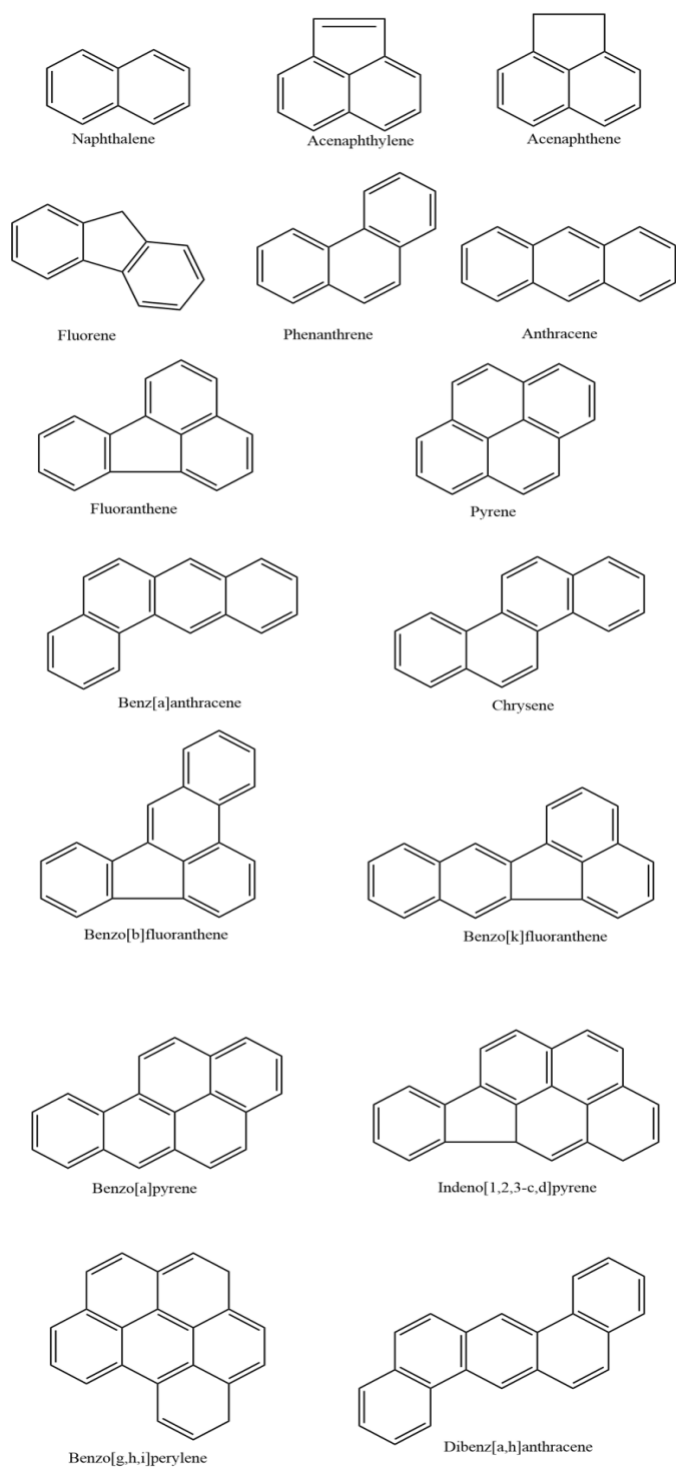
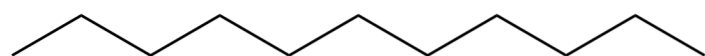


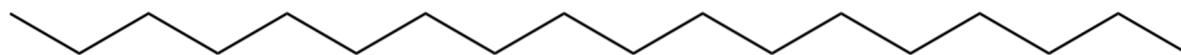
Figure 1.1. Chemical structures of the 16 USEPA priority PAHs, produced in ChemDraw Professional (ver. 22.0).

When crude oil is spilled in an open environment, many lighter MW PAHs are susceptible to volatilization/ evaporation from the liquid state into a gas within the open atmosphere. This serves as a major source of potential PAH exposure for biota when in relatively close proximity to crude oil (Lawal, 2017). PAHs are persistent organic pollutants (Head et al., 2006; Lawal, 2017; Medić et al., 2020). Their recalcitrance is dependent on their size, the higher MW PAHs being more persistent. This is due to both the increased stability and hydrophobicity associated with increasing molecule size (Head et al., 2006; Lawal, 2017). Under particular circumstances, PAHs have been known to persist for years to decades when released (Head et al., 2006; Prince et al., 2002; Zhendi. Wang et al., 1995).

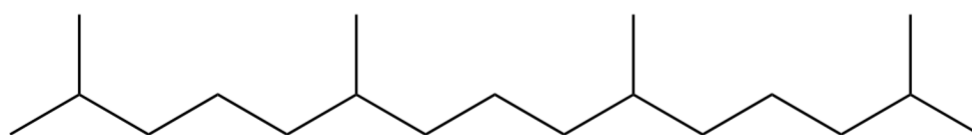
The alkanes are a major component of the saturate fraction of crude oil. Alkanes are represented by linear, circular, and branched forms (Vergeynst, Greer, et al., 2019) (Figure 1.2). The saturates generally constitute the largest relative proportion of hydrocarbons within petroleum, and are essentially insoluble in water (Head et al., 2006; Wentzel et al., 2007).



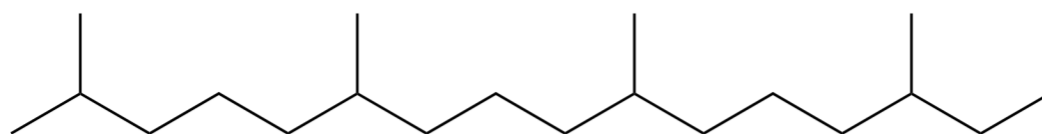
Undecane (nC11)



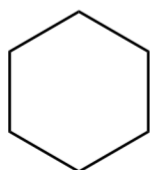
Octadecane (nC18)



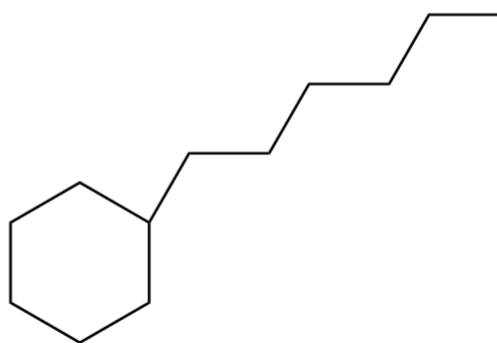
Pristane



Phytane



Cyclohexane



Hexylcyclohexane

Figure 1.2. Chemical structures of representative linear n-alkanes, branched alkanes, and cycloalkanes, produced in ChemDraw Professional (ver. 22.0).

Alkanes are largely inert compounds. Although they may not carry toxic characteristics, they remain for very long within the environment that they are introduced into due to their lack of reactivity (Wentzel et al., 2007). Cycloalkanes exist in purely their cyclic forms, but most cycloalkanes found in crude oil contain alkyl substituents (Harayama et al., 1999) (Figure 1.2). Both branched and cyclic alkanes are more resistant to degradation than simple, linear n-alkanes (Wardroper et al., 1984). Increasing complexity of chemical structures leads to higher specificity of enzymatic pathways for degrading hydrocarbons (Alvarez et al., 2009; Johnson et al., 2012; Rocha et al., 2011). As such, these compounds are quite recalcitrant, but still incur biodegradation (Alvarez et al., 2009).

Alkylbenzenes are another common component of the aromatic fraction of crude oil (Sinninghe Damste et al., 1988). There exist hundreds of alkylbenzenes, along with great potential for isomerization of the alkyl substituents of varying shapes, positions, and lengths (Francis, 1948). As such, ongoing efforts towards differentiating and identifying the various species of alkylbenzenes has been progressing as the domain of analytical instrumentation evolves (Francis, 1948; Griffiths et al., 1981; Sinninghe Damste et al., 1988; Solli et al., 1980). As their name suggests, alkylbenzenes are organic compounds composed of a benzene ring and at least one alkyl substituent (Francis, 1948) (Figure 1.3). Some compounds with alkyl chains of up to C₃₅ have been detected in crude oils (Solli et al., 1980).

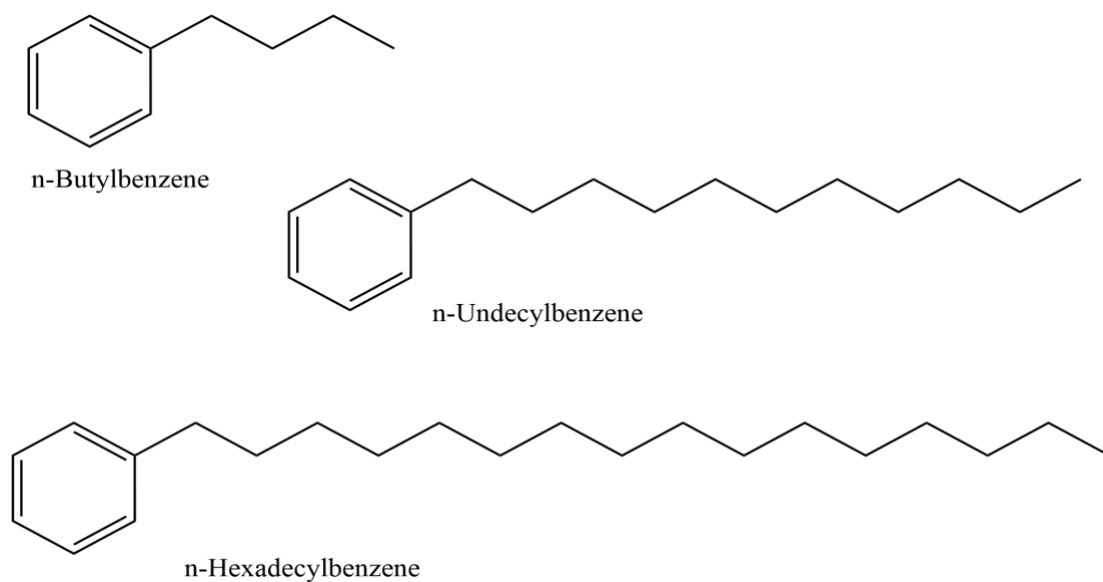


Figure 1.3. Chemical structures of representative alkylbenzenes, produced in ChemDraw Professional (ver. 22.0).

Biomarkers involve an intriguing group of hydrocarbons within crude oil. These compounds form in petroleum from biological precursors such as sterols, chlorophyll, and hopanoids (Peters & Moldowan, 1991). The most common types of biomarkers are referred to as hopanes and steranes. Structurally, biomarkers are similar to steroids, wherein they are largely made up of hexacyclic and pentacyclic saturated rings (Venosa et al., 1997) (Figure 1.4).

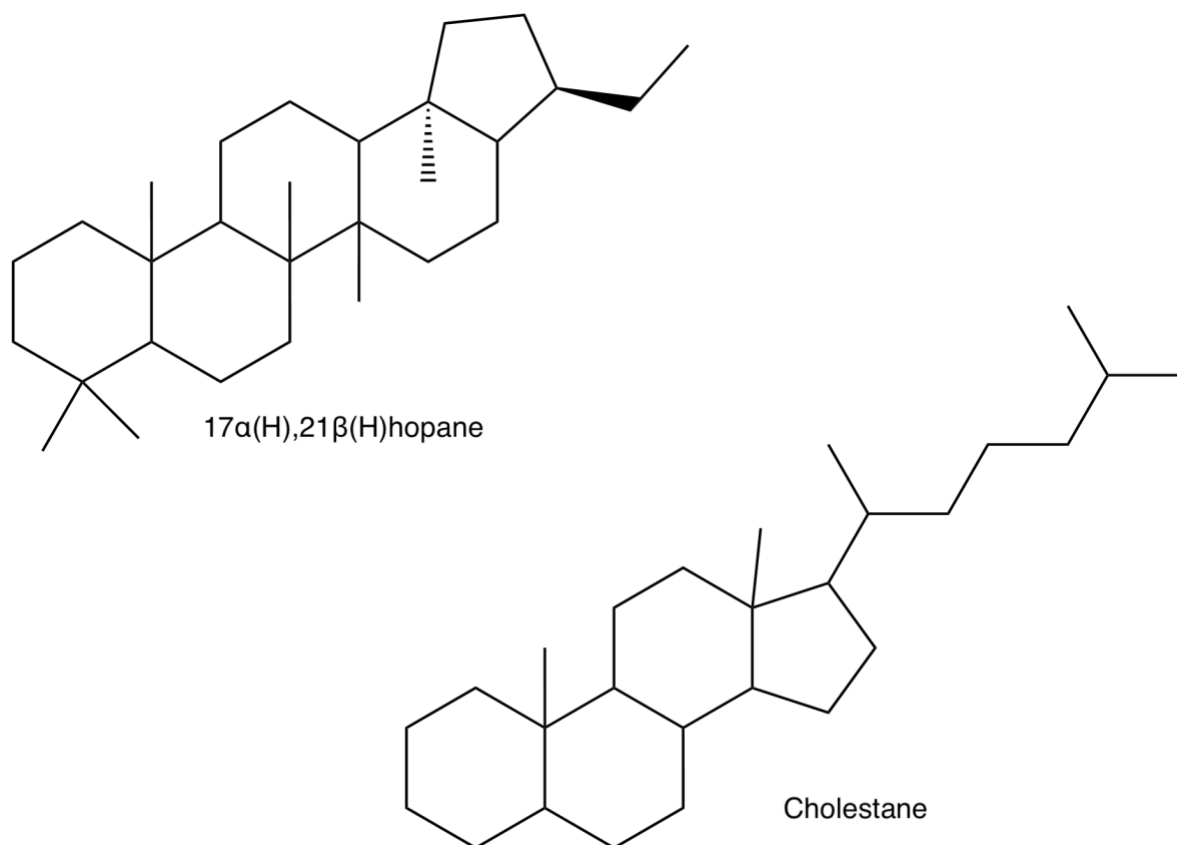


Figure 1.4. Chemical structures of the conserved biomarker, 17 α (H)21 β (H)hopane, and a general cholestane molecule, produced in ChemDraw Professional (ver. 22.0).

These compounds are termed as biomarkers, because the hopanoid precursor molecules are common cellular membrane components, and are extremely resistant to degradation (Bost et al., 2001; Peters & Moldowan, 1991; Rubinstein et al., 1977). Consequently, the compositions of biomarkers within crude oils are often unique and diagnostic, allowing for estimation of their source rock (Bost et al., 2001; W. E. Reed, 1977). Although the degradation of various biomarkers has been observed over time in both environmental and laboratory settings, this process generally occurs at a much slower rate than compared to other recalcitrant crude oil residues such as PAHs and alkanes (Peters & Moldowan, 1991; W. E. Reed, 1977; Rubinstein et al., 1977; Wardroper et al., 1984). The biomarker 17 α (H)21 β (H)hopane has been extensively

studied within the literature surrounding crude oil degradation. It is understood to be widespread in various types of crude oils, and is one of the most recalcitrant biomarkers, with incredible resistance to biodegradation (Peters et al., 1996; Prince et al., 1994; Venosa et al., 1997, 2002; Vergeynst, Greer, et al., 2019; Z. Wang et al., 1999). The measured concentrations of $17\alpha(H)21\beta(H)$ hopane can be used to account for bulk removal, or physical losses of crude oil residues when examining the fate of petroleum (Venosa et al., 1996). This provides a vital tool when attempting to compare the degradation of individual hydrocarbons in a particular study site over time. By eliminating one of the major potential sources of crude oil loss in environmental samples, normalizing hydrocarbon concentrations to that of $17\alpha(H)21\beta(H)$ hopane allows users to examine the extent of fewer concurrent remediation processes, such as biodegradation.

Degradation of crude oil

When spilled at sea, crude oil forms a slick with high surface area, and becomes subject to a collection of degradation processes including evaporation/volatilization, dissolution, photooxidation, and microbial degradation/biodegradation (Ehrhardt et al., 1992; Garrett et al., 1998). The contamination of crude oil on coastal sediments upon encroachment from the nearshore environment does not occur uniformly (Beyer et al., 2016). Specifically, the hydrophobicity of organic contaminants such as petroleum hydrocarbons influences the interactions with the organic and mineral fractions of sediments and soils, ultimately impacting the persistence of various compounds found within crude oil when exposed to different sediments (Chikere et al., 2011). This process is largely determined by the sediment compositions and organic matter content (Chikere et al., 2011; Moreda et al., 1998). The potential extent of petroleum degradation within seawater is largely dependent on volume, as the

spread and dilution of crude oil are crucial factors that affect the time in which it takes to sufficiently degrade a spill (Prince et al., 2017; Ward et al., 2018).

Aromatic compounds such as PAHs and alkylbenzenes are known to readily undergo photochemical reactions, such as photooxidation (Dabestani & Ivanov, 1999; Yu et al., 1997). Saturated compounds such as alkanes and hopanes have been observed to be largely unaffected by the effects of photooxidation (Garrett et al., 1998). This is mainly due to the lack of reactive centres within saturated molecules. These compounds are inert and thus insensitive to the initial reactions caused by exposure to UV irradiance (Larson et al., 1979). The beginning reactions of photooxidation of aromatic compounds in crude oil takes place *via* two main mechanisms: The first involves the generation of free radicals from ground-state triplet oxygens ($^3\text{O}_2$), which forms peroxy-radicals, which in turn extract hydrogens from other reactive centres to form hydroxy-radicals (Larson et al., 1979). The second mechanism also generates hydroxy-radicals from singlet oxygens ($^1\text{O}_2$) that react with unsaturated, or double-bonded carbons (Larson et al., 1979). When present in seawater, solar radiation that penetrates onto crude oil residues is capable of transforming and degrading PAHs (Jesus et al., 2022). Photooxidation is positively influenced by increased light intensity, increasing temperatures, and higher oxygen availability (Fasnacht & Blough, 2003; Xiao & Shao, 2017). General trends and observations of PAH photooxidation are strongest when experimentally driven results focus on single compounds, or simple mixtures. However, these associations when examining complex mixtures such as crude oil are not always as consistent (Garrett et al., 1998). The implications of interactions between hydrocarbons within extensively complicated mixtures must be considered when performing such studies. The degree of photooxidation of PAHs increases with increasing substitution. As such, the parent molecules

are more resistant to photooxidation than their alkylated counterparts (Ehrhardt et al., 1992; Garrett et al., 1998).

Evaporation, or volatilization (which are used interchangeably) involves the process of light MW hydrocarbons transforming from a liquid to gaseous state under natural conditions. In many types of crude oils, volatilization accounts for roughly 45 % of hydrocarbon loss by volume (Fingas, 2011). The process of volatilization is primarily driven by the Henry's Law constant, K_H , which represents the equilibrium distribution of a compound between its liquid and gaseous phases (Southworth, 1979). Additionally, the gas and liquid phase exchange constants, K_g and K_l , which denote the rate of transport of a compound away from the liquid-air interface, are important factors that influence volatilization (Southworth, 1979). Apart from the physiochemical properties of the compound being examined, environmental factors such as temperature, wind, and water turbulence affect the rate of volatilization (Southworth, 1979). Through experimentation, these three conditions have been positively associated with volatilization rates (Southworth, 1979). A few of the lighter MW PAHs such as naphthalene, phenanthrene, and fluorene are known to readily evaporate into the open atmosphere (H. Wang et al., 2015). Light MW alkanes ($\leq nC_{14}$) are also known to volatilize readily into the atmosphere (Kristensen et al., 2015; H. Wang et al., 2015). However, larger hydrocarbons also evaporate when left exposed to the open environment for sufficient lengths of time.

Biodegradation is a dominant process regarding the breakdown of crude oil. It involves marine microorganisms such as bacteria, whom use various hydrocarbons within crude oil as an energy source, thereby consuming it to grow and reproduce (Beyer et al., 2016). The relative population sizes of various hydrocarbon-degrading microorganisms depend on a number of factors including nutrient availability, environmental conditions, and the particular hydrocarbons

present (Dubinsky et al., 2013). Ultimately, certain microorganisms “prefer” consuming specific hydrocarbons, depending on their size and structure. As such, if any particularly favourable hydrocarbon becomes depleted, the populations of microorganisms degrading this compound will begin to decrease if they are unable to degrade the other chemical species present (Dubinsky et al., 2013; Kleindienst et al., 2016). The crude oil residues that are consumed by microorganisms often are degraded in tandem with available nutrient supplies such as phosphate and bioavailable nitrogen species, which can become limiting factors when assessing biodegradation (Atlas & Hazen, 2011; Edwards et al., 2011). There is a general knowledge gap as it pertains to the interactions between and behaviours of hydrocarbon-degrading microorganisms *in situ* (Head et al., 2006), hence the ongoing need for direct monitoring of these processes within an Arctic setting. However, researchers have noted the capability of various microorganisms native to the Arctic to degrade crude oil-related compounds, such as alkanes (Vergeynst, Christensen, et al., 2019). Hydrocarbons with varying structures are generally broken down in different fashions, but many are degraded into fewer unique final products (Abbasian et al., 2015). Consequently, the presence of certain final products of biodegradation can be used as an indicator of microbial degradation of crude oil. In general, lower MW hydrocarbons are more readily degraded by microorganisms than higher MW congeners, due to their solubilities in marine systems and uptake ability of the microbes (Abbasian et al., 2015). Of the aliphatic hydrocarbons, n-alkanes are some of the most readily biodegraded, due to the simplicity of their chemical structures (Abbasian et al., 2015). A widely used indicator of biodegradation of crude oil involves the comparison of n-alkanes to respective branched alkanes, or isoprenoids pristane and phytane (Figure 4), since they are less prone to being degraded

(Vergeynst, Christensen, et al., 2019; Z. Wang et al., 1998). Biodegradation is suggested to be the predominant form of PAH breakdown (Bumpus, 1989; Yuan et al., 2001).

Generally, biodegradation occurs most readily to unsubstituted PAHs, then the rates of degradation tend to decrease with increasing degrees of alkylation (Garrett et al., 1998). This trend is the opposite of what is expected to occur when observing the trends of PAH photooxidation.

Analysis using Gas Chromatography Mass Spectrometry (GCMS)

As stated earlier, crude oil exists as a complex mixture of potentially hundreds of thousands of individual compounds (Bartle & Myers, 2002; Demirbas & Taylan, 2016; Harayama et al., 1999; Z. Wang et al., 1999). When first attempting to identify individual compounds within a mixture, there must be a method of separating them. This necessary step can be achieved by chromatography (Bartle & Myers, 2002; Jalali-Heravi & Parastar, 2010). In this case, gas chromatography (GC) will be discussed. In simple terms, GC functions by serial partitioning of compounds between a mobile gas phase and a stationary liquid phase within a small diameter column, upon heated injection of a sample mixture (Bartle & Myers, 2002; Harvey, 2023). In relatively recent years, the introduction of helium or hydrogen as the carrier, or mobile gas was implemented. This gas is passed from a cylinder to the column inlet (Bartle & Myers, 2002). The type of column that is most efficient at separating complex mixtures is the capillary column. These are made of fused silica with a protective polymer coating, and are generally 30-100m in length (Harvey, 2023). The compounds within the mixtures being examined are separated within the capillary columns based on their boiling points and their polarities/non-polarities (Harvey, 2023). Choosing a column with the appropriate stationary

phase is of utmost importance; it must not react with the analytes, the polarity must be similar to that of the analytes, it must be thermally stable, and non-volatile (Harvey, 2023). In order to maintain steady, proper rates of compound emergence, or elution, the column must be kept at a high temperature. As such, modern GC instruments come equipped with a small oven that houses the column (Bartle & Myers, 2002; Harvey, 2023). Additionally, pneumatic control systems were put in place to ensure proper forward and backward pressures of gases flowing throughout the analyses (Bartle & Myers, 2002). The final major component of the GC is the detector. As compounds within the sample begin to elute through the column, the detector receives a signal and produces a distinguishable peak on its corresponding chromatogram. If compounds separate well, they elute one by one, rather than multiple at once; however, particular groups of hydrocarbons and their isomers often co-elute (Jalali-Heravi & Parastar, 2010). By using GC, the separated compounds within a complex mixture can be displayed on the resulting chromatogram as a function of their signal vs. the time in which the analyte eluted from the column, otherwise known as retention time.

Mass Spectrometry (MS) is a key tool used in the identification of various substances, including but not limited to: proteins, pesticides, pharmaceuticals, and contaminants (Glish & Vachet, 2003). The main components of a mass spectrometer include an ionization, or ion source, a mass analyzer, and a detector (Glish & Vachet, 2003). The premise of this technique is to ionize molecules within a sample, which in turn hit a detector that reads both the ion abundance, as well as the mass to charge ratio (m/z), which is relayed as Daltons (DA) per unit charge (Glish & Vachet, 2003). When comparing the m/z to the molecular mass of a compound, they are often the same values (e.g. benzene has a MW of 78 g/mol and is detected as an ion with m/z of 78) however, isotopes do not follow this pattern (Glish & Vachet, 2003). When the MW

of a compound is expressed, it is presented as the weighted average of its isotopes. In the mass spectrum, the m/z values would be diagnostic of each individual isotope, rather than the average (Dittwald et al., 2014; Glish & Vachet, 2003). Adding MS to an analysis allows users to distinguish the compounds within the mixture of interest *via* their m/z or mass, rather than based on the time in which they were detected. Since the molecular mass of known compounds can be easily found, this is an easy method to estimate which compounds are present within any given sample.

There is far greater certainty of properly determining compounds within a mixture when performing a Gas Chromatography Mass Spectrometry (GCMS) analysis, as opposed to relying on either gas chromatography or mass spectrometry alone. When operating in tandem, GCMS can provide meaningful insight towards identifying and quantifying various hydrocarbons based largely on their retention times and their m/z values. As such, GCMS has become one of the most widespread analytical tools globally (Jalali-Heravi & Parastar, 2010). Additionally, GCMS is an analytical technique that is constantly evolving, as scientists strive to increase analytical resolution and sensitivity to more confidently identify compounds at smaller concentrations (Dittwald et al., 2014). There are a number of analytical methods employed to identify and quantify compounds within sample mixtures, and each have their unique utilities. The following examples are some of the most commonly used, and ones that were used during this MSc project.

Full Scan

Full scan mode is the most basic, and generally least sensitive form of mass spectrometry. This method presents the mass spectra for every signal obtained within the allowed m/z range, which is dictated by the user. This method is extremely useful when performing preliminary

analyses of a sample mixture, and can be used to begin annotating signal peaks as a basic survey (Dittwald et al., 2014). Full scan allows users to observe the predominant m/z values detected that are considered diagnostic of particular compounds. This information is vital when developing more complex methods of analysis, which will be discussed in subsequent sections (Andrianova & Quimby, 2021; Dittwald et al., 2014). Another application of this method is to observe whether there is any background contamination being detected within a chromatogram when running a blank, as a signal is produced whenever an ion hits the detector. Finally, another function of full scan is to monitor the potential changes in retention times when the GC column needs to be shortened for maintenance purposes.

Single Ion Monitoring

A step up when considering sensitivity and specificity of analysis from full scan would be Selected, or Single Ion Monitoring (SIM) (Zeigler et al., 2008). SIM allows for users to select specific ions that they wish to examine, rather than including all m/z possibilities within their set range. Doing so increases the signal-to-noise ratio (S/N) of analyte peaks, as the MS dwell times when measuring each specified ion are longer (Wells & Huston, 1995). In essence, two main mechanisms are responsible for making SIM possible; a single quadrupole or an ion trap mass spectrometer, which has higher sensitivity than the former (Wells & Huston, 1995). Ionization of the analytes within a sample occurs prior to passing through the single quadrupole or ion trap, which then filter out all ions that have not been programmed into the instrument for examination by the user (Wells & Huston, 1995). Consequently, only selected ions of interest will reach the detector.

Multiple Reaction Monitoring

Multiple Reaction Monitoring (MRM) is one of the most sensitive and selective methods of MS (Andrianova & Quimby, 2021; Churley et al., 2019). It is incredibly effective at examining the presence of trace-level compounds in complex mixtures but is a very specific form of methodology. The utilization of MRM would normally occur after preliminary analyses using other methods such as full scan. MRM is only made possible when equipped with a triple quadrupole (QQQ) mass spectrometer (Churley et al., 2019). Theoretically, the QQQ functions by ionizing the analytes before reaching the first quadrupole, as with the preceding methods of analysis. Within the first quadrupole, the user selects a parent, or precursor ion of interest with a particular m/z value. Any precursor ions not selected will not be detected by the instrument. Subsequently, as these filtered ions move to the second quadrupole, a collision energy is applied which acts to fragment those ions into smaller daughter, or product ions with their own m/z value. Finally, the third quadrupole acts similarly to the first, wherein the user selects the product ions of interest that are generated from their initial precursor ion being fragmented (Churley et al., 2019). MRM outcompetes SIM in terms of selectivity, as it requires the combination of both parent and daughter ions, and eliminates possible matrix interferences experienced with SIM analyses (Churley et al., 2019; Zeigler et al., 2008). The sensitivity of MRM also outcompetes that of SIM, as there are less signals being sent to the detector, allowing for lower baseline responses. The output of an MRM analysis is generally much cleaner and easy to interpret than compared to full scan or SIM (Churley et al., 2019), but users will only be able to examine signals for compounds that they have already programmed the instrument to search for.

Time of Flight

One of the conceptually simplest forms of MS analysis is Time-of-Flight (TOF) (Weickhardt et al., 1996). TOF operates in full scan mode but has a high resolution and works well to separate various compounds, depending on certain physiochemical properties. The TOF spectrometers form all the ions at the same place and time, then are accelerated towards the detector. The separation is based on the velocities of the individual ions (Glish & Vachet, 2003). The electrostatic forces that produce the acceleration only function on charged particles. As such, TOF analysis still requires ionization as one of the first steps (Weickhardt et al., 1996). The TOF of individual ions is proportional to the square root of each respective ions mass, which allows for their separation when observing their retention times (Glish & Vachet, 2003; Weickhardt et al., 1996). Resolution, or resolving power is a performance parameter, which measures $m/\Delta m$, where m denotes the mass of an ion, and Δm signifies the width of the peak produced in the chromatogram by the mass m (Fiehn Lab, 2016). In essence, the higher the resolution, the lower the width of each peak, allowing for increased separation and identification of individual compounds within a particular sample. TOF-MS techniques often have high resolutions ($>10,000$) (Fiehn Lab, 2016; Macherone, 2015). When pairing high resolution with full-scan settings, the user is able to identify many compounds within a complex mixture with relative ease. TOF is an extremely useful tool to examine and identify groups of hydrocarbons such as n-alkanes, as the chromatogram can be configured to observe their diagnostic m/z ratios, such as m/z 71 (Medić et al., 2020). However, TOF analyses do not exhibit the same degree of selectivity as other analyses such as MRM. As such, it is important for users to understand the benefits and limitations of each analytical technique, prior to carrying out their experiments.

Often times, using a combination of different instrumental strategies can lead to the most comprehensive set of results.

The Baffin Island Oil Spill (BIOS) Project

By the late 1970s, the research and development of Arctic oil spill response measures had reached a point where field experiments became necessary to make meaningful progress (Sergy & Blackall, 1987). Performing experimental releases of oil within a pristine Arctic setting would allow for timely answers as it pertains to understanding their true environmental effects (Sergy & Blackall, 1987). Collaboration between representatives of Canadian oil industry, academia, government, public environmental groups, and inhabitants of Arctic communities led to the design of two particular experiments; one monitoring the impacts of an oil spill within the nearshore, and another along shorelines of Cape Hatt, Baffin Island (Sergy & Blackall, 1987). These two studies became what is now known as the Baffin Island Oil Spill (BIOS) project. The complex nature and design of the BIOS project required the establishment of five study topics: physical, chemical, and biological fates, oil discharge, and shoreline countermeasures. The BIOS project was mainly funded by Canadian oil industry and government (~75 %), with additional financial support from three other nations (Sergy & Blackall, 1987). There were two main objectives pertaining to the BIOS project. The first was to observe whether the application of chemical dispersants increases or decreases the environmental impacts of the spilled oil, and to compare dispersant use with other methods of shoreline cleanup and protection. The second goal of the BIOS project was to assess the physical and chemical fate of the crude oil released within the Arctic nearshore and shoreline (Sergy & Blackall, 1987). When designing this project, measures to reduce the likelihood of environmental damage as a consequence of releasing crude

oil into an otherwise pristine Arctic setting were considered and implemented. The basecamp and study locations of the BIOS project were located in Baffin Island, roughly 65 km southwest of Pond Inlet (Figure 1.5). The general area is characterized by mountainous terrain separated by various valleys and fjords. Low lying wetlands are present in certain areas surrounding the BIOS site, supporting limited vegetation. However, the area is mainly composed of polar semi-desert and desert conditions (Sergy & Blackall, 1987). To acquire a deep understanding of the physical features within the BIOS site prior to any oil spill experimentation, examinations of the ice conditions (Dickins, 1987), climate (Meeres, 1987), geomorphology (Sempels, 1987), and oceanography (Buckley et al., 1987) were conducted. Cape Hatt, Baffin Island was observed to have slightly shorter open-water seasons than many other representative areas within the Arctic (Dickins, 1987). A 17-year dataset of ice condition monitoring provided a mean 63 days of open waters within the study locations of the BIOS project, whereas some other areas experienced up to 98 days of open water (Allen, 1977 in Dickins, 1987). Such conditions were taken into account as it pertains to sediment transport by ice movement, capacity for crude oil to move, and the potential hindrance of degradation processes such as photooxidation and dissolution. The array and distribution of biological organisms at the BIOS site was determined to be representative of Eastern Arctic coastlines. Most of the faunal abundance was found in the marine benthic zones, with limited records of organisms such as phytoplankton, zooplankton, fish, birds and mammals (Snow et al., 1987). Additionally, studies were conducted to monitor the baseline concentrations of petroleum-related hydrocarbons within sediments (Cretney et al., 1987b), water (Cretney et al., 1987a), and the biological organisms (Cretney, 1987) found within the study region of the BIOS project. The recorded concentrations were determined to be as low as what might be found anywhere in an untouched, Arctic setting, and thus supported the choice

of the BIOS site as the geographic setting to conduct the experimental oil spills (Sergy & Blackall, 1987).

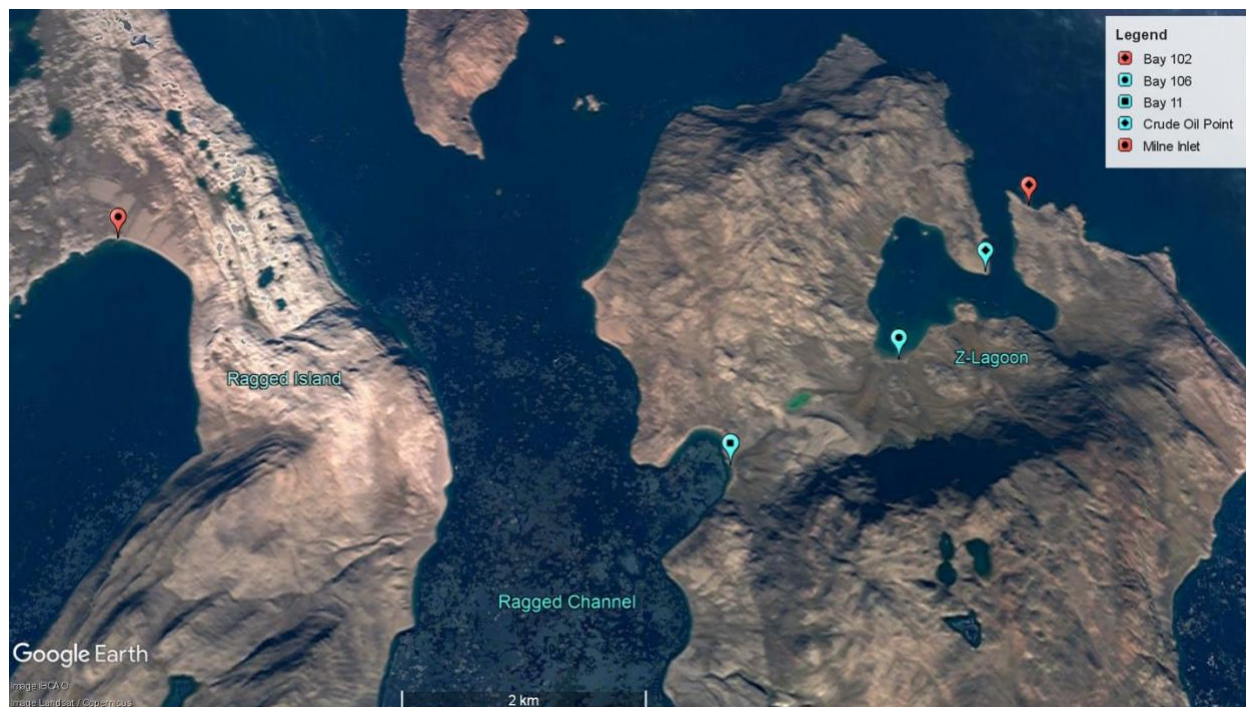


Figure 1.5. The geographical location of the Baffin Island Oil Spill (BIOS) project. Light blue pinpoints represent oiled sites, and red pinpoints denote field blank stations which were sampled from during the most recent revisitation of the BIOS site during the 2019 CCGS Amundsen expedition.

The nearshore component of the BIOS project was chosen to take place within the sheltered bays of the Ragged Channel (Figure 1.5). The design of this study was implemented as a four-year plan, with pre-spill studies conducted in 1980, the experimental spills in 1981, then two years of follow-up measurements during open-water periods (Sergy & Blackall, 1987). Bay 11 was the site chosen for the surface oil slick to be released (Figure 1.5), and the chemically dispersed oil spill was planned to occur at Bay 9 (Sergy & Blackall, 1987). The intention behind the surface release of crude oil at Bay 11 was to enclose the spill, forcing wave action to physically move the petroleum onto the intertidal sediments along the shoreline. Additionally,

crude oil behaviour and losses would be tracked over time (Sergy & Blackall, 1987). In each case, 15 m³ of a sweet medium gravity, Venezuelan Lagomedio crude oil was applied. With shorelines being only roughly 400m in length, this volume of petroleum was effective in emulating a spill that could heavily contaminate (75 – 100 % coverage) the intertidal zone of the respective bays (Owens et al., 1987; Owens et al., 2002). In the case of Bay 9, the Corexit 9527 chemical dispersant was fed through a pipe directly into the water column (Sergy & Blackall, 1987). The dispersed oil produced some unexpected results. Most notably, the dispersal of the crude oil caused transport of many toxic aromatic residues to the benthos of Bay 10. Thankfully, Bay 10 had been set up as a site that could receive cross-contamination from Bay 9 in the event of unexpected oil movement (Sergy & Blackall, 1987). The sedimentology of the intertidal sediments at Bay 11 are largely comprised of gravel and sand, with very little mud; whereas the nearshore surface sediments are mostly made up of sand and mud (Sempels, 1987). These parameters are important when observing the fate of crude oil in beach sediments.

A large component of the shoreline studies was to monitor the fate of crude oil when applied to different types of beach sediments, and exposure to wave and tidal action (E. H. Owens & Robson, 1987; Sergy & Blackall, 1987). Additionally, the testing of different crude oil countermeasures was conducted as part of the shoreline studies. These were done within a sheltered area called the Z-Lagoon (Figure 1.5) at two different sampling stations: Crude Oil Point and Bay 106 (E. H. Owens & Robson, 1987). Other sites such as Bays 102 and 103 within the Z-lagoon were selected for similar experiments (E. H. Owens & Robson, 1987), but were not considered as part of this Masters project. Crude Oil Point was chosen to be a site with no countermeasure techniques utilized (E. H. Owens & Robson, 1987). The sediments of Crude Oil Point were not fully characterized however, the nearest site, Bay 109 is made up almost entirely

of gravel and sand, with little mud present (Sempels, 1987). At Crude Oil Point, two 40 m² plots were created on the beach surface, above the limit of tidal action to eliminate any contact with the marine interface. The first plot, T1 had the same Venezuelan Lagomedio crude oil applied, whereas the second plot, T2 had a 1:1 crude oil-water emulsion added in 1980 (E. H. Owens & Robson, 1987). Bay 106 hosted a sediment mixing experiment in 1982 (E. H. Owens, Robson, et al., 1987; E. H. Owens & Robson, 1987). Two sub-sectioned plots within the supratidal area were created; one receiving crude oil (IMC) and the second receiving the 1:1 emulsion (IME). These two plots were separated by both a mixing section *via* tillage (suffix c), or no mixing (suffix e) (E. H. Owens, Robson, et al., 1987). The positioning of these plots were selected with the expectation that tidal action would reach these sediments under spring tides or storm activity (E. H. Owens & Robson, 1987). The sediments in the upper intertidal zone of Bay 106 are characterized by large amounts of sand and mud, with relatively little gravel (Sempels, 1987).

To monitor the fate and behaviour of crude oil within an Arctic setting over long periods of time, the BIOS site has been revisited on a number of occasions. The revisitations have spanned from a single year post-oil application to twenty years post-spills. Reports disseminating results from Total Petroleum Hydrocarbon (TPH) analyses, crude oil weathering ratios, oil budgets and volumes are provided (Boehm, 1981, 1983; Humphrey, 1984; Humphrey et al., 1992b; E. Owens et al., 2002; H. Owens, 1984; Prince et al., 2002; Zhendi. Wang et al., 1995). Most recently, the BIOS site was revisited during the third leg of the 2019 CCGS Amundsen expedition. This sampling regime was held nearly four decades after the initial experiments had been conducted. This was a truly unique and once-in-a-lifetime excursion to take part in, as large-scale crude oil experiments such as the BIOS project are legally and logistically impractical to begin implementing today. As such, the continued research on existing field

studies must be maintained to understand the long-term trends of crude oil degradation within the Arctic. The three main sites of the BIOS project; Crude Oil Point, Bay 11, and Bay 106 were visited to collect surface (0-2cm) and subsurface (5-10cm) sediment samples, in order to continue the legacy of this long-term monitoring project. The collected samples will incur hydrocarbon analyses using GCMS methods described above. Detailed chemical information, such as the total concentrations of n-alkanes, PAHs, alkylcycloalkanes, biomarkers, and alkylbenzenes, chemical compositions, weathering ratios, potential toxicity, and percent residual data will be provided regarding these sediments. Whenever possible, direct comparisons to previous work will be done.

Thesis Topic, Objectives, and Hypotheses

The overarching topic that this Master's thesis will be addressing is the continuation of the long-term monitoring study, the BIOS project. By applying analytical chemistry techniques such as GCMS, I will work to provide a chemical assessment of the recalcitrant crude oil residues within the samples collected during the 2019 CCGS Amundsen expedition. Doing so will offer pertinent information regarding the degradation of crude oil within a previously pristine Arctic setting, over the course of nearly four decades. It is critically important to ensure continued, long-term monitoring of experiments such as this to educate and inform officials responsible for policy-making decisions, and to reduce the potential for catastrophic errors with regards to oil spills in an Arctic environment.

This Master's thesis will be accomplished by addressing the objectives denoted below:

- Examine the individual identities and concentrations of hydrocarbons (PAHs, n-alkanes, biomarkers, alkylbenzenes, alkylcycloalkanes) within the oiled sediments collected from the BIOS site.
- Compare wherever applicable current hydrocarbon data to that found in previous literature from the BIOS site, to assess the extents of natural attenuation processes affecting crude oil within the Arctic.
- By completing the above two points, determine the long-term chemical fate and behaviour of crude oil-contaminated beach sediments within the Arctic, as no other studies on similar temporal & geographical scales have ever been completed.

Given the highest potential for degradation to occur at Bay 11, I hypothesize that this station will host the lowest recorded concentrations of hydrocarbons across the BIOS site. I hypothesize that the sediments collected from Crude Oil Point will exhibit the least amount of degradation, as there is no access to the marine interface. I hypothesize that significant losses of total and individual hydrocarbons will be observed when comparing with data acquired from previous revisitations to the BIOS site.

References

- Abbasian, F., Lockington, R., Mallavarapu, M., & Naidu, R. (2015). A comprehensive review of aliphatic hydrocarbon biodegradation by bacteria. *Applied Biochemistry and Biotechnology*, *176*(3), 670–699. <https://doi.org/10.1007/s12010-015-1603-5>
- Acevedo, S., Castro, A., Negrin, J. G., Fernández, A., Escobar, G., Piscitelli, V., Delolme, F., & Dessalces, G. (2007). Relations between asphaltene structures and their physical and chemical properties: The rosary-type structure. *Energy & Fuels*, *21*(4), 2165–2175. <https://doi.org/10.1021/ef070089v>
- Akmaz, S., Iscan, O., Gurkaynak, M. A., & Yasar, M. (2011). The structural characterization of saturate, aromatic, resin, and asphaltene fractions of batiraman crude oil. *Petroleum Science and Technology*, *29*(2), 160–171. <https://doi.org/10.1080/10916460903330361>
- Alvarez, L. A., Exton, D. A., Timmis, K. N., Suggett, D. J., & McGenity, T. J. (2009). Characterization of marine isoprene-degrading communities. *Environmental Microbiology*, *11*(12), 3280–3291. <https://doi.org/10.1111/j.1462-2920.2009.02069.x>
- Andersson, J. T., & Achten, C. (2015). Time to say goodbye to the 16 EPA PAHs? Toward an up-to-date use of PACs for environmental purposes. *Polycyclic Aromatic Compounds*, *35*(2–4), 330–354. <https://doi.org/10.1080/10406638.2014.991042>
- Andrianova, A., & Quimby, B. (2021). *Full scan quantitative analysis of semivolatile organic compounds* (p. 10) [Application Note]. Agilent Technologies, Inc.
- Arctic Monitoring and Assessment Programme. (2017). *Snow, water, ice and permafrost in the Arctic—Summary for policy-makers*. Arctic Monitoring and Assessment Programme (AMAP).

- Ashoori, S., Sharifi, M., Masoumi, M., & Mohammad Salehi, M. (2017). The relationship between SARA fractions and crude oil stability. *Egyptian Journal of Petroleum*, 26(1), 209–213. <https://doi.org/10.1016/j.ejpe.2016.04.002>
- Atlas, R. M., & Hazen, T. C. (2011). Oil biodegradation and bioremediation: A tale of the two worst spills in U.S. history. *Environmental Science & Technology*, 45(16), 6709–6715. <https://doi.org/10.1021/es2013227>
- Bakan, S., Chlond, A., Cubasch, U., Feichter, H., Graf, H., Grassl, H., Hasselmann, K., Kirchner, I., Latif, M., Roeckner, E., Sausen, R., Schlese, U., Schrieffer, D., Schlut, I., Schumann, U., Sielmann, F., & Welke, W. (1991). Climate response to smoke from the burning oil wells in Kuwait. *Nature*, 351(6325), 367–371.
- Bartle, K. D., & Myers, P. (2002). History of gas chromatography. *Trends in Analytical Chemistry*, 21(9–10), 547–557. [https://doi.org/10.1016/S0165-9936\(02\)00806-3](https://doi.org/10.1016/S0165-9936(02)00806-3)
- Bejarano, A. C., Levine, E., & Mearns, A. J. (2013). Effectiveness and potential ecological effects of offshore surface dispersant use during the Deepwater Horizon oil spill: A retrospective analysis of monitoring data. *Environmental Monitoring and Assessment*, 185(12), 10281–10295. <https://doi.org/10.1007/s10661-013-3332-y>
- Beyer, J., Trannum, H. C., Bakke, T., Hodson, P. V., & Collier, T. K. (2016). Environmental effects of the Deepwater Horizon oil spill: A review. *Marine Pollution Bulletin*, 110(1), 28–51. <https://doi.org/10.1016/j.marpolbul.2016.06.027>
- Blumer, M., & Sass, J. (1972). Oil pollution: Persistence and degradation of spilled fuel oil. *Science*, 176(4039), 1120–1122.
- Boehm, P. D. (1981). *Chemistry:2 Hydrocarbon chemistry—1980 study results. (BIOS) Baffin Island Oil Spill Working Report* (p. 184) [Working Report].

- Boehm, P. D. (1983). *Chemistry: 2. Analytical biogeochemistry—1982 study results* (p. 231).
- Boehm, P. D., Page, D. S., Burns, W. A., Bence, A. E., Mankiewicz, P. J., & Brown, J. S. (2001). Resolving the origin of the petrogenic hydrocarbon background in Prince William Sound, Alaska. *Environmental Science & Technology*, *35*(3), 471–479.
<https://doi.org/10.1021/es001421j>
- Bost, F. D., Frontera-Suau, R., McDonald, T. J., Peters, K. E., & Morris, P. J. (2001). Aerobic biodegradation of hopanes and norhopanes in Venezuelan crude oils. *Organic Geochemistry*, *32*(1), 105–114. [https://doi.org/10.1016/S0146-6380\(00\)00147-9](https://doi.org/10.1016/S0146-6380(00)00147-9)
- Box, J. E., Colgan, W. T., Christensen, T. R., Schmidt, N. M., Lund, M., Parmentier, F.-J. W., Brown, R., Bhatt, U. S., Euskirchen, E. S., Romanovsky, V. E., Walsh, J. E., Overland, J. E., Wang, M., Corell, R. W., Meier, W. N., Wouters, B., Mernild, S., Mård, J., Pawlak, J., & Olsen, M. S. (2019). Key indicators of Arctic climate change: 1971–2017. *Environmental Research Letters*, *14*(4), 045010. <https://doi.org/10.1088/1748-9326/aafc1b>
- Brubaker, L., Anderson, P., & Hu, F. (1995). Arctic tundra biodiversity: A temporal perspective from late quaternary pollen records. In *Arctic and Alpine Biodiversity: Patterns, Causes and Ecosystem Consequences* (Vol. 113, pp. 111–125). Springer.
- Buckley, J. R., De Lange Boom, B. R., & Reimer, E. M. (1987). The physical oceanography of the Cape Hatt Region, Eclipse Sound, N.W.T. *ARCTIC*, *40*(5), 20–33.
<https://doi.org/10.14430/arctic1799>
- Bumpus, J. A. (1989). Biodegradation of polycyclic hydrocarbons by *Phanerochaete chrysosporium*. *Applied and Environmental Microbiology*, *55*(1), 154–158.
<https://doi.org/10.1128/aem.55.1.154-158.1989>

- Chapin, F. S., Sturm, M., Serreze, M. C., McFadden, J. P., Key, J. R., Lloyd, A. H., McGuire, A. D., Rupp, T. S., Lynch, A. H., Schimel, J. P., Beringer, J., Chapman, W. L., Epstein, H. E., Euskirchen, E. S., Hinzman, L. D., Jia, G., Ping, C.-L., Tape, K. D., Thompson, C. D. C., ... Welker, J. M. (2005). Role of land-surface changes in Arctic summer warming. *Science*, *310*(5748), 657–660. <https://doi.org/10.1126/science.1117368>
- Chikere, C. B., Okpokwasili, G. C., & Chikere, B. O. (2011). Monitoring of microbial hydrocarbon remediation in the soil. *3 Biotech*, *1*(3), 117–138. <https://doi.org/10.1007/s13205-011-0014-8>
- Churley, M., Quimby, B., & Andrianova, A. (2019). *A fast method for EPA 8270 in MRM mode using the 7000 series triple quadrupole GC/MS* (p. 10) [Application Note]. Agilent Technologies, Inc.
- Cretney, W. J. (1987). Hydrocarbon biogeochemical setting of the Baffin Island Oil Spill experimental sites. III. Biota. *ARCTIC*, *40*, 9.
- Cretney, W. J., Green, D. R., Fowler, B. R., Humphrey, B., Fiest, D. L., & Boehm, P. D. (1987a). Hydrocarbon biogeochemical setting of the Baffin Island Oil Spill experimental sites. II. Water. *Arctic*, *40*, 66–70.
- Cretney, W. J., Green, D. R., Fowler, B. R., Humphrey, B., Fiest, D. L., & Boehm, P. D. (1987b). Hydrocarbon biogeochemical setting of the Baffin Island Oil Spill experimental sites. I. Sediments. *ARCTIC*, *40*(5), 51–65. <https://doi.org/10.14430/arctic1802>
- Dabestani, R., & Ivanov, I. N. (1999). A compilation of physical, spectroscopic and photophysical properties of polycyclic aromatic hydrocarbons. *Photochemistry and Photobiology*, *70*(1), 10–34. <https://doi.org/10.1111/j.1751-1097.1999.tb01945.x>

- Dawson, J., Pizzolato, L., Howell, S. E. L., Copland, L., & Johnston, M. E. (2018). Temporal and spatial patterns of ship traffic in the Canadian Arctic from 1990 to 2015. *ARCTIC*, *71*(1), Article 1. <https://doi.org/10.14430/arctic4698>
- Demirbas, A., & Taylan, O. (2016). Removing of resins from crude oils. *Petroleum Science and Technology*, *34*(8), 771–777. <https://doi.org/10.1080/10916466.2016.1163397>
- Dickins, D. F. (1987). Ice conditions at Cape Hatt, Baffin Island. *ARCTIC*, *40*(5), 34–41. <https://doi.org/10.14430/arctic1800>
- Dittwald, P., Vu, T. N., Harris, G. A., Caprioli, R. M., Van de Plas, R., Laukens, K., Gambin, A., & Valkenburg, D. (2014). Towards automated discrimination of lipids versus peptides from full scan mass spectra. *EuPA Open Proteomics*, *4*, 87–100. <https://doi.org/10.1016/j.euprot.2014.05.002>
- Dubinsky, E. A., Conrad, M. E., Chakraborty, R., Bill, M., Borglin, S. E., Hollibaugh, J. T., Mason, O. U., M. Piceno, Y., Reid, F. C., Stringfellow, W. T., Tom, L. M., Hazen, T. C., & Andersen, G. L. (2013). Succession of hydrocarbon-degrading bacteria in the aftermath of the *Deepwater Horizon* oil spill in the Gulf of Mexico. *Environmental Science & Technology*, *47*(19), 10860–10867. <https://doi.org/10.1021/es401676y>
- Edwards, B. R., Reddy, C. M., Camilli, R., Carmichael, C. A., Longnecker, K., & Van Mooy, B. A. S. (2011). Rapid microbial respiration of oil from the *Deepwater Horizon* spill in offshore surface waters of the Gulf of Mexico. *Environmental Research Letters*, *6*(3), 035301. <https://doi.org/10.1088/1748-9326/6/3/035301>
- Ehrhardt, M. G., Burns, K. A., & Bicego, M. C. (1992). Sunlight-induced compositional alterations in the seawater-soluble fraction of a crude oil. *Marine Chemistry*, *37*(1–2), 53–64. [https://doi.org/10.1016/0304-4203\(92\)90056-G](https://doi.org/10.1016/0304-4203(92)90056-G)

- Fasnacht, M. P., & Blough, N. V. (2003). Kinetic analysis of the photodegradation of polycyclic aromatic hydrocarbons in aqueous solution. *Aquatic Sciences - Research Across Boundaries*, 65(4), 352–358. <https://doi.org/10.1007/s00027-003-0680-7>
- Feihn. (2016). *Mass resolution and resolving power*. UC Davis.
<https://fiehnlab.ucdavis.edu/projects/seven-golden-rules/mass-resolution>
- Fingas, M. (2011). *Oil and petroleum evaporation*. <https://doi.org/10.1002/9781118989982.ch7>
- Fiocco, R., & Lewis, A. (1999). Oil spill dispersants. *Pure Applied Chemistry*, 71(1), 27–42.
<https://doi.org/10.1351/pac199971010027>
- Francis, A. W. (1948). Properties of alkylbenzenes. *Chemical Reviews*, 42(1), 107–162.
<https://doi.org/10.1021/cr60131a003>
- Galt, J. A., Lehr, W. J., & Payton, D. L. (1991). Fate and transport of the Exxon Valdez oil spill. Part 4. *Environmental Science & Technology*, 25(2), 202–209.
<https://doi.org/10.1021/es00014a001>
- Garrett, R. M., Pickering, I. J., Haith, C. E., & Prince, R. C. (1998). Photooxidation of crude oils. *Environmental Science & Technology*, 32(23), 3719–3723.
<https://doi.org/10.1021/es980201r>
- Garti, N. (1997). Progress in stabilization and transport phenomena of double emulsions in food applications. *LWT - Food Science and Technology*, 30(3), 222–235.
<https://doi.org/10.1006/fstl.1996.0176>
- Glish, G. L., & Vachet, R. W. (2003). The basics of mass spectrometry in the twenty-first century. *Nature Reviews Drug Discovery*, 2(2), 140–150. <https://doi.org/10.1038/nrd1011>

- Griffiths, I., Harris, F., Mukhtar, E., & Beynon, J. (1981). Calculation of the abundance ratio [91+/92+] from n-Butylbenzene molecular ions as a function of internal energy. *International Journal of Mass Spectrometry and Ion Physics*, 41, 83–88.
- Groenzin, H., & Mullins, O. C. (1999). Asphaltene molecular size and structure. *The Journal of Physical Chemistry A*, 103(50), 11237–11245. <https://doi.org/10.1021/jp992609w>
- Harayama, S., Kishira, H., Kasai, Y., & Shutsubo, K. (1999). Petroleum biodegradation in marine environments. *Journal of Molecular Microbiology and Biotechnology*, 1(1), 63–70.
- Haritash, A. K., & Kaushik, C. P. (2009). Biodegradation aspects of polycyclic aromatic hydrocarbons (PAHs): A review. *Journal of Hazardous Materials*, 169(1–3), 1–15. <https://doi.org/10.1016/j.jhazmat.2009.03.137>
- Harvey, D. (2023). *Analytical Chemistry 2.1* (2.1). LibreTexts.
- Harwell, M. A., & Gentile, J. H. (2006). Ecological significance of residual exposures and effects from the *Exxon Valdez* oil spill: Ecological significance of EVOS. *Integrated Environmental Assessment and Management*, 2(3), 204–246. <https://doi.org/10.1002/ieam.5630020303>
- Head, I. M., Jones, D. M., & Röling, W. F. M. (2006). Marine microorganisms make a meal of oil. *Nature Reviews Microbiology*, 4(3), 173–182. <https://doi.org/10.1038/nrmicro1348>
- Humphrey, B. (1984). *Chemistry 1: Field sampling and measurements—1983 study results* (Baffin Island Oil Spill, p. 64) [Working Report]. Environmental Protection Service.
- Humphrey, B., Owens, E., & Sergy, G. (1992). *The fate and persistence of stranded crude oil: A nine-year overview from the BIOS project, Baffin Island, N.W.T., Canada* (p. 60) [Working Report]. Environment Canada.

- Inkley, D., Kronenthal, S., & McCormick, L. (2013). *Restoring a degraded Gulf of Mexico: Wildlife and wetlands three years into the gulf oil disaster* (p. 15). National Wildlife Federation.
- Jalali-Heravi, M., & Parastar, H. (2010). Assessment of the co-elution problem in gas chromatography-mass spectrometry using non-linear optimization techniques. *Chemometrics and Intelligent Laboratory Systems*, *101*(1), 1–13. <https://doi.org/10.1016/j.chemolab.2009.11.010>
- Jeffries, M. O., Overland, J. E., & Perovich, D. K. (2013). The Arctic shifts to a new normal. *Physics Today*, *66*(10), 35–40. <https://doi.org/10.1063/PT.3.2147>
- Jesus, F., Pereira, J. L., Campos, I., Santos, M., Ré, A., Keizer, J., Nogueira, A., Gonçalves, F. J. M., Abrantes, N., & Serpa, D. (2022). A review on polycyclic aromatic hydrocarbons distribution in freshwater ecosystems and their toxicity to benthic fauna. *Science of The Total Environment*, *820*, 153282. <https://doi.org/10.1016/j.scitotenv.2022.153282>
- Jia, H. (2018). Crude oil trade and green shipping choices. *Transportation Research Part D: Transport and Environment*, *65*, 618–634. <https://doi.org/10.1016/j.trd.2018.10.003>
- Johnson, R. J., West, C. E., Swaih, A. M., Folwell, B. D., Smith, B. E., Rowland, S. J., & Whitby, C. (2012). Aerobic biotransformation of alkyl branched aromatic alkanonic naphthenic acids via two different pathways by a new isolate of Mycobacterium: Isolation and characterization of an aromatic NA degrading Mycobacterium spp. *Environmental Microbiology*, *14*(4), 872–882. <https://doi.org/10.1111/j.1462-2920.2011.02649.x>
- Keith, L. H. (2015). The source of U.S. EPA's sixteen PAH priority pollutants. *Polycyclic Aromatic Compounds*, *35*(2–4), 147–160. <https://doi.org/10.1080/10406638.2014.892886>

- Kleindienst, S., Grim, S., Sogin, M., Bracco, A., Crespo-Medina, M., & Joye, S. B. (2016). Diverse, rare microbial taxa responded to the Deepwater Horizon deep-sea hydrocarbon plume. *The ISME Journal*, *10*(2), 400–415. <https://doi.org/10.1038/ismej.2015.121>
- Knol, M., & Arbo, P. (2014). Oil spill response in the Arctic: Norwegian experiences and future perspectives. *Marine Policy*, *50*, 171–177. <https://doi.org/10.1016/j.marpol.2014.06.003>
- Kristensen, M., Johnsen, A. R., & Christensen, J. H. (2015). Marine biodegradation of crude oil in temperate and Arctic water samples. *Journal of Hazardous Materials*, *300*, 75–83. <https://doi.org/10.1016/j.jhazmat.2015.06.046>
- Larson, R. A., Bott, T. L., Hunt, L. L., & Rogenmuser, K. (1979). Photooxidation products of a fuel oil and their antimicrobial activity. *Environmental Science & Technology*, *13*(8), 965–969. <https://doi.org/10.1021/es60156a011>
- Lawal, A. T. (2017). Polycyclic aromatic hydrocarbons. A review. *Cogent Environmental Science*, *3*(1), 1339841. <https://doi.org/10.1080/23311843.2017.1339841>
- Lee, J.-S., Kim, J.-W., Han, S.-H., Chang, I.-S., Kang, H.-H., Lee, O.-S., Oh, S.-G., & Suh, K.-D. (2004). The stabilization of L-ascorbic acid in aqueous solution and water-in-oil-in-water double emulsion by controlling pH and electrolyte concentration. *International Journal of Cosmetic Science*, *26*(4), 217–217. https://doi.org/10.1111/j.0142-5463.2004.00223_1.x
- Lim, J., Wong, S., Law, M., Samyudia, Y., & Dol, S. (2015). A review on the effects of emulsions on flow behaviours and common factors affecting the stability of emulsions. *Journal of Applied Sciences*, *15*(2), 167–172. <https://doi.org/10.3923/jas.2015.167.172>
- Macherone, A. (2015). *Resolving power and mass resolution* (p. 4) [Technical Overview]. Agilent Technologies, Inc.

- Markus, T., Stroeve, J. C., & Miller, J. (2009). Recent changes in Arctic sea ice melt onset, freezeup, and melt season length. *Journal of Geophysical Research: Oceans*, *114*(C12).
<https://doi.org/10.1029/2009JC005436>
- Masnadi, M. S., El-Houjeiri, H. M., Schunack, D., Li, Y., Englander, J. G., Badahdah, A., Monfort, J.-C., Anderson, J. E., Wallington, T. J., Bergerson, J. A., Gordon, D., Koomey, J., Przesmitzki, S., Azevedo, I. L., Bi, X. T., Duffy, J. E., Heath, G. A., Keoleian, G. A., McGlade, C., ... Brandt, A. R. (2018). Global carbon intensity of crude oil production. *Science*, *361*(6405), 851–853. <https://doi.org/10.1126/science.aar6859>
- McCarthy, E. D., & Calvin, M. (1967). Organic geochemical studies. I. Molecular criteria for hydrocarbon genesis. *Nature*, *216*(5116), 642–647. <https://doi.org/10.1038/216642a0>
- Medić, A., Lješević, M., Inui, H., Beškoski, V., Kojić, I., Stojanović, K., & Karadžić, I. (2020). Efficient biodegradation of petroleum *n*-alkanes and polycyclic aromatic hydrocarbons by polyextremophilic *Pseudomonas aeruginosa* strain with multidegradative capacity. *RSC Advances*, *10*(24), 14060–14070. <https://doi.org/10.1039/C9RA10371F>
- Meeres, L. S. (1987). Meteorological operations at Cape Hatt in support of the Baffin Island Oil Spill project. *ARCTIC*, *40*(5), 42–50. <https://doi.org/10.14430/arctic1801>
- Moreda, J. M., Arranz, A., De Betono, S., & Arranz, J. (1998). Chromatographic determination of aliphatic hydrocarbons and polyaromatic hydrocarbons (PAHs) in a sewage sludge. *The Science of the Total Environment*, *220*, 33–43.
- Mostafawi, N. (2001). How severely was the Persian Gulf affected by oil spills following the 1991 Gulf War? *Environmental Geology*, *40*(10), 1185–1191.
<https://doi.org/10.1007/s002540100238>

- Murray, J., Hacquebord, L., Gregor, D., & Loeng, H. (1998). *AMAP assessment report: Physical/geographical characteristics of the Arctic* (p. 16) [Assessment Report]. Arctic Monitoring and Assessment Programme.
- Neff, W., Compo, G. P., Martin Ralph, F., & Shupe, M. D. (2014). Continental heat anomalies and the extreme melting of the Greenland ice surface in 2012 and 1889: Melting of Greenland in 1889 and 2012. *Journal of Geophysical Research: Atmospheres*, *119*(11), 6520–6536. <https://doi.org/10.1002/2014JD021470>
- Owens, E. H., & Robson, W. (1987). Experimental design and the retention of oil on Arctic test beaches. *ARCTIC*, *40*(5), 230–243. <https://doi.org/10.14430/arctic1817>
- Owens, E. H., Robson, W., & Foget, C. R. (1987). A field evaluation of selected beach-cleaning techniques. *ARCTIC*, *40*(5), 244–257. <https://doi.org/10.14430/arctic1818>
- Owens, E., Sergy, G. A., & Prince, R. (2002). The fate of stranded oil at the BIOS site twenty years after the experiment. *Environment Canada Arctic and Marine Oil Spill Program Technical Seminar (AMOP) Proceedings*, *25*, 1–11.
- Owens, H. (1984). *Shoreline Countermeasures—1983 Results. Baffin Island Oil Spill project working report 83-4* (pp. 1–115) [Working Report]. Environmental Protection Service, Environment Canada, Ottawa.
- Pashaei, R., Mortaza Gholizadeh, Ahad Hanifi, & Iran, K. J. (2015). *The effects of oil spills on ecosystem at the Persian Gulf*. <https://doi.org/10.13140/RG.2.1.2239.3684>
- Peters, K. E., & Moldowan, J. M. (1991). Effects of source, thermal maturity, and biodegradation on the distribution and isomerization of homohopanes in petroleum. *Organic Geochemistry*, *17*(1), 47–61. [https://doi.org/10.1016/0146-6380\(91\)90039-M](https://doi.org/10.1016/0146-6380(91)90039-M)

- Peters, K. E., Moldowan, J. M., McCaffrey, M. A., & Fago, F. J. (1996). Selective biodegradation of extended hopanes to 25-norhopanes in petroleum reservoirs. Insights from molecular mechanics. *Organic Geochemistry*, 24(8–9), 765–783.
[https://doi.org/10.1016/S0146-6380\(96\)00086-1](https://doi.org/10.1016/S0146-6380(96)00086-1)
- Pew Charitable Trusts. (2013). *Arctic standards: Recommendations on oil spill prevention, response, and safety in the U.S. Arctic Ocean* (p. 142).
- Piatt, J., & Ford, R. (1996). *How many seabirds were killed by the Exxon Valdez oil spill?* 18, 712–719.
- Pizzolato, L., Howell, S. E. L., Dawson, J., Laliberté, F., & Copland, L. (2016). The influence of declining sea ice on shipping activity in the Canadian Arctic. *Geophysical Research Letters*, 43(23), 12,146–12,154. <https://doi.org/10.1002/2016GL071489>
- Pizzolato, L., Howell, S. E. L., Derksen, C., Dawson, J., & Copland, L. (2014). Changing sea ice conditions and marine transportation activity in Canadian Arctic waters between 1990 and 2012. *Climatic Change*, 123(2), 161–173. <https://doi.org/10.1007/s10584-013-1038-3>
- Prince, R. C., & Butler, J. D. (2014). A protocol for assessing the effectiveness of oil spill dispersants in stimulating the biodegradation of oil. *Environmental Science and Pollution Research*, 21(16), 9506–9510. <https://doi.org/10.1007/s11356-013-2053-7>
- Prince, R. C., Butler, J. D., & Redman, A. D. (2017). The rate of crude oil biodegradation in the sea. *Environmental Science & Technology*, 51(3), 1278–1284.
<https://doi.org/10.1021/acs.est.6b03207>
- Prince, R. C., Coolbaugh, T. S., & Parkerton, T. F. (2016). Oil dispersants do facilitate biodegradation of spilled oil. *Proceedings of the National Academy of Sciences*, 113(11).
<https://doi.org/10.1073/pnas.1525333113>

- Prince, R. C., Elmendorf, D. L., Lute, J. R., Hsu, C. S., Haith, C. E., Senius, J. D., Dechert, G. J., Douglas, G. S., & Butler, E. L. (1994). 17.alpha.(H)-21.beta.(H)-hopane as a conserved internal marker for estimating the biodegradation of crude oil. *Environmental Science & Technology*, 28(1), 142–145. <https://doi.org/10.1021/es00050a019>
- Prince, R. C., Owens, E. H., & Sergy, G. A. (2002). Weathering of an Arctic oil spill over 20 years: The BIOS experiment revisited. *Marine Pollution Bulletin*, 44(11), 1236–1242. [https://doi.org/10.1016/S0025-326X\(02\)00214-X](https://doi.org/10.1016/S0025-326X(02)00214-X)
- Reed, M., Johansen, Ø., Brandvik, P. J., Daling, P., Lewis, A., Fiocco, R., Mackay, D., & Prentki, R. (1999). Oil spill modeling towards the close of the 20th century: Overview of the state of the art. *Spill Science & Technology Bulletin*, 5(1), 3–16. [https://doi.org/10.1016/S1353-2561\(98\)00029-2](https://doi.org/10.1016/S1353-2561(98)00029-2)
- Reed, W. E. (1977). Molecular compositions of weathered petroleum and comparison with its possible source. *Geochimica et Cosmochimica Acta*, 41(2), 237–247. [https://doi.org/10.1016/0016-7037\(77\)90231-9](https://doi.org/10.1016/0016-7037(77)90231-9)
- Rocha, C. A., Pedregosa, A. M., & Laborda, F. (2011). Biosurfactant-mediated biodegradation of straight and methyl-branched alkanes by *Pseudomonas aeruginosa* ATCC 55925. *AMB Express*, 1(1), 9. <https://doi.org/10.1186/2191-0855-1-9>
- Rubinstein, I., Strausz, O. P., Spyckerelle, C., Crawford, R. J., & Westlake, D. W. S. (1977). The origin of the oil sand bitumens of Alberta: A chemical and a microbiological simulation study. *Geochimica et Cosmochimica Acta*, 41(9), 1341–1353. [https://doi.org/10.1016/0016-7037\(77\)90077-1](https://doi.org/10.1016/0016-7037(77)90077-1)
- Saha, M., Togo, A., Mizukawa, K., Murakami, M., Takada, H., Zakaria, M. P., Chiem, N. H., Tuyen, B. C., Prudente, M., Boonyatumanond, R., Sarkar, S. K., Bhattacharya, B.,

- Mishra, P., & Tana, T. S. (2009). Sources of sedimentary PAHs in tropical Asian waters: Differentiation between pyrogenic and petrogenic sources by alkyl homolog abundance. *Marine Pollution Bulletin*, 58(2), 189–200.
<https://doi.org/10.1016/j.marpolbul.2008.04.049>
- Salager, J.-L. (2000). Emulsion properties and related know-how to attain them. In F. Nielloud & G. Marti-Mestres, *Pharmaceutical Emulsions and Suspensions* (Vol. 20000573, pp. 73–125). CRC Press. <https://doi.org/10.1201/b14005-4>
- Saltymakova, D., Desmond, D. S., Isleifson, D., Firoozy, N., Neusitzer, T. D., Xu, Z., Lemes, M., Barber, D. G., & Stern, G. A. (2020). Effect of dissolution, evaporation, and photooxidation on crude oil chemical composition, dielectric properties and its radar signature in the Arctic environment. *Marine Pollution Bulletin*, 151, 110629.
<https://doi.org/10.1016/j.marpolbul.2019.110629>
- Seal, R. (2021, December 11). 'Gushing oil and roaring fires': 30 years on Kuwait is still scarred by catastrophic pollution. *The Guardian*.
<https://www.theguardian.com/environment/2021/dec/11/the-sound-of-roaring-fires-is-still-in-my-memory-30-years-on-from-kuwaits-oil-blazes>
- Sempels, J.-M. (1987). The coastal morphology and sedimentology of Cape Hatt peninsula. *ARCTIC*, 40(5), 10–19. <https://doi.org/10.14430/arctic1798>
- Sergy, G. A., & Blackall, P. J. (1987). Design and conclusions of the Baffin Island Oil Spill project. *ARCTIC*, 40(5), 1–9. <https://doi.org/10.14430/arctic1797>
- Serreze, M. C., Holland, M. M., & Stroeve, J. (2007). Perspectives on the Arctic's shrinking sea-ice cover. *Science*, 315(5818), 1533–1536. <https://doi.org/10.1126/science.1139426>

- Sinninghe Damste, J. S., Kock-van Dalen, A. C., & De Leeuw, J. W. (1988). Identification of long-chain isoprenoid alkylbenzenes in sediments and crude oils. *Geochimica et Cosmochimica Acta*, *52*, 2671–2677.
- Snow, N. B., Cross, W. E., Green, R. H., & Bunch, J. N. (1987). The biological setting of the BIOS site at Cape Hatt, N.W.T., Including the sampling design, methodology and baseline results for macrobenthos. *ARCTIC*, *40*(5), 80–99.
<https://doi.org/10.14430/arctic1805>
- Solli, H., Larter, S., & Douglas, A. (1980). Analysis of kerogens by pyrolysis-gas chromatography-mass spectrometry using selective ion monitoring. III. Long-chain alkylbenzenes. *Physics and Chemistry of the Earth*, *12*, 591–597.
[https://doi.org/10.1016/0079-1946\(79\)90141-1](https://doi.org/10.1016/0079-1946(79)90141-1)
- Southworth, G. R. (1979). The role of volatilization in removing polycyclic aromatic hydrocarbons from aquatic environments. *Bulletin of Environmental Contamination and Toxicology*, *21*(1), 507–514. <https://doi.org/10.1007/BF01685462>
- Stroeve, J. C., Serreze, M. C., Holland, M. M., Kay, J. E., Malanik, J., & Barrett, A. P. (2012). The Arctic's rapidly shrinking sea ice cover: A research synthesis. *Climatic Change*, *110*(3–4), 1005–1027. <https://doi.org/10.1007/s10584-011-0101-1>
- Sturm, M., Racine, C., & Tape, K. (2001). Increasing shrub abundance in the Arctic. *Nature*, *411*(6837), 546–547. <https://doi.org/10.1038/35079180>
- Tamizhdurai, P., Sakthipriya, N., Sivagami, K., Rajasekhar, B., & Nambi, I. M. (2022). Field studies on monitoring the marine oil spill bioremediation site in Chennai. *Process Safety and Environmental Protection*, *163*, 227–235. <https://doi.org/10.1016/j.psep.2022.05.005>

- Venosa, A. D., Lee, K., Suidan, M. T., Garcia-Blanco, S., Cobanli, S., Moteleb, M., Haines, J. R., Tremblay, G., & Hazelwood, M. (2002). Bioremediation and biorestitution of a crude oil-contaminated freshwater wetland on the St. Lawrence River. *Bioremediation Journal*, 6(3), 261–281. <https://doi.org/10.1080/10889860290777602>
- Venosa, A. D., Suidan, M. T., King, D., & Wrenn, B. A. (1997). Use of hopane as a conservative biomarker for monitoring the bioremediation effectiveness of crude oil contaminating a sandy beach. *Journal of Industrial Microbiology and Biotechnology*, 18(2–3), 131–139. <https://doi.org/10.1038/sj.jim.2900304>
- Venosa, A. D., Suidan, M. T., Wrenn, B. A., Strohmeier, K. L., Haines, J. R., Eberhart, B. L., King, D., & Holder, E. (1996). Bioremediation of an experimental oil spill on the shoreline of Delaware Bay. *Environmental Science & Technology*, 30(5), 1764–1775. <https://doi.org/10.1021/es950754r>
- Vergeynst, L., Christensen, J. H., Kjeldsen, K. U., Meire, L., Boone, W., Malmquist, L. M. V., & Rysgaard, S. (2019). In situ biodegradation, photooxidation and dissolution of petroleum compounds in Arctic seawater and sea ice. *Water Research*, 148, 459–468. <https://doi.org/10.1016/j.watres.2018.10.066>
- Vergeynst, L., Greer, C. W., Mosbech, A., Gustavson, K., Meire, L., Poulsen, K. G., & Christensen, J. H. (2019). Biodegradation, photo-oxidation, and dissolution of petroleum compounds in an Arctic fjord during summer. *Environmental Science & Technology*, 53(21), 12197–12206. <https://doi.org/10.1021/acs.est.9b03336>
- Wang, H., Geppert, H., Fischer, T., Wieprecht, W., & Möller, D. (2015). Determination of volatile organic and polycyclic aromatic hydrocarbons in crude oil with efficient gas-

- chromatographic methods. *Journal of Chromatographic Science*, 53(5), 647–654.
<https://doi.org/10.1093/chromsci/bmu113>
- Wang, Z., Fingas, M., Blenkinsopp, S., Sergy, G., Landriault, M., Sigouin, L., Foght, J., Semple, K., & Westlake, D. W. S. (1998). Comparison of oil composition changes due to biodegradation and physical weathering in different oils. *Journal of Chromatography A*, 809(1–2), 89–107. [https://doi.org/10.1016/S0021-9673\(98\)00166-6](https://doi.org/10.1016/S0021-9673(98)00166-6)
- Wang, Z., Fingas, M., & Page, D. S. (1999). Oil spill identification. *Journal of Chromatography A*, 843, 369–411.
- Wang, Zhendi., Fingas, Merv., & Sergy, Gary. (1995). Chemical characterization of crude oil residues from an Arctic beach by GC/MS and GC/FID. *Environmental Science & Technology*, 29(10), 2622–2631. <https://doi.org/10.1021/es00010a025>
- Ward, C. P., Sharpless, C. M., Valentine, D. L., French-McCay, D. P., Aeppli, C., White, H. K., Rodgers, R. P., Gosselin, K. M., Nelson, R. K., & Reddy, C. M. (2018). Partial photochemical oxidation was a dominant fate of *Deepwater Horizon* surface oil. *Environmental Science & Technology*, 52(4), 1797–1805.
<https://doi.org/10.1021/acs.est.7b05948>
- Wardroper, A. M. K., Hoffmann, C. F., Maxwell, J. R., Barwise, A. J. G., Goodwin, N. S., & Park, P. J. D. (1984). Crude oil biodegradation under simulated and natural conditions—II. Aromatic steroid hydrocarbons. *Organic Geochemistry*, 6, 605–617.
[https://doi.org/10.1016/0146-6380\(84\)90083-4](https://doi.org/10.1016/0146-6380(84)90083-4)
- Weickhardt, C., Moritz, F., & Grotemeyer, J. (1996). Time-of-flight mass spectrometry: State-of-the-art in chemical analysis and molecular science. *Mass Spectrometry Reviews*, 15(3),

139–162. [https://doi.org/10.1002/\(SICI\)1098-2787\(1996\)15:3<139::AID-MAS1>3.0.CO;2-J](https://doi.org/10.1002/(SICI)1098-2787(1996)15:3<139::AID-MAS1>3.0.CO;2-J)

Wells, Greg., & Huston, Chuck. (1995). High-resolution selected ion monitoring in a quadrupole ion trap mass spectrometer. *Analytical Chemistry*, 67(20), 3650–3655.

<https://doi.org/10.1021/ac00116a006>

Wenning, R. J., Robinson, H., Bock, M., Rempel-Hester, M. A., & Gardiner, W. (2018). Current practices and knowledge supporting oil spill risk assessment in the Arctic. *Marine Environmental Research*, 141, 289–304. <https://doi.org/10.1016/j.marenvres.2018.09.006>

Wentzel, A., Ellingsen, T. E., Kotlar, H.-K., Zotchev, S. B., & Throne-Holst, M. (2007). Bacterial metabolism of long-chain n-alkanes. *Applied Microbiology and Biotechnology*, 76(6), 1209–1221. <https://doi.org/10.1007/s00253-007-1119-1>

Wiens, J., Day, R., Murphy, S., & Fraker, M. (2006). Assessing cause-effect relationships in environmental accidents: Harlequin ducks and the Exxon Valdez oil spill. In *Current Ornithology* (Vol. 17, pp. 131–189). Springer.

Wong, S. F., Lim, J. S., & Dol, S. S. (2015). Crude oil emulsion: A review on formation, classification and stability of water-in-oil emulsions. *Journal of Petroleum Science and Engineering*, 135, 498–504. <https://doi.org/10.1016/j.petrol.2015.10.006>

Xiao, W., & Shao, Y. (2017). Study of kinetics mechanism of PAHs photodegradation in solution. *Procedia Earth and Planetary Science*, 17, 348–351.

<https://doi.org/10.1016/j.proeps.2016.12.088>

Yamanouchi, T., & Takata, K. (2020). Rapid change of the Arctic climate system and its global influences—Overview of GRENE Arctic climate change research project (2011–2016). *Polar Science*, 25, 100548. <https://doi.org/10.1016/j.polar.2020.100548>

- Yu, J., Jeffries, E., & Sexton, G. (1997). Atmospheric photooxidation of alkylbenzenes—I. Carbonyl product analyses. *Atmospheric Environment*, 31(15), 2261–2280.
- Yuan, S. Y., Chang, J. S., Yen, J. H., & Chang, B.-V. (2001). Biodegradation of phenanthrene in river sediment. *Chemosphere*, 43(3), 273–278. [https://doi.org/10.1016/S0045-6535\(00\)00139-9](https://doi.org/10.1016/S0045-6535(00)00139-9)
- Zeigler, C., MacNamara, K., Wang, Z., & Robbat, A. (2008). Total alkylated polycyclic aromatic hydrocarbon characterization and quantitative comparison of selected ion monitoring versus full scan gas chromatography/mass spectrometry based on spectral deconvolution. *Journal of Chromatography A*, 1205(1–2), 109–116. <https://doi.org/10.1016/j.chroma.2008.07.086>
- Zhang, X., He, J., Zhang, J., Polyakov, I., Gerdes, R., Inoue, J., & Wu, P. (2013). Enhanced poleward moisture transport and amplified northern high-latitude wetting trend. *Nature Climate Change*, 3(1), 47–51. <https://doi.org/10.1038/nclimate1631>
- Zhang, Y., Lu, Y., Xu, J., Yu, T., & Zhao, W. (2011). Spatial distribution of polycyclic aromatic hydrocarbons from Lake Taihu, China. *Bulletin of Environmental Contamination and Toxicology*, 87(1), 80–85. <https://doi.org/10.1007/s00128-011-0292-1>

Chapter 2: The recalcitrance and potential toxicity of polycyclic aromatic hydrocarbon residues within beach sediments at the Baffin Island Oil Spill (BIOS) site, nearly forty years later

Blake E. Hunnie^a, Lars Schreiber^b, Charles W. Greer^{b,c}, Gary A. Stern^a

hunnieb@myumanitoba.ca, lars.schreiber@cnrc-nrc.gc.ca, Charles.greer@cnrc-nrc.gc.ca,

gary.stern@umanitoba.ca

^aUniversity of Manitoba, 125 Dysart Rd Winnipeg, MB R3T 2N2

^bNational Research Council Canada, 6100 Royalmount Ave Montreal, QC H4P 2R2

^cMcGill University, Department of Natural Resource Sciences, 21111 Lakeshore Rd Ste-Anne-de-Bellevue, QC, H9X 3V9

Corresponding Author:

Gary Stern (Gary.stern@umanitoba.ca) University of Manitoba, 125 Dysart Rd, Winnipeg, MB, Canada. R3T 2N2

Contributions of authors

Blake Hunnie: Methodology, Validation, Formal Analysis, Investigation, Resources, Data Curation, Writing – Original Draft, Writing – Review & Editing, Visualization, Project Administration

Lars Schreiber: Conceptualization, Methodology, Investigation, Resources, Data Curation, Visualization, Supervision, Project Administration

Charles Greer: Funding acquisition, Writing – Review & Editing, Conceptualization, Methodology, Resources,

Gary Stern: Conceptualization, Methodology, Formal Analysis, Resources, Writing – Original Draft, Supervision, Project Administration

Abstract

The Arctic is a unique environment characterized by extreme conditions, including daylight patterns, sea ice cover, and some of the lowest temperatures on Earth. Such characteristics in tandem present challenges when extrapolating information from oil spill research within warmer, more temperate regions. Consequently, oil spill studies must be conducted within the Arctic to yield accurate and reliable results. Sites of the Baffin Island Oil Spill (BIOS) project (Cape Hatt, Baffin Island, Canadian Arctic) were revisited nearly 40 years after the original oil application to provide long-term monitoring data for Arctic oil spill research. Surface and subsurface sediment samples were collected from the intertidal zone of the 1981 nearshore oil spill experiment (Bay 11), from 1980 supratidal control plots (Crude Oil Point) and 1982 supratidal treatment plots (Bay 106). Samples were analyzed for Polycyclic Aromatic Hydrocarbons (PAHs) and alkylated homologues via Gas Chromatography – Mass Spectrometry (GC-MS). Our results suggest that total mean concentrations of all measured PAHs range from 0.049 – 14 mg/kg, whereas total mean concentrations of the 16 US EPA priority PAHs range from 0.02 – 2.1 mg/kg. The relative proportions of individual PAHs were compared between sampling sites and with the original technical mixture. Where available, percent loss of individual PAHs was compared with data from samples collected at the BIOS site, in 2001. All three sites featured samples where concentrations of various priority PAHs exceeded the established Interim Marine Sediment Quality Guidelines. All supratidal samples contained potentially toxic levels of PAHs. Even after nearly four decades of weathering, the recalcitrant crude oil residues remain a potential hazard for the native organisms. Continued monitoring of this unique study site is crucial for establishing a timeline for oil degradation, and to observe a reduction in toxicity over time.

Keywords: The Arctic, Oil Spill, Persistence, Weathering, Long-term Monitoring, BIOS project

Introduction

There is an increasing awareness and concern regarding anthropogenic impacts on global climate change. Over the past 30 years, the Arctic has warmed more than any other region on earth, resulting in an acceleration of sea-ice melt and a shift toward annual ice types. For the entire Arctic, the length of the melt season has increased by 20 days over the last 30 years (Arctic Monitoring and Assessment Programme, 2017; Markus et al., 2009). These progressively longer open-water seasons have given rise to a 75 % increase in Arctic shipping traffic over the past decade (Dawson et al., 2017, 2018; Pizzolato et al., 2014, 2016). This, in combination with a rising interest in oil exploration within the Arctic, increases the risk of a fuel or crude oil spill into the marine Arctic environment (Arctic Monitoring and Assessment Programme, 2010a; Harsem et al., 2011). Oil spill response measures can fundamentally affect the environmental health of the marine ecosystem (Dawson et al., 2018). It became clear that a field study approach was required in ascertaining pertinent information in a timely fashion, regarding Arctic oil spill research (Sergy & Blackall, 1987). The idea behind sacrificing the environmental health of a relatively small, pristine Arctic region to make large advances in oil spill research was what led to the Baffin Island Oil Spill (BIOS) project. In 1979, Cape Hatt, Baffin Island in the Canadian Arctic, was chosen as the location for the project to be performed (Sergy & Blackall, 1987). Important components of the BIOS project included a beached, surface oil slick, and oiled test plot experiments. These were monitored to compare the oil's short, and long-term chemical and physical fate when left subject to natural attenuation processes in the Arctic (Sergy & Blackall, 1987).

One of the top priorities prior to carrying out the simulated oil spills in the original experiment was to establish a database of pre-existing hydrocarbons within the sediments, water, and tissues of marine organisms at the study locations, as this data is often missing when studying accidental oil spills (Cretney et al., 1987b). In all three cases, total concentrations of polycyclic aromatic hydrocarbons (PAHs) were detected in the low to sub mg/kg concentration range (Cretney, 1987; Cretney et al., 1987a, 1987b). The PAH concentrations in marine and riverine sediments in other Arctic regions have also been reported in the low to sub mg/kg range (Foster et al., 2015; Yunker et al., 2002). Since the PAH concentrations at the BIOS site were as low as what might be found anywhere within the Arctic, it was confirmed that the designated locations were well suited to carry out the planned oil spills (Cretney, 1987; Cretney et al., 1987a, 1987b).

The crude oil chosen for the main experiments at the BIOS site was a medium weight Venezuelan Lagomedio, which was artificially weathered 8 % by volume *via* evaporation to simulate the natural degradation processes anticipated when oil is first stranded (Sergy & Blackall, 1987). The BIOS site hosted several oiled sampling stations within two main areas: Ragged Channel and the Z-lagoon (Figure 2.1). This current study focuses on only a subset of the original BIOS stations, mainly due to time constraints during sampling. Bay 11, an open, moderately exposed beach of approximately 400 m in length found on the eastern side of the Ragged Channel (E. H. Owens & Robson, 1987) was one of the chosen sites for the 1981 nearshore oil spill experiment. At this site, an experimentally controlled release of 15 m³ of crude oil was added directly to the surface water. The stranded oil was left to encroach onto the intertidal zone of the beach, then attenuate under natural conditions (E. Owens et al., 2002). Crude Oil Point was chosen as the oiled control site for the 1980 shoreline cleanup

countermeasure experiment, which largely involved applications of the pure weathered oil and a 50 % mixture of oil and water to 20-40 m² test plots dug within beach sediments (E. H. Owens, Robson, et al., 1987; Sergy & Blackall, 1987). This site is located near the entrance of the Z-lagoon (Figure 2.1). The T1 (weathered crude) and T2 (emulsified oil) plots were created in 1980 as backshore control plots, positioned above the normal level of tidal and wave action with the expectation that they would not be affected by marine processes (E. H. Owens, Robson, et al., 1987; E. H. Owens & Robson, 1987). Bay 106 is a well-sheltered area in the southern end of the Z-lagoon (Figure 2.1). The samples included from Bay 106 in the current study are those from the four plots created for the 1982 backshore (supratidal) mixing experiment (E. H. Owens, Robson, et al., 1987). The plots involved were separated by oil type IMC (weathered crude Lagomedio oil) and IME (emulsified Lagomedio crude), then again by treatment type c (tilled) and e (no mixing) (E. H. Owens, Robson, et al., 1987). To follow up on the results acquired before and after the oil spills, the BIOS site has been revisited on a few occasions to record the quantities of remaining oil and the composition of recalcitrant oil residues. Until now, this was done most recently in 2001, roughly twenty years after the original experiments were conducted (E. Owens et al., 2002; Prince et al., 2002).

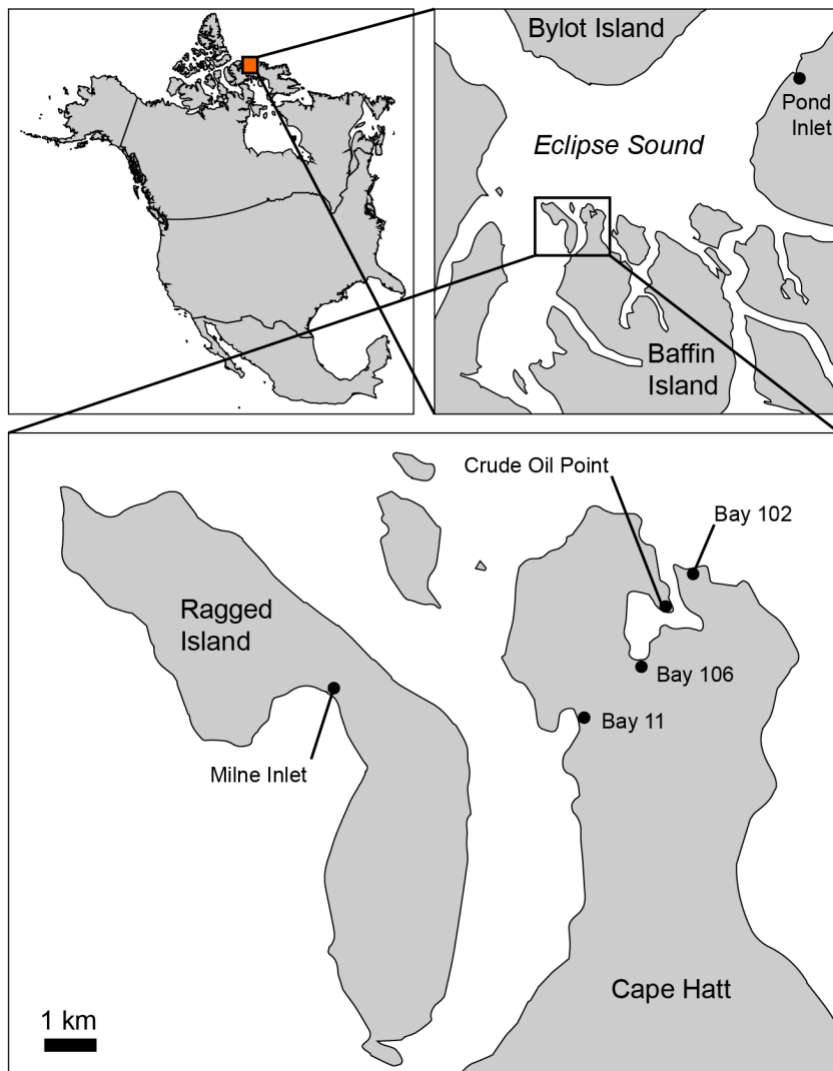


Figure 2.1. Location of the BIOS site in Cape Hatt, Baffin Island, NU. Sites visited during the 2019 sampling regime are shown. Oiled sampling stations include Crude Oil Point and Bay 106 within Z-lagoon, and Bay 11 in the Ragged Channel. Field blanks were collected from Bay 102 and Milne Inlet within Z-lagoon and Ragged Island, respectively.

PAHs are organic compounds of high interest, especially with respect to their ecotoxicological properties. They are found in crude oil (petrogenic), and are mainly produced from combustion of fossil fuels and coal (pyrogenic) (Cerniglia, 1993; Saha et al., 2012; Samanta et al., 2002). In this work, light, medium, and heavy molecular weight (MW) PAHs are defined as PAHs composed of 2-3 rings, 4 rings, and 5-6 rings, respectively. PAHs are well-

known for their persistence in the environment, as well as their potential for toxic, mutagenic, and carcinogenic effects (Cerniglia, 1993; Saha et al., 2012; Samanta et al., 2002). Due to these hazardous properties, sixteen PAHs of particular concern have been listed as priority pollutants by the United States Environment Protection Agency (US EPA). Toxic Equivalency Factors (TEFs) have been established (Nisbet & LaGoy, 1992) to assign the degree of carcinogenicity to the 16 US EPA priority PAHs. Benzo[a]pyrene, one of these priority PAHs is a well-studied compound in cancer research, known for having the greatest measure of carcinogenicity among all PAHs, (Collins et al., 1991; B. M. Lee & Shim, 2007; Saffiotti et al., 1972) and therefore serves as a surrogate with a TEF value of 1. Subsequently, other PAHs are assigned a TEF based on their relative potency to Benzo[a]pyrene (Nisbet & LaGoy, 1992). Toxic Equivalency Quotients (TEQs) are a representation of potential toxicity, either for individual compounds or total PAHs (Fisher et al., 2011). The TEQ system was designed mainly as a means of reporting toxicity of mixtures to assist in regulatory efforts and risk assessment (Bhavsar et al., 2008; Choudhury et al., 2000). From a toxicological point of view, the group of compounds must operate under a similar mode of action for the TEQ system to be applicable (Choudhury et al., 2000). The US EPA priority PAHs share common toxicological characteristics, and can therefore adopt the TEQ system (Tongo et al., 2017). Sediment Quality Guidelines (SQGs) have been established by the Canadian Council of Ministers of the Environment (CCME) to denote the acceptable limits of individual PAH concentrations in both freshwater and marine sediments, with the goal of protecting aquatic organisms (Canadian Council of Ministers of the Environment, 2001). To determine whether a considerable risk for toxicity remains, these limits will be compared with the concentrations found within the samples collected from the BIOS sites.

It is critically important to ensure continued, long-term monitoring of experiments such as this to educate and inform policymakers and reduce the potential for catastrophic errors regarding oil spills in an Arctic setting. It is also becoming incredibly difficult to obtain permission to begin conducting new oil spill-related field studies. As such, progressing ongoing research should be a top priority to further our general knowledge surrounding the implications of Arctic oil spills. A significant gap in currently available literature exists, concerning the assessment of PAH concentrations, composition, and ecotoxicological characteristics at the BIOS site. Many previous chemical analyses of samples collected from the BIOS site provide bulk values, rather than individual PAH concentrations. Understanding how individual PAH concentrations change over time in the global Arctic is essential towards building a framework for further ecotoxicological research, since PAHs contribute a significant proportion of crude oil's overall toxicity (Carls et al., 1999; Ramachandran et al., 2004). Such opportunities include the design of toxicity tests to address the deleterious effects of PAH concentrations measured nearly forty years post-spill on native Arctic organisms. Additionally, we are currently unaware of any other studies examining the chemical and toxicological fate of PAHs within crude oil, conducted on a similar time scale within the Arctic. Work has been done to observe the long-term fate and effects of oil spills in other geographical regions, such as the Exxon Valdez oil spill (EVOS) within the Prince William Sound (Boehm et al., 2004; Payne et al., 2008), the Metula oil spill within the Strait of Magellan (Z. Wang et al., 2001), and the Deepwater Horizon spill within the Gulf of Mexico (Yin et al., 2015); however, the natural attenuation of crude oil is deeply affected by environmental parameters such as the presence of sea ice, temperature, sunlight, percent organic matter, and indigenous microbial communities (Cerniglia, 1993; Ferguson et al., 2020). Despite rough similarities between environmental conditions and time scales at the BIOS

and the EVOS, a heavier emphasis is placed on PAH concentrations in mussel tissues at the EVOS site, rather than sediments (Boehm et al., 2004; Payne et al., 2008, 2021). To properly characterize the extreme environmental conditions of the Arctic, direct monitoring within this region is necessary. This work serves to begin establishing a coherent timeline regarding the degradation of PAHs found in beach sediments, and their respective potential toxicities, within an Arctic setting.

Materials and Methods

Sample collection

Cape Hatt (Baffin Island, Nunavut, Canada) was chosen for the original study because it is a rarely visited, remote location with pristine, natural conditions (Figure 2.1) (Cretney, 1987; Cretney et al., 1987a, 1987b). Consequently, long-term monitoring for effects and outcomes of the BIOS project poses both logistical and financial challenges. However, two full days of the CCGS Amundsen 2019 expedition were reserved for revisiting the BIOS site. The sampling sites were accessed with a small barge, operated by the Canadian Coast Guard. Oiled BIOS plots were identified and documented using ground and drone photography, then their precise locations were recorded by Global Positioning System (GPS) (Table 2.S1). Most of the original sampling sites could be identified based on metal stakes remaining from the original experiments. Bay 102 is a sampling station located at the mouth of the Z-lagoon (Figure 2.1), and was established as intertidal oiled, control plots in 1980 (E. H. Owens, Robson, et al., 1987). The metal stakes from this site could not be found, so based on the available coordinates, sediments were collected from an area adjacent to Bay 102, and were designated as field blanks. Additional field blanks were

collected from Milne Inlet, Ragged Island (Figure 2.1), which was scouted and sampled from during the 2019 CCGS Amundsen expedition. This site was untouched by any potential contamination from the various BIOS experiments.

Bulk surface (0-2 cm) and sub-surface (5-10 cm) sediment samples from Bays 106 and 102 were collected on August 17, 2019 (Figure 2.1). The remaining samples were collected from Bay 11, Milne Inlet and Crude Oil Point on August 18, 2019 (Figure 2.1). All sediment samples were obtained using a garden trowel, then collected within sterile WhirlPak bags. In total, 86 samples were collected, including field blanks and replicates (Table 2.S1). For the sake of maintaining a logical system of sample nomenclature consistently into the future, we devised our sample nomenclature based on plot designations made during the original experimental designs (E. H. Owens & Robson, 1987). For clarity, the sample names of this study consist of a prefix that indicates the sampling location and a suffix that indicates the sampled depth horizon. Used sample prefixes include: T1 and T2 for the Crude Oil Point test plots; IMC-c, IMC-e, IME-c and IME-e for the Bay 106 test plots; B11-BS for Bay 11 backshore sediments; and finally, B11-I for Bay 11 intertidal sediments (E. H. Owens & Robson, 1987). The suffixes 0-2 and 5-10 indicate the surface (0-2 cm sediment depth) and subsurface (5-10 cm depth) sediment horizons, respectively. These collected samples were stored away from direct sunlight at ambient temperature for 1.5-9.0 hours until they could be transported onto the CCGS Amundsen and stored at 4.0 °C until demobilization in Quebec City on September 5, 2019. All samples were shipped in a -20 °C delivery truck from Quebec City, QC to Winnipeg, MB (Canada). Upon delivery to the University of Manitoba, the samples were immediately stored in -20 °C chest freezers at the Centre for Earth and Observation Science (CEOS).

Sample preparation

Samples were subjected to hydrocarbon fractionation extractions, following standardized procedures (Asihene, 2019) with minor alterations (Section S1). Samples were spiked with 4.0-10 μ L Cambridge Isotope Laboratories (CIL) PAH surrogate standard mixture ES-5164 (16 compounds; prepared to 5.0 ppm; Table 2.S2) (Cambridge Isotope Laboratories, 2016) to monitor PAH recovery. 2-Fluorobiphenyl was used as an internal standard for PAH quantification.

A 20 mL vial of the original technical mixture, the Venezuelan Lagomedio crude oil, was provided to use for this study by Environment and Climate Change Canada on November 13th, 2019. This sample vial was stored at room temperature. The Lagomedio crude oil was prepared for analysis by series dilution in methylene chloride. The technical mixture was treated with the same CIL PAH surrogates standard mixture and 2-Fluorobiphenyl internal standard.

Depending on the number of samples being extracted (≤ 11), one or two laboratory duplicates were included in each batch. Average reproducibility of individual PAH concentrations within duplicates was 82 %. Standard Reference Materials (SRM) 1941b and 1944 were chosen for this experiment (Gonzalez & Choquette, 2017; Gonzalez & Watters, 2015). A single SRM was added to each batch of samples and was subject to the same extraction process as all samples and duplicates. Average reproducibility of individual PAH concentrations within SRMs was 88 %. An additional measure taken to account for quality assurance of analysis was the inclusion of lab blanks. The used material was pre-washed sand that was baked at 550 $^{\circ}$ C for eight hours and stored in a desiccator. In a similar fashion to the laboratory duplicates, laboratory blanks were included in each sample batch. Concentrations of PAHs detected within

the lab blanks were subtracted from sample compound concentrations to account for any contamination during the extractions.

PAH Analysis

The analysis of a suite of 36 PAHs (Table 2.S3) was quantified using an Agilent 7010B Triple Quadrupole GC-MS system, in the Multiple Reaction Monitoring (MRM) mode. The MRM method was based on parameters included in Saltymakova et al. (2020) with minor adjustments (Table 2.S4). A list of the ion transitions can be found in Table 2.S5. Analyses were also conducted to detect n-alkanes, as well as various biomarkers, the results of which will be presented in a subsequent manuscript. Tunes were performed and validated, prior to each batch of samples analyzed on the GC-MS system. Instrument quantitation limits can be found in table 2.S6. Qualitative and quantitative analyses of the PAH residues were executed in the Agilent MassHunter Qualitative Analysis B.07.00 and the Agilent MassHunter Quantitative Analysis (for QQQ) softwares, respectively. Due to highly variable PAH concentrations between samples collected from different sites, two ranges of calibration curves were used for PAH quantification. Calibration standards were produced as a mixture of three standards: RESTEK SV calibration mix #5 31011, Chiron AS PAH/Dibenzothiophenes mixture S-4406-200-T, and the abovementioned CIL PAH surrogate standard mixture ES-5164. A 9-point calibration curve with a $1/x$ weighted R^2 value of ≥ 0.95 for all compounds, ranging from 0.5-135 ng/mL was applied to all samples. Samples with compound concentrations exceeding the quantification limit were quantified using a second calibration curve, with a range of 67.5-1080 ng/mL. This was a 5-point calibration curve with a $1/x$ weighted R^2 value of ≥ 0.97 for all compounds. A signal-to-noise ratio limit of 5.0 was set for every compound. Those flagged below the limit were scrutinized

and either accepted or rejected, based on the presence of a discernable peak within the chromatogram.

Toxic Equivalency Quotients

The TEF values for each US EPA priority PAH presented in Nisbet and LaGoy (1992) were multiplied by the concentrations of their respective PAH to obtain TEQ values (eq1):

$$(1) TEQ_x = TEF_x * [x]$$

Where x represents any individual US EPA PAH.

Total Carbon and Total Inorganic Carbon Analysis

Total Organic Carbon (TOC) values are important when disseminating information pertaining to TEQs as these values tend to display high correlations, and thus TEQ results are often normalized to their respective percentage of TOC (Kanematsu et al., 2006; Wu et al., 1997). TOC data was generated by subtraction of Total Inorganic Carbon (TIC) values from Total Carbon (TC) values. Sediment subsamples that were previously freeze-dried and ground for hydrocarbon extractions were subjected to both TIC and TC analyses. TIC and TC analyses were carried out using a Carbon/Sulfur Analyzer (Helios, Eltra™) and a 4010 Elemental Analyzer (Costech™), coupled with a Delta V Plus Isotope-Ratio Mass-Spectrometer (IRMS; Thermo Finnigan™) respectively. Further details on these analyses are presented in the supplemental information section S2.

Principal Component Analysis

For statistical analyses, a Principal Component Analysis (PCA) was carried out in SYSTAT SigmaStat V4.0. Mean values were produced from replicates of each sample, then incorporated for further data manipulation to fit PCA requirements as follows: Non-detected PAH concentration values were replaced with the minimum detection values for respective compounds. Compound concentrations were then converted to percentages of the total PAH concentration for each sample. Finally, values were log-transformed, using log base 10. Centering of the data was not required, as it was done automatically through SigmaStat. Principle components were calculated based on a 36x36 covariance matrix, consisting of the quantified compounds.

Results and Discussion

Σ 16PAH and Σ 36PAH concentrations

Despite nearly forty years of natural attenuation, considerable amounts of oil remain in the collected sediments (Table 2.1). Total PAH (Σ 36PAH) concentrations and total US EPA PAH (Σ 16PAH) concentrations vary mainly between samples from different sites and tidal zones, rather than from within sites or sampling depth. The recalcitrance of the oil appears to be mainly dependent on the extent of interaction with marine processes such as wave and tidal action, and physical removal.

Bay 11

Previous surveys of the BIOS site indicate that most of the initially spilled oil at Bay 11, the site of the surface water oil slick, had been degraded or removed through tidal and wave action to a higher degree than other sites (E. Owens et al., 2002; E. H. Owens, Harper, et al., 1987; E. H. Owens, Robson, et al., 1987; Prince et al., 2002; Wang et al., 1995). The $\Sigma 36\text{PAH}$ and $\Sigma 16\text{PAH}$ concentrations listed in Table 2.1 agree with this conclusion. The lowest $\Sigma 36\text{PAH}$ concentrations were those collected from the intertidal zone. The $\Sigma 36\text{PAH}$ concentrations within the surface samples were about half those within the subsurface. $\Sigma 36\text{PAH}$ concentration values in the B11-I surface and subsurface samples represent $< 0.0020\%$ and $< 0.0040\%$ of the PAHs found within the technical mixture, respectively. The back-beach sediments at this site were not intentionally oiled during the BIOS project, as the stranded oil only encroached into the intertidal zone. However, increased levels of oil-degrading bacteria in these sediments have been previously reported and was attributed to the involuntary oiling due to logistic activities associated with the 1981 nearshore oil spill of the BIOS project (Boehm, 1983). Consequently, backshore sediments (B11-BS) were collected from the few accessible spaces within the supratidal zone and analyzed in an identical fashion to the other oiled samples. The $\Sigma 36\text{PAH}$ concentrations within the backshore replicates (B11-BS) followed the same pattern between depth horizons as those from the intertidal area (Table 2.1). Interestingly, the $\Sigma 16\text{PAH}$ concentrations decrease with increased sample depth in the backshore sediments but increase with depth in the intertidal zone (Table 2.1). Two-factor ANOVA exposed statistically significant differences in $\Sigma 36\text{PAH}$ concentrations between tidal zone ($P = 0.042$), sample depth ($P = 0.00052$), and the interaction between the two variables ($P = 0.0043$).

Crude Oil Point

The acquired samples from Crude Oil Point are the least degraded amongst all the samples from the BIOS site, exhibiting the highest $\Sigma 36\text{PAH}$ concentrations, ranging from 7.0 – 14 mg/kg (Table 2.1). During the 2019 sampling, sediments of the T1 and T2 plots were visibly still contaminated with dark oil compared to sediments outside the plot areas. Since these two plots were located above any potential tidal action, this wasn't an unexpected observation. Both the oiled crude and emulsified plots show consistent $\Sigma 36\text{PAH}$ concentrations, as well as $\Sigma 16\text{PAH}$ concentrations (Table 2.1). Two-way ANOVA determined that there were no statistically significant differences between oil type ($P = 0.24$), nor sample depth ($P = 0.15$), and there were no significant interactions between the two variables ($P = 0.076$) for $\Sigma 36\text{PAH}$ concentrations.

Bay 106

The $\Sigma 36\text{PAH}$ concentrations varied between samples but fell within a 20-fold range and were 0.4 – 8 mg/kg at the time of sampling, whereas the $\Sigma 16\text{PAH}$ concentrations fell within a 10-fold range (Table 2.1). Based on two-way ANOVA, there is a statistically significant difference between treatment types ($P = 0.036$), but there are no statistically significant differences between sample depths ($P = 0.46$), nor interactions between oil type and sample depth ($P = 0.39$), regarding $\Sigma 36\text{PAH}$ concentrations. Nearly forty years of freeze-thaw cycles, ice scouring, evaporation, dissolution, photooxidation, and microbial degradation in combination with different oil types, mixing, and sample depths (Prince et al., 2003; Sempels, 1987) have made interpretations difficult to attribute cause to any specific variable.

Table 2.1. Total PAH concentrations of oiled samples at the BIOS site and the technical mixture.

Sample ID ^a	Sample Depth ^b	Total PAHs (Σ 36PAH)		16 Priority PAHs (Σ 16PAH)		N ^c	Site
		(mg/kg)		(mg/kg)			
		Mean (std. dev)	Range	Mean (std. dev)	Range		
Technical							
Mixture	-	3200 (48)	3200 - 3300	620 (14)	600 - 630	2	-
IMC-c ^d	s	8.0 (5.6)	0.77 - 14	1.2 (0.78)	0.22 - 2.4	6	Bay 106
	ss	4.3 (1.6)	1.6 - 6.4	0.61 (0.31)	0.14 - 0.97	5	Bay 106
IMC-e ^d	s	0.43 (0.43)	0.086 - 1.0	0.11 (0.087)	0.024 - 0.23	3	Bay 106
	ss	0.91 (1.0)	0.081 - 2.4	0.36 (0.39)	0.028 - 0.91	3	Bay 106
IME-c ^d	s	3.7 (5.1)	0.24 - 13	0.79 (0.79)	0.091 - 2.1	4	Bay 106
	ss	1.5 (1.2)	0.20 - 3.1	0.59 (0.52)	0.078 - 1.3	3	Bay 106
IME-e ^d	s	0.53 (0.25)	0.34 - 0.89	0.26 (0.13)	0.16 - 0.44	3	Bay 106
	ss	5.1 (3.4)	0.89 - 9.5	0.81 (0.55)	0.33 - 1.6	3	Bay 106
B11-BS ^d	s	0.93 (0.40)	0.46 - 1.4	0.34 (0.16)	0.13 - 0.52	3	Bay 11
	ss	0.19 (0.056)	0.14 - 0.25	0.081 (0.026)	0.056 - 0.11	2	Bay 11
T1 ^d	s	7.1 (1.6)	6.3 - 9.4	1.3 (0.45)	0.74 - 1.8	3	Crude Oil Point
	ss	14 (1.8)	12 - 16	2.1 (0.64)	1.5 - 2.8	2	Crude Oil Point
T2 ^d	s	13 (0.17)	13 - 13	2.1 (0.11)	2.0 - 2.2	2	Crude Oil Point
	ss	12 (1.9)	10 - 14	1.8 (0.060)	1.7 - 1.8	2	Crude Oil Point
B11-I ^e	s	0.049 (0.033)	0.010 - 0.13	0.020 (0.015)	0.0032 - 0.053	11	Bay 11
	ss	0.083 (0.032)	0.044 - 0.15	0.039 (0.017)	0.015 - 0.063	8	Bay 11

^aTotal mean PAH concentrations of control samples = 0.11 mg/kg (std. dev = 0.085, n = 39)

^bs = surface (0-2cm), ss = subsurface (5-10cm)

^cnumber of replicates analyzed per sample

^dCollected from the supratidal zone

^eCollected from the upper intertidal zone

Oil Composition and Weathering

Not surprisingly, over the course of the last four decades extensive weathering had occurred in all samples evident by the changes in PAH compositions amongst the collected samples. Exposure to weathering mechanisms differed between sites (Figures 2.2, 2.3, and 2.4). While difficult to quantify, Crude Oil Point, for example, would have been exposed to longer periods of solar radiation than the ice-covered intertidal sediments at Bay 11, resulting in increased photooxidation and volatilization. Contrarily, intertidal plots were subjected to much greater physical removal processes through wave action, and biodegradation. Of the compounds included in this dataset, Naphthalene and its 1C, 2C, and 3C homologues account for 56 % of the overall PAH profile in the technical mixture. In contrast, the same group of compounds in the 2019 BIOS samples contributed between 1.3 and 12 % towards the $\Sigma 36\text{PAH}$ concentration. It is important to consider that despite the percent proportions that each PAH contribute to their total concentration, the $\Sigma 36\text{PAH}$ concentrations between the technical mixture, the field blanks, and the oiled samples differ greatly (Table 2.1).

Bay 11

The PAH compositions of the oil found within the samples from Bay 11 follow a loose uniformity across depth and tidal zone (Figure 2.2). Both the B11-I and B11-BS profiles exhibit a shift from high abundance of two-ringed PAHs in the technical mixture to larger relative proportions of the three-ringed PAHs and some of their alkylated congeners (Figure 2.2). Additionally, the intertidal sediments contain a greater abundance of medium and heavy MW PAHs including Chrysene, Triphenylene, 1-Methylchrysene, 6-Ethylchrysene

Benzo[j]fluoranthene, Benzo[a]pyrene, Perylene, Dibenz[a,h]anthracene, and Benz[g,h,i]perylene, compared to the other samples from Bay 11 (Figure 2.2). The dissolution of PAHs is expected to readily occur within the intertidal sediments. PAH solubility has been observed to decrease with increasing MW, as well as with increasing alkylation (Saltymakova et al., 2020). This trend is especially highlighted when observing the relative percentages of Dibenzothiophene and its alkylated counterparts, as well as for Phenanthrene and its mono and dimethylated congeners (Figure 2.2). The effects of dissolution are present, but less robust when considering Chrysene, 1-Methylchrysene, and 6-Ethylchrysene. The percent organic carbon found within sediments is a key driver of PAH adsorption, as well as the hydrophobicity of the individual PAHs (Ahangar, 2010). The TOC content of the intertidal sediments is the lowest recorded across all the samples collected from the BIOS site (Table 2.2). This observation supports the conclusion that the dominant force of oil degradation occurring in the intertidal sediments is physical removal through tidal action and dissolution, as the 2-ringed PAHs are unlikely to adsorb to sediment particles; conversely, medium and heavy MW PAHs will exhibit a higher propensity to remain sorbed to any available organic matter (Ahangar, 2010).

(Figure 2.2), and even more so than the technical mixture (Figure 2.3). Despite these samples containing the highest recorded concentrations of total PAHs from the BIOS site in 2019, the relative concentrations of the 2-ringed PAHs which contribute to over half of the overall $\Sigma 36$ PAH concentrations within the technical mixture are negligible within these plots, likely due to volatilization (Figure 2.3) which targets smaller ringed species more readily than larger ones. Measured concentrations of Phenanthrenes and Dibenzothiophenes increased with increasing alkylation, which is indicative of biodegradation, rather than photooxidation which was expected to be the dominant force of degradation occurring at this site (Prince et al., 2002, 2003). In this context, no distinct pattern of weathering processes was observed amongst Chrysene and its alkylated congeners; however, Chrysene was the only PAH within the analyzed suite of compounds that had methylated and ethylated species, rather than mono and dimethylated species. When observing the changes solely between the unsubstituted Chrysene and 1-Methylchrysene, the trend shown in the Phenanthrenes and Dibenzothiophenes emerges within the subsurface samples (Figure 2.3). There is no contact with the marine interface at these plots. Therefore, there is no opportunity for dissolution or physical removal of oil through tidal action, and the effects of microbial degradation would be only attributable to the microorganisms found within the sediments.

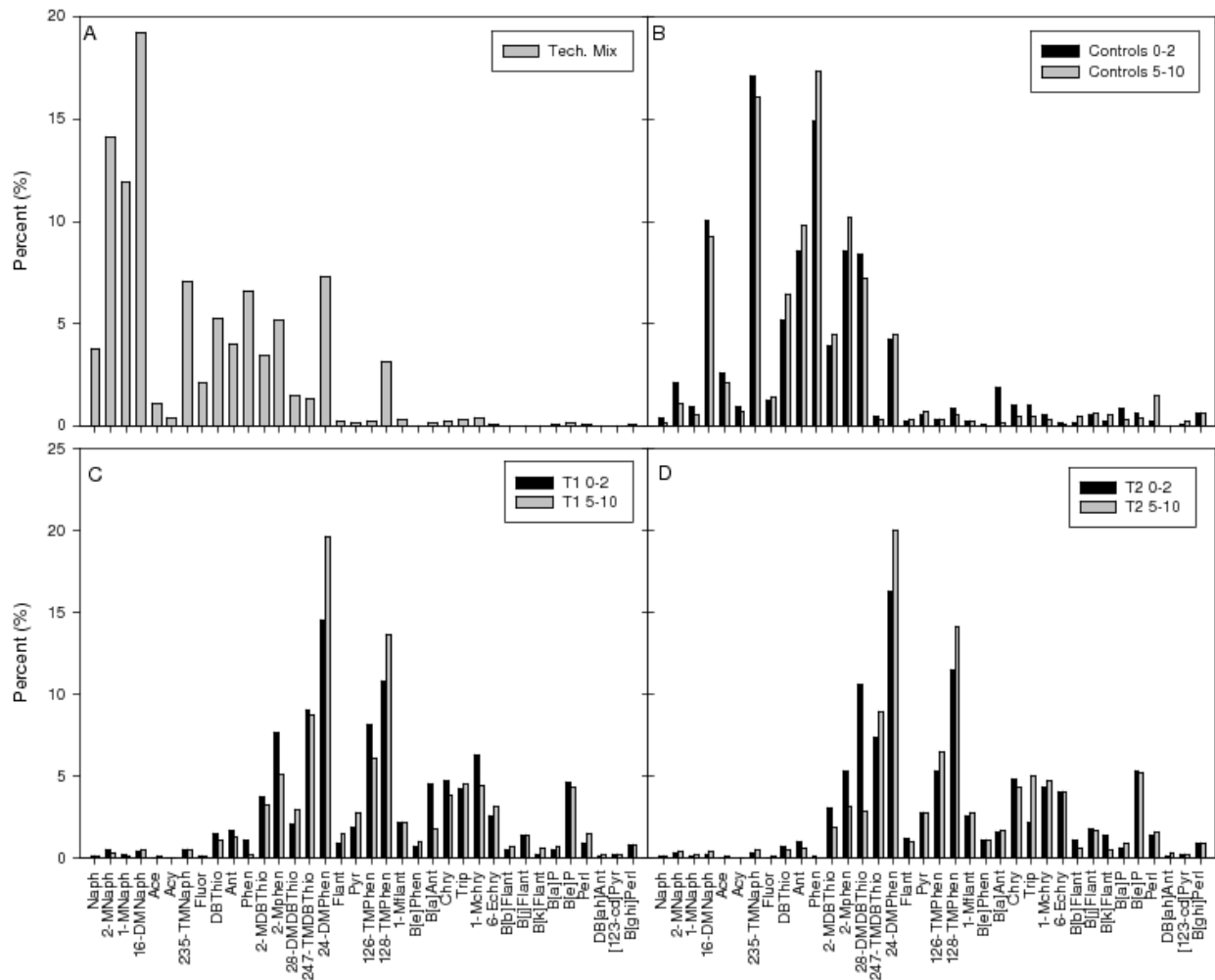


Figure 2.3. PAH profiles shown as percentages of each analyzed PAH relative to their total abundance for (A) the technical mixture, (B) the field blanks, (C) the weathered crude oil plot from Crude Oil Point, and (D) the emulsified oil plot from Crude Oil Point.

Bay 106

This site was part of the 1982 BIOS mixing experiment, therefore the samples collected from Bay 106 differ by oil type (crude (IMC) vs. emulsion (IME)), treatment type (mixing (c) vs. control (e)) and depth (surface (0-2cm) vs. subsurface (5-10cm)) (E. H. Owens & Robson, 1987). As seen in the samples from both Bay 11 and Crude Oil Point, the relative concentrations of Naphthalene and its methylated species are negligible compared to those found within the

technical mixture (Figure 2.4). The degradation patterns of Phenanthrene and its alkylated forms are similar to what is observed in the samples from Crude Oil Point, which are in agreement with expected outcomes of biodegradation (Prince et al., 2002) for all samples except IME-e 0-2cm, which had roughly equivalent concentrations of trimethylated Phenanthrenes to the unsubstituted form (Figure 2.4). A similar theme was observed for the degradation of Dibenzothiophenes, although these values were less consistent with the expected outcomes of biodegradation; however, it is very likely that many degradation processes are occurring at once. The plots of this experiment are located on the berm of the beach, but receive infrequent tidal inundation, which could contribute to influx of hydrocarbon-degrading microbes, as well as the dissolution and physical removal of light MW PAHs. As mentioned earlier, it is difficult to tease concrete conclusions from the observations, since these plots had been oiled nearly forty years ago and have since incurred numerous sources of degradation and were designed with numerous experimental variables. In general, the PAH compositions within the Bay 106 sediments more closely resemble those from Crude Oil Point than from Bay 11; however, there is little consistency between experimental conditions for samples from different sampling stations at the BIOS site, which impedes the opportunity for simple data comparison.

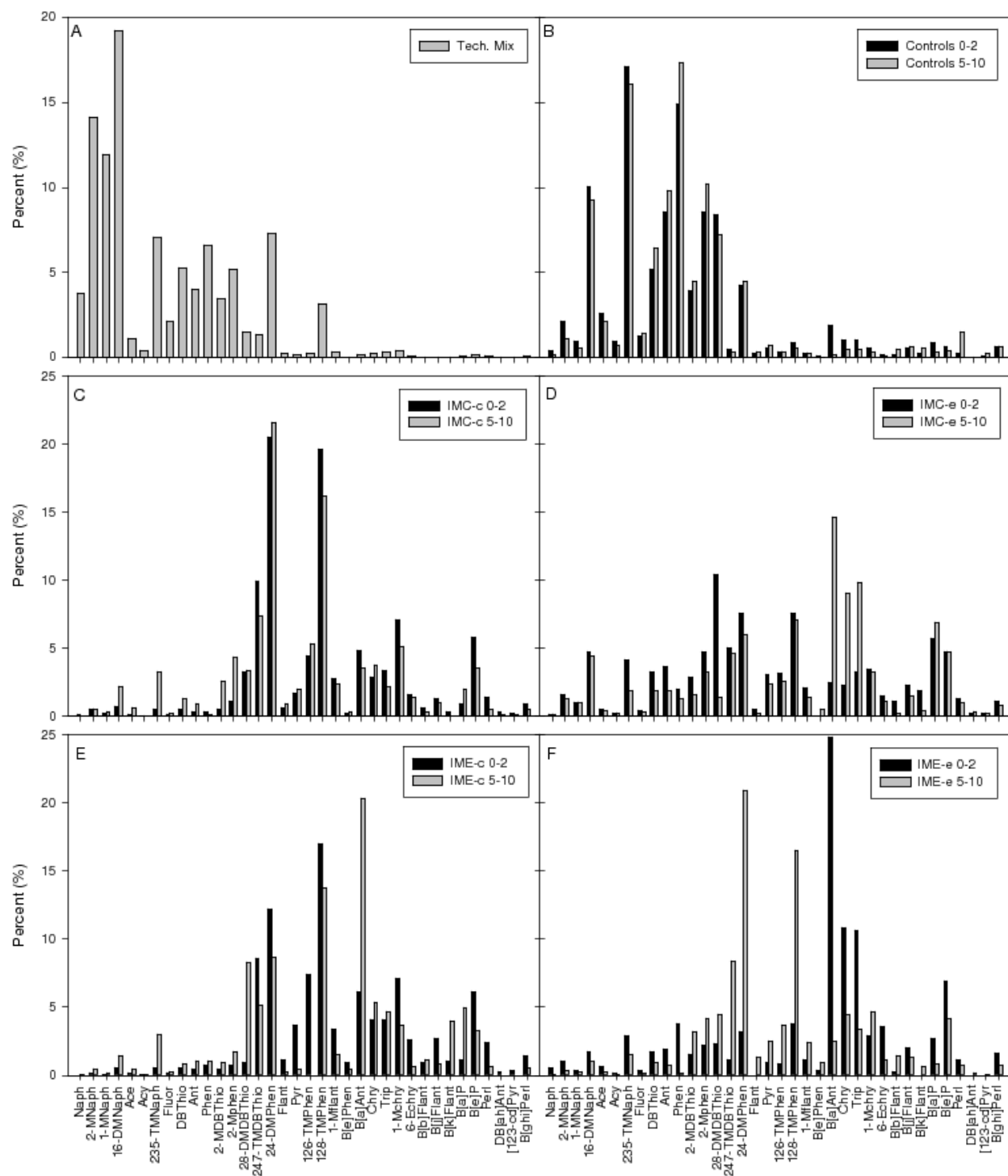


Figure 2.4. PAH profiles shown as percentages of each analyzed PAH relative to their total abundance for (A) the technical mixture, (B) the field blanks, (C) the tilled crude plot from Bay 106, (D) the tilled emulsion plot from Bay 106, (E) the control crude plot from Bay 106, and (F) the control emulsion plot from Bay 106.

Comparison to Previous Data

Sampling stations from the BIOS site were revisited in 2001 and percent loss data of Phenanthrenes and Chrysenes were subsequently reported (Prince et al., 2002). This particular analysis included samples from Bay 11 (B11 0-2 and B11 5-10), Crude Oil Point (T1 0-2 and T2 0-2), and Bay 106 (IMC-c 0-2 and IMC-c 5-10). The percent losses observed for Phenanthrene and Methylphenanthrene across nearly all collected samples were 100 %, but less extensive losses were reported for Dimethylphenanthrene (Prince et al., 2002). As such, the 2001 percent loss data for Dimethylphenanthrene was taken and converted to a concentration, using the concentration measured within the technical mixture as follows (eq2):

$$(2) [x]_{sample} = [x]_{tech.mix} * \left(\frac{100 - \%loss}{100}\right)$$

This process was repeated for Chrysene, as the percent loss values for this compound were also available in Prince et al., (2002). To observe the changes in concentrations for Dimethylphenanthrene and Chrysene between 2001 and 2019, this data has been included in Table 2.2. We believe that reporting the concentrations would be more meaningful than comparing percent losses, as the percent loss values between the 2019 samples and the technical mixture are essentially 100 %. The largest observed decrease in concentration between the two compounds from 2001 to 2019 was Dimethylphenanthrene in T1 0-2 (Table 2.2). This result was expected, as certain weathering and transformation processes tend to occur more readily in 3-ringed PAHs than 4-ringed PAHs. Surprisingly, there were no recorded percent loss of Dimethylphenanthrene for this particular sample in 2001, but the concentration from 2001 to

2019 has decreased by 240-fold. The subsurface Bay 11 sample displayed the largest decrease in Chrysene concentration between 2001 and 2019.

Table 2.2. Percent (%) loss of Dimethylphenanthrene and Chrysene in BIOS samples collected during 2001 (Prince et al., 2002), and associated concentrations between 2001 and 2019.

Sample ID	Dimethylphenanthrene			Chrysene		
	2001 (% loss)	2001 ($\mu\text{g}/\text{kg}$)	2019 ($\mu\text{g}/\text{kg}$)	2001 (% loss)	2001 ($\mu\text{g}/\text{kg}$)	2019 ($\mu\text{g}/\text{kg}$)
B11-I 0-2	85	36000	2.4	33	5800	1.9
B11-I 5-10	42	140000	3.6	11	7700	1.7
TI 0-2	0.0	240000	1000	7.0	8000	330
T2 0-2	7.0	220000	2100	1.0	8500	640
IMC-c 0-2	64	85000	1600	23	6600	230
IMC-c 5-10	48	120000	920	8.0	7900	160

PCA

A Principal Component Analysis (PCA) ordination was carried out to identify potential trends or relationships within the data (Holland, 2019; Maitra & Yan, 2008). This PCA analysis included all samples collected during the 2019 Amundsen expedition, including field blanks, as well as the technical mixture (Table 2.S1). PC1 and PC2 represent 39 and 30 % of the total variance, respectively. Three distinct clusters are observed in the corresponding score plot representing the supratidal oiled sediments, the technical mixture, and the controls grouped with the intertidal oiled samples. Based on the PCA loadings, the technical mixture featured increased proportions of light MW PAHs such as Naphthalene, 1-Methylnaphthalene, and 2-Methylnaphthalene. The control and intertidal sediments were mainly characterized by higher

concentrations of light MW PAHs, such as 1,6-Dimethylnaphthalene, 2,3,5-Trimethylnaphthalene, Acenaphthene, Acenaphthylene, Fluorene, Dibenzothiophene, 2-Methyldibenzothiophene, 2,8-Dimethyldibenzothiophene, and Phenanthrene, compared to the technical mixture and oiled, supratidal sediments. The supratidal samples collected from the oiled plots demonstrate increased proportions of three, four, and five-ringed PAHs, among which include 2,4,7-Trimethyldibenzothiophene, Fluoranthene, 1-Methylfluoranthene, 1,2,6-Trimethylphenanthrene, 1,2,8-Trimethylphenanthrene, Chrysene, Triphenylene, 1-Methylchrysene, Benz[a]anthracene, and Benzo[e]pyrene. When considering the amount of time these sediments have remained untouched, such patterns reflect the recalcitrance of larger PAHs compared to the lighter, more volatile PAHs that are also more readily subject to microbial degradation (Mozo et al., 2012; Prince, 2002).

The component scores of the oiled sediment samples in the first PCA were well clustered, but that made it difficult to differentiate any patterns between sampling site, depth, or oil type. As such, a second PCA was conducted, excluding the technical mixture and controls (Figure 2.5). Principal components 1 (PC1) and 2 (PC2) accounted for 52 and 13% of the total variance, respectively. Three distinct clusters of samples are apparent from the component scores plot (Figure 2.5b). The rightmost cluster (quadrants 2 and 4) represents Bay 11 sediments, mainly characterized by higher abundances of PAHs such as Fluorene, Phenanthrene, Anthracene, Dibenzothiophene, 2-Methyldibenzothiophene, 2,8-Dimethyldibenzothiophene, 2-Methylphenanthrene, Benzo[j]phenanthrene, and Benzo[g,h,i]perylene (bottom-right quadrant and just above; Figure 2.5). There is also a strong negative correlation involving these samples and Benz[a]anthracene. The second cluster (quadrants 1 and 2) represent selected supratidal sediments from Bay 106. These are relatively higher in 1-Methylnaphthalene, 2-

Methylnaphthalene, 1,6-Dimethylnaphthalene, Fluoranthene, Triphenylene, Benz[a]anthracene, and most notably Benzo[a]pyrene. Finally, the third cluster (quadrants 1 and 4) consists of the remaining Bay 106 and Crude Oil Point supratidal sediments. This cluster is mainly comprised of increased abundances of Benzo[e]phenanthrene, 6-Ethylchrysene, Fluoranthene, 1-Methylfluoranthene, 2,4,7-Trimethyldibenzothiophene, Pyrene, 2,4-Dimethylphenanthrene, and predominantly 1,2,6-Trimethylphenanthrene (bottom-left quadrant; Figure 2.5). These points also share a strong negative correlation to Phenanthrene abundance. PC3 and PC4 represent 9.6 and 6.5 % of the variance, respectively (not shown).

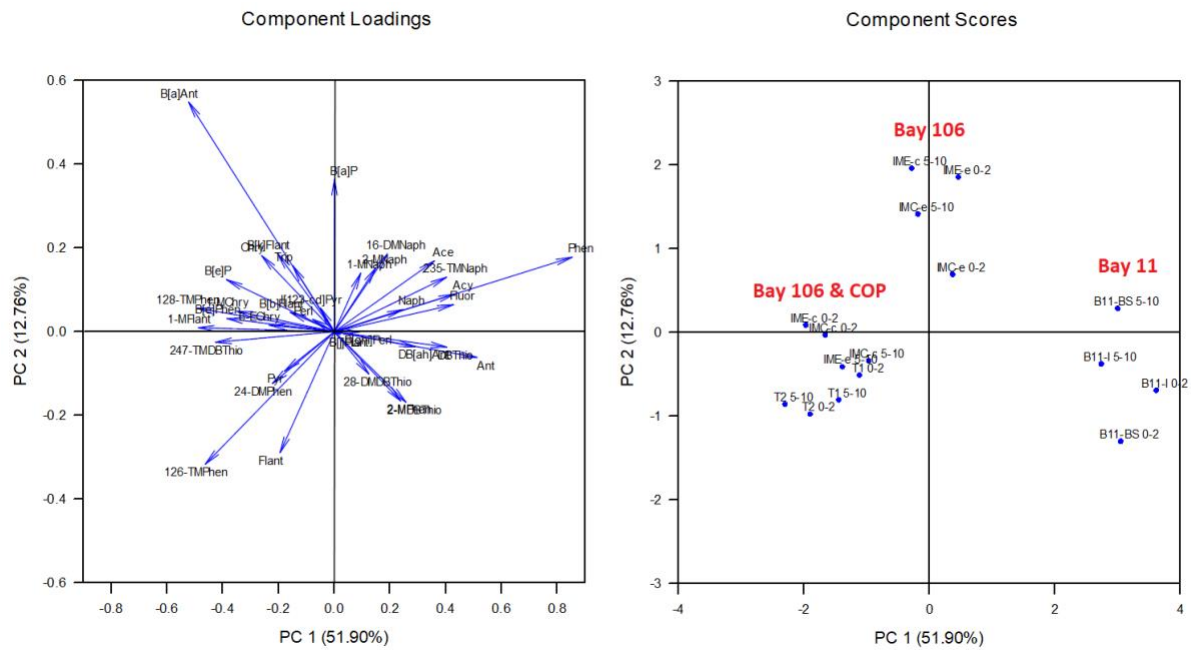


Figure 2.5. PCA, demonstrated by PC1 and PC2, of the weathered PAH concentrations for the oiled samples from the BIOS site. Plot a represents the component loading vectors, and plot b represents the component scores.

Potential Toxicity

The system of TEFs and TEQs originated upon examination of polychlorinated dibenzo-p-dioxins (PCDDs) and dibenzofurans (PCDFs) (NATO, 1988). As such, this method of characterizing carcinogenicity and toxicity was adopted for PAHs since they pose similar health risks (Nisbet & LaGoy, 1992). PCDDs, PCDFs, and various PAHs have high propensities to sorb to organic carbon in the sediments (Sahu & Pandit, 2003; Shiu et al., 1988). In turn, strong correlations ($R^2 \geq 0.79$) between TEQs and percent organic carbon (%OC) in sediments have been reported for PCDDs and PCDFs. As a result, there have been descriptions of TEQ values that have been normalized to %OC (Kanematsu et al., 2006); however, doing so has been questioned due to preferential partitioning of various dioxins to different types of organic matter in sediments (Yeager et al., 2007). As such, relationships between TEQ values measured from the 2019 BIOS samples and %OC are presented in Table 2.3. In general, the relationship between the two variables were generally weak, particularly in the 4-ringed PAHs. The R^2 values for the light MW PAHs in both the surface and subsurface sediments were identical ($R^2 = 0.61$); however, the R^2 values for the medium and heavy MW PAHs were higher in the subsurface sediments, compared to the surface sediments (Table 2.3). The average particle sizes of the sediments at each sampling station could play a role in the observed results, as each beach was characterized by slightly different sediment types, ranging from fine sands to gravel. Based on these results, the decision was made not to normalize TEQ values to the %OC calculated for each sample, as the correlations were weaker than what has been reported for the relationship between dioxin TEQs and %OC.

Table 2.3. Coefficient of determination (R^2) values between percent Organic Carbon (OC) and Toxic Equivalency Quotients (TEQs) for light (2 and 3-ringed), medium (4-ringed), and heavy (5 and 6-ringed) MW PAHs in surface and subsurface sediments from the BIOS site.

Sample	Surface				Subsurface			
	TEQ ($\mu\text{g}/\text{kg}$)			OC (%)	TEQ ($\mu\text{g}/\text{kg}$)			OC (%)
	Light	Medium	Heavy	-	Light	Medium	Heavy	-
IMC-c	0.28	41	230	2.8	0.42	17	110	2.0
IMC-e	0.17	1.2	31	1.6	0.20	14	78	1.8
IME-c	0.19	24	95	3.2	0.17	31	80	1.4
IME-e	0.13	14	15	2.4	0.41	15	86	2.0
B11-BS	1.2	0.22	0.0071	6.7	0.23	0.25	24	3.0
TI	1.3	36	78	3.4	1.9	31	310	4.1
T2	1.3	27	170	4.6	0.80	27	310	4.1
B11-I	0.060	0.032	1.4	1.2	0.14	0.046	1.5	1.2
R^2 value	0.61	0.0018	0.0042	-	0.61	0.17	0.73	-

The total TEQ values of individual US EPA PAHs for each sample are reported in Table 2.4. In a similar fashion to mean $\Sigma 16\text{PAH}$ and $\Sigma 36\text{PAH}$ concentrations, the highest total TEQ values on average were observed within the sediments from Crude Oil Point, followed by those from Bay 106, then finally from Bay 11, with minor exceptions (Table 2.4). Regarding the total TEQs within the Bay 11 sediments, two-way ANOVA determined that there were no statistically significant differences among tidal zone ($P = 0.66$), sample depth ($P = 0.71$), nor interactions between both variables ($P = 0.86$). Surprisingly, two-way ANOVA suggests that total TEQs for the samples collected from Crude Oil Point show statistically significant differences between oil type (weathered crude vs. emulsion) ($P = 0.017$) despite there being no significant differences in total PAH concentrations between oil type at this site. It is anticipated that the crude oil exhibits altered physical parameters upon emulsification, which could contribute to the noticeable

differences in the PAH compositions between the weathered crude and emulsified samples (Figure 2.3) and thus the TEQs. Conversely, there were no significant differences amongst sample depth ($P = 0.29$) nor the interaction between the two variables ($P = 0.22$) for the Crude Oil Point site. Upon examination of the Bay 106 samples, two-factor ANOVA results indicate that there were no significant differences between the total TEQ values amongst treatment type ($P = 0.78$), sample depth ($P = 0.24$), nor the interaction between the two variables ($P = 0.87$). It is important to be aware of the associated potential toxicity of crude oil residues within various environmental compartments to understand the possible implications and risks for human and environmental health. As accidental oil spills within Arctic waters are expected to increase in frequency over time, establishing databases of TEQs for compound groups such as PAHs will serve to facilitate risk assessment efforts to maintain the health and safety of remote communities in the Arctic, as well as the organisms in which they depend on for sustenance.

Sediment Quality Guidelines (SQGs) have been established and updated by the Canadian Council of Ministers of the Environment (CCME) for a variety of metals, pesticides, and other organic compounds (Canadian Council of Ministers of the Environment, 2001). The CCME SQGs include information for twelve of the sixteen EPA priority PAHs. Values for the four remaining PAHs were obtained from other sources (Ingersoll et al., 1996; Menchaca et al., 2014). Together, these SQGs were compared to the concentration values from the oiled surface and subsurface beach sediment samples obtained in 2019 (Table 2.4). To remain conservative in our estimates of toxicity, based on dry weight, if the concentration value for a single PAH exceeds the SQG limit provided by CCME (Canadian Council of Ministers of the Environment, 2001; Ingersoll et al., 1996; Menchaca et al., 2014), that sample is considered to be potentially toxic. Based on this, even after nearly forty years, back-beach “terrestrial” oiled sediments from

Bay 106 and Crude Oil Point would still be classified as potentially toxic (Table 2.4). However, there is no potential toxicity attributed to the intertidal sediments from Bay 11. Within the surface samples, there are thirty-three total cases where individual PAH concentrations exceed the SQG limits, and there are forty cases of SQG limits that were exceeded within the subsurface samples. The surface sediments are more exposed to weathering and atmospheric conditions such as solar radiation, air temperature change, and wind; therefore, it is unsurprising to observe more exceedances of the SQGs in the subsurface sediments than those in the surface. Interestingly, the two samples exhibiting the largest increases in SQG exceedance from surface to subsurface samples are the emulsified control plot from Bay 106 (IME-e), and the weathered crude plot from Crude Oil Point (T1). No samples contain levels of Naphthalene or Fluorene that exceed the SQG value (Table 2.4). It is understood that these SQGs are primarily relevant to marine sediments, whereas this analysis focuses mostly on supratidal beach sediments. However, the potential for redistribution into the intertidal zone from rare weather patterns cannot be disregarded.

The values previously calculated for the concentrations of Chrysene from the samples described in Prince et al. (2002) are presented in Table 2.4. All values included in the 2001 dataset exceed the SQG limit for Chrysene, by at least fifty-three times. The least concentrated sample from the 2001 data is the surface intertidal Bay 11 sediments, B11-I 0-2. Comparatively, the same sample collected in 2019 now only contains levels of Chrysene that meet 1.8 % of the SQG threshold. As such, there has been a 93 – 100 % degradation of Chrysene within the comparable samples between 2001 and now. Coincidentally, eight of the sixteen samples from the 2019 sampling event still contain potentially toxic levels of Chrysene, exceeding the limit by 150 – 590 %.

Table 2.4. Interim Marine Sediment Quality Guidelines (ISQGs) (Canadian Council of Ministers of the Environment, 2001) and TEQs for the 16 EPA Priority PAHs. SQG values are provided on a dry weight, threshold effect level (TEL) basis. The TEQ values are derived from TEFs provided in Nisbet and LaGoy (1992), unless otherwise specified. The lightly highlighted values represent concentrations that exceed the proposed SQGs.

Mean Concentration (µg/kg) (TEQ (µg/kg))										
Surface		Subsurface								
T2	B11-I	IMC-c	IMC-e	IME-c	IME-e	B11-BS	T1	T2	B11-I	B11-I
16 (0.016)	0.16 (0.00016)	1.4 (0.0014)	0.80 (0.00080)	0.84 (0.00084)	1.9 (0.0019)	0.53 (0.00053)	12 (0.012)	15 (0.015)	0.82 (0.00082)	
7.9 (0.0079)	0.43 (0.00043)	25 (0.025)	3.9 (0.0039)	6.2 (0.0062)	13 (0.013)	3.1 (0.031)	11 (0.011)	13 (0.013)	0.30 (0.00030)	
2.2 (0.0022)	-	1.3 (0.0013)	2.3 (0.0023)	1.4 (0.0014)	3.1 (0.0031)	-	7.4 (0.0074)	5.8 (0.0058)	0.61 (0.00061)	
7.1 (0.0071)	0.92 (0.00092)	9.8 (0.0098)	3.0 (0.0030)	4.1 (0.0041)	9.7 (0.0097)	1.9 (0.0019)	13 (0.013)	11 (0.011)	1.0 (0.0010)	
130 (1.3)	5.1 (0.051)	37 (0.37)	18 (0.18)	15 (0.15)	37 (0.37)	18 (0.18)	190 (1.9)	75 (0.75)	13 (0.13)	
18 (0.017)	7.4 (0.0074)	6.1 (0.0061)	12 (0.012)	15 (0.015)	6.5 (0.0065)	37 (0.037)	34 (0.034)	-	14 (0.014)	
160 (0.16)	0.26 (0.00026)	40 (0.040)	20 (0.020)	4.3 (0.0043)	65 (0.065)	0.67 (0.00067)	220 (0.22)	130 (0.13)	0.58 (0.00058)	
360 (0.36)	0.94 (0.00094)	85 (0.085)	21 (0.021)	6.5 (0.0065)	130 (0.13)	1.2 (0.0012)	390 (0.39)	340 (0.34)	1.9 (0.0019)	
200 (20)	0.12 (0.012)	150 (15)	130 (13)	300 (30)	130 (13)	2.4 (0.24)	250 (25)	210 (21)	0.26 (0.026)	
640 (6.4)	1.9 (0.019)	160 (1.6)	82 (0.82)	79 (0.79)	230 (2.3)	-	540 (5.4)	530 (5.3)	1.7 (0.017)	
8500 (85)	5800 (58)	7800 (78)	n/a	n/a	n/a	n/a	n/a	n/a	7600 (76)	
150 (15)	-	15 (1.5)	2.1 (0.21)	17 (1.7)	72 (7.2)	2.5 (0.25)	100 (10)	72 (7.2)	0.73 (0.072)	
180 (18)	-	-	3.6 (0.36)	58 (5.8)	32 (3.2)	-	87 (8.7)	59 (5.9)	0.15 (0.015)	
85 (85)	1.4 (1.4)	87 (87)	63 (63)	73 (73)	45 (45)	4.8 (4.8)	110 (110)	110 (110)	1.40 (1.4)	
11 (54)	-	4.2 (21)	2.7 (14)	-	6.1 (30)	3.7 (19)	37 (190)	38 (190)	-	
26 (2.6)	-	3.8 (0.38)	2.3 (0.23)	-	5.0 (0.50)	3.0 (0.30)	27 (2.7)	25 (2.5)	0.41 (0.041)	
120 (0.12)	1.8 (0.0018)	22 (0.022)	7.2 (0.0072)	8.4 (0.0084)	35 (0.035)	2.2 (0.0022)	120 (0.12)	110 (0.11)	2.2 (0.0022)	
2100 (200)	20 (1.5)	650 (130)	380 (92)	590 (110)	810 (100)	81 (25)	2100 (350)	1800 (340)	39 (1.7)	

Compound	SQG (µg/kg)	IMC-c	IMC-e	IME-c	IME-e	B11-BS	T1
Naphthlene	35	7.8 (0.0078)	0.51 (0.00051)	1.2 (0.0012)	3.1 (0.0031)	0.27 (0.00027)	11 (0.011)
Acenaphthene	6.7	7.0 (0.0070)	2.2 (0.0022)	4.5 (0.0045)	3.4 (0.0034)	5.1 (0.0051)	4.5 (0.0044)
Acenaphthylene	5.9	3.7 (0.0037)	1.1 (0.0011)	2.4 (0.0024)	0.90 (0.00090)	4.6 (0.0046)	4.5 (0.0045)
Fluorene	21	9.2 (0.0091)	1.8 (0.0018)	4.1 (0.0041)	2.0 (0.0020)	8.7 (0.0087)	7.2 (0.0072)
Anthracene	47	23 (0.23)	16 (0.15)	15 (0.15)	10 (0.10)	98 (0.98)	120 (1.2)
Phenanthrene	87	28 (0.028)	8.7 (0.0087)	27 (0.027)	20 (0.020)	200 (0.20)	80 (0.080)
Fluoranthene	110	50 (0.050)	2.4 (0.0024)	42 (0.042)	0.18 (0.00018)	3.7 (0.0037)	65 (0.065)
Pyrene	150	130 (0.13)	13 (0.013)	140 (0.14)	4.9 (0.0049)	6.4 (0.0064)	130 (0.13)
Benz[a]anthracene	75	390 (39)	11 (1.0)	220 (22)	130 (13)	1.8 (0.18)	320 (32)
Chrysene ^a	110	230 (2.3)	9.7 (0.10)	150 (1.5)	58 (0.58)	2.7 (0.027)	330 (3.3)
Chrysene ^b	110	6600 (66)	n/a	n/a	n/a	n/a	7900 (79)
Benzo[b]fluoranthene ^c	5.8	49 (4.9)	4.9 (0.49)	34 (3.4)	1.4 (0.14)	-	39 (3.9)
Benzo[k]fluoranthene ^d	27	24 (2.4)	8.1 (0.81)	38 (3.8)	-	-	20 (2.0)
Benzo[a]pyrene	89	76 (76)	24 (24)	40 (40)	15 (15)	-	36 (36)
Dibenz[a,h]anthracene	6.2	29 (140)	0.96 (4.8)	9.2 (46)	-	-	7.0 (35)
Indeno[1,2,3-c,d]pyrene ^d	17	18 (1.8)	0.86 (0.086)	11 (1.1)	-	-	13 (1.3)
Benzo[g,h,i]perylene ^d	16	76 (0.076)	4.9 (0.0049)	54 (0.049)	8.6 (0.0086)	7.2 (0.0071)	56 (0.056)
Total	920	1200 (270)	110 (32)	790 (120)	260 (29)	340 (1.4)	1300 (120)

^aData from current study

^bData calculated from the 2001 percent loss values (excluded from total)

^cSQG value was obtained from Menchaca et al. (2014)

^dSQG values were acquired from Ingersoll et al. (1996)

Conclusion

This work marks a step forward in the continued search towards answering a myriad of questions pertaining to the behaviour of PAH degradation within the Arctic. Additionally, it begins to address how long PAH toxicity will last within marine sediments when crude oil is left to degrade under natural conditions. Unfortunately, data on individual PAH concentrations from previous experiments at the BIOS site is extremely limited. The underlying importance of these results is that potential toxicity remains in all the originally oiled sites, based on the concentrations of PAHs recorded within the collected sediments. Crude Oil Point remains the site with the highest potential toxicity, followed by Bay 106, then Bay 11. This was expected, given that the plots of Crude Oil Point were intentionally setup with little to no access to the marine interface (E. H. Owens, Robson, et al., 1987; E. H. Owens & Robson, 1987).

The BIOS site was initially chosen as a representation of any pristine area that might be found in any Arctic climate, meaning that these results can be applied on an international scale (Cretney, 1987; Cretney et al., 1987a, 1987b; Foster et al., 2015; Yunker et al., 2002). Despite the increasing interest and efforts towards Arctic oil exploration; extreme, remote environments such as this lack sufficient infrastructure to properly and timely respond to and contain large-scale oil spills (Knol & Arbo, 2014). The results of this study demonstrate roughly forty years of natural attenuation processes alone are insufficient to remediate the priority PAHs within the crude oil. There exists hence a remaining risk at the BIOS site to the indigenous, terrestrial biota, even almost four decades after the initial application of the oils (Thomas et al., 1992). We have established the presence of an extensive suite of PAHs that have toxic properties associated to them. Nearly all these PAHs have exceeded the well-established aforementioned SQGs a grand total of 73 times, implicating the potential toxicity after nearly forty years within the oiled

sediments at the study locations. The fate of the crude oil observed at the BIOS site, and its ongoing serious, deleterious impacts serve as an example of what might occur in similar Arctic settings, when oil is accidentally released.

References

- Ahangar, A. G. (2010). Sorption of PAHs in the soil environment with emphasis on the role of soil organic matter: A review. *World Applied Sciences*, 11(7), 7.
- Arctic Monitoring and Assessment Programme. (2010). *AMAP assessment 2007: Oil and gas activities in the Arctic - effects and potential effects. 1*. AMAP Arctic Monitoring and Assessment Programme.
- Arctic Monitoring and Assessment Programme. (2017). *Snow, water, ice and permafrost in the Arctic—Summary for policy-makers*. Arctic Monitoring and Assessment Programme (AMAP).
- Asihene, W. (2019). *Sources and geochemical controls on hydrocarbons in Arctic sediments, Kivalliq Region, Nunavut*.
- Bhavsar, S. P., Reiner, E. J., Hayton, A., Fletcher, R., & MacPherson, K. (2008). Converting Toxic Equivalents (TEQ) of dioxins and dioxin-like compounds in fish from one Toxic Equivalency Factor (TEF) scheme to another. *Environment International*, 34(7), 915–921. <https://doi.org/10.1016/j.envint.2008.02.001>
- Boehm, P. D. (1983). *Chemistry: 2. Analytical biogeochemistry—1982 Study results* (p. 231).
- Boehm, P. D., Page, D. S., Brown, J. S., Neff, J. M., & Burns, W. A. (2004). Polycyclic aromatic hydrocarbon levels in mussels from Prince William Sound, Alaska, USA, document the return to baseline conditions. *Environmental Toxicology and Chemistry*, 23(12), 2916–2929. <https://doi.org/10.1897/03-514.1>
- Cambridge Isotope Laboratories. (2016). *Certificate of analysis, PAH surrogates standard mixture*.

- Canadian Council of Ministers of the Environment. (2001). *Canadian sediment quality guidelines for the protection of aquatic life* (pp. 1–5). CCME.
- Carls, M., Rice, S., & Hose, J. E. (1999). Sensitivity of fish embryos to weathered crude oil: PART I. Low-level exposure during incubation causes malformations, genetic damage, and mortality in larval Pacific Herring (*Clupea Pallasii*). *Environmental Toxicology and Chemistry*, 18(3), 481–493.
- Cerniglia, C. E. (1993). Biodegradation of polycyclic aromatic hydrocarbons. *Current Opinion in Biotechnology*, 4, 331–338.
- Choudhury, H., Hertzberg, R., Rice, G., Cogliano, J., Mukerjee, D., & Teuschler, L. (2000). *Supplementary guidance for conducting health risk assessment of chemical mixtures* (p. 209) [Technical Panel]. U.S. Environmental Protection Agency.
- Collins, J. F., Brown, J. P., Dawson, S. V., & Marty, M. A. (1991). Risk assessment for benzo[a]pyrene. *Regulatory Toxicology and Pharmacology*, 13(2), 170–184.
[https://doi.org/10.1016/0273-2300\(91\)90020-V](https://doi.org/10.1016/0273-2300(91)90020-V)
- Cretney, W. J. (1987). Hydrocarbon biogeochemical setting of the Baffin Island Oil Spill experimental sites. III. Biota. *ARCTIC*, 40, 9.
- Cretney, W. J., Green, D. R., Fowler, B. R., Humphrey, B., Fiest, D. L., & Boehm, P. D. (1987a). Hydrocarbon biogeochemical setting of the Baffin Island Oil Spill experimental sites. II. Water. *Arctic*, 40, 66–70.
- Cretney, W. J., Green, D. R., Fowler, B. R., Humphrey, B., Fiest, D. L., & Boehm, P. D. (1987b). Hydrocarbon biogeochemical setting of the Baffin Island Oil Spill experimental sites. I. Sediments. *ARCTIC*, 40(5), 51–65. <https://doi.org/10.14430/arctic1802>

- Dawson, J., Copland, L., Johnston, M., Pizzolato, L., Howell, S., Pelot, R., Etienne, L., Matthews, L., & Parsons, J. (2017). *Climate change adaptation strategies and* (p. 156).
- Dawson, J., Pizzolato, L., Howell, S. E. L., Copland, L., & Johnston, M. E. (2018). Temporal and spatial patterns of ship traffic in the Canadian Arctic from 1990 to 2015. *ARCTIC*, 71(1), Article 1. <https://doi.org/10.14430/arctic4698>
- Ferguson, D. K., Li, C., Jiang, C., Chakraborty, A., Grasby, S. E., & Hubert, C. R. J. (2020). Natural attenuation of spilled crude oil by cold-adapted soil bacterial communities at a decommissioned high Arctic oil well site. *Science of The Total Environment*, 722, 137258. <https://doi.org/10.1016/j.scitotenv.2020.137258>
- Fisher, T. T., Law, R. J., Rumney, H. S., Kirby, M. F., & Kelly, C. (2011). Towards a scheme of toxic equivalency factors (TEFs) for the acute toxicity of PAHs in sediment. *Ecotoxicology and Environmental Safety*, 74(8), 2245–2251. <https://doi.org/10.1016/j.ecoenv.2011.07.023>
- Foster, K. L., Stern, G. A., Carrie, J., Bailey, J. N. L., Outridge, P. M., Sanei, H., & Macdonald, R. W. (2015). Spatial, temporal, and source variations of hydrocarbons in marine sediments from Baffin Bay, Eastern Canadian Arctic. *Science of the Total Environment*, 506(507), 430–443.
- Gonzalez, C., & Choquette, S. (2017). *Certificate of analysis—Standard reference material 1944*. National Institute of Standards & Technology.
- Gonzalez, C., & Watters, R. (2015). *Certificate of analysis—Standard reference material 1941b*. National Institute of Standards & Technology.
- Harsem, Ø., Eide, A., & Heen, K. (2011). Factors influencing future oil and gas prospects in the Arctic. *Energy Policy*, 39(12), 8037–8045. <https://doi.org/10.1016/j.enpol.2011.09.058>

- Holland, S. M. (2019). *Principal components analysis (PCA)* (p. 12). Department of Geology, University of Georgia, Athens, GA.
- Ingersoll, C. G., Haverland, P. S., Brunson, E. L., Canfield, T. J., James Dwyer, F., Henke, C. E., Kemble, N. E., Mount, D. R., & Fox, R. G. (1996). Calculation and evaluation of sediment effect concentrations for the amphipod *Hyalella azteca* and the midge *Chironomus riparius*. *Journal of Great Lakes Research*, 22(3), 602–623.
[https://doi.org/10.1016/S0380-1330\(96\)70984-X](https://doi.org/10.1016/S0380-1330(96)70984-X)
- Kanematsu, M., Shimizu, Y., Sato, K., Kim, S., Suzuki, T., Park, B., Hattori, K., Nakamura, M., Yabushita, H., & Yokota, K. (2006). Distribution of dioxins in surface soils and river-mouth sediments and their relevance to watershed properties. *Water Science and Technology*, 53(2), 11–21. <https://doi.org/10.2166/wst.2006.034>
- Knol, M., & Arbo, P. (2014). Oil spill response in the Arctic: Norwegian experiences and future perspectives. *Marine Policy*, 50, 171–177. <https://doi.org/10.1016/j.marpol.2014.06.003>
- Lee, B. M., & Shim, G. A. (2007). Dietary exposure estimation of benzo[a]pyrene and cancer risk assessment. *Journal of Toxicology and Environmental Health, Part A*, 70(15–16), 1391–1394. <https://doi.org/10.1080/15287390701434182>
- Maitra, S., & Yan, J. (2008). *Principle component analysis and partial least squares: Two dimension reduction techniques for regression*. 12.
- Markus, T., Stroeve, J. C., & Miller, J. (2009). Recent changes in Arctic sea ice melt onset, freezeup, and melt season length. *Journal of Geophysical Research: Oceans*, 114(C12).
<https://doi.org/10.1029/2009JC005436>
- Menchaca, I., Rodríguez, J. G., Borja, Á., Belzunce-Segarra, M. J., Franco, J., Garmendia, J. M., & Larreta, J. (2014). Determination of polychlorinated biphenyl and polycyclic aromatic

- hydrocarbon marine regional sediment quality guidelines within the European water framework directive. *Chemistry and Ecology*, 30(8), 693–700.
<https://doi.org/10.1080/02757540.2014.917175>
- Mozo, I., Lesage, G., Yin, J., Bessiere, Y., Barna, L., & Sperandio, M. (2012). Dynamic modeling of biodegradation and volatilization of hazardous aromatic substances in aerobic bioreactor. *Water Research*, 46(16), 5327–5342.
<https://doi.org/10.1016/j.watres.2012.07.014>
- NATO. (1988). *Pilot study on international information exchange on dioxins and related compounds. International Toxic Equivalency Factor (I-TEF) method of risk assessment for complex mixtures of dioxins and related compounds.* (No. 176; p. 32). North Atlantic Treaty Organization (NATO).
- Nisbet, I. C. T., & LaGoy, P. K. (1992). Toxic equivalency factors (TEFs) for polycyclic aromatic hydrocarbons (PAHs). *Regulatory Toxicology and Pharmacology*, 16(3), 290–300. [https://doi.org/10.1016/0273-2300\(92\)90009-X](https://doi.org/10.1016/0273-2300(92)90009-X)
- Owens, E. H., & Robson, W. (1987). Experimental design and the retention of oil on Arctic test beaches. *ARCTIC*, 40(5), 230–243. <https://doi.org/10.14430/arctic1817>
- Owens, E. H., Robson, W., & Foget, C. R. (1987). A field evaluation of selected beach-cleaning techniques. *ARCTIC*, 40(5), 244–257. <https://doi.org/10.14430/arctic1818>
- Owens, E., Sergy, G. A., & Prince, R. (2002). The fate of stranded oil at the BIOS site twenty years after the experiment. *Environment Canada Arctic and Marine Oil Spill Program Technical Seminar (AMOP) Proceedings*, 25, 1–11.
- Payne, J. R., Driskell, W. B., Janka, D., Ka’aihue, L., Banta, J., Love, A., & Litman, E. (2021). EVOS and the Prince William Sound long term environmental monitoring program.

- International Oil Spill Conference Proceedings*, 2021(1), 688991.
<https://doi.org/10.7901/2169-3358-2021.1.688991>
- Payne, J. R., Driskell, W. B., Short, J. W., & Larsen, M. L. (2008). Long term monitoring for oil in the Exxon Valdez spill region. *Marine Pollution Bulletin*, 56(12), 2067–2081.
<https://doi.org/10.1016/j.marpolbul.2008.07.014>
- Pizzolato, L., Howell, S. E. L., Dawson, J., Laliberté, F., & Copland, L. (2016). The influence of declining sea ice on shipping activity in the Canadian Arctic. *Geophysical Research Letters*, 43(23), 12,146–12,154. <https://doi.org/10.1002/2016GL071489>
- Pizzolato, L., Howell, S. E. L., Derksen, C., Dawson, J., & Copland, L. (2014). Changing sea ice conditions and marine transportation activity in Canadian Arctic waters between 1990 and 2012. *Climatic Change*, 123(2), 161–173. <https://doi.org/10.1007/s10584-013-1038-3>
- Prince, R. C. (2002). Biodegradation of petroleum and other hydrocarbons. In *Encyclopedia of Environmental Microbiology* (pp. 2402–2416).
- Prince, R. C., Garrett, R. M., Bare, R. E., Grossman, M. J., Townsend, T., Suflita, J. M., Lee, K., Owens, E. H., Sergy, G. A., Braddock, J. F., Lindstrom, J. E., & Lessard, R. R. (2003). The Roles of photooxidation and biodegradation in long-term weathering of crude and heavy fuel oils. *Spill Science & Technology Bulletin*, 8(2), 145–156.
[https://doi.org/10.1016/S1353-2561\(03\)00017-3](https://doi.org/10.1016/S1353-2561(03)00017-3)
- Prince, R. C., Owens, E. H., & Sergy, G. A. (2002). Weathering of an Arctic oil spill over 20 years: The BIOS experiment revisited. *Marine Pollution Bulletin*, 44(11), 1236–1242.
[https://doi.org/10.1016/S0025-326X\(02\)00214-X](https://doi.org/10.1016/S0025-326X(02)00214-X)

- Ramachandran, S. D., Hodson, P. V., Khan, C. W., & Lee, K. (2004). Oil dispersant increases PAH uptake by fish exposed to crude oil. *Ecotoxicology and Environmental Safety*, 59(3), 300–308. <https://doi.org/10.1016/j.ecoenv.2003.08.018>
- Saffiotti, U., Montesano, R., & Sellaku, A. R. (1972). Respiratory tract carcinogenesis induced in hamsters by different dose levels of benzo- [a] pyrene and ferric oxide I' 2. *JOURNAL OF THE NATIONAL CANCER INSTITUTE*, 49(4), 1199–1204.
- Saha, M., Takada, H., & Bhattacharya, B. (2012). Establishing criteria of relative abundance of alkyl polycyclic aromatic hydrocarbons (PAHs) for differentiation of pyrogenic and petrogenic PAHs: An application to Indian sediment. *Environmental Forensics*, 13(4), 312–331. <https://doi.org/10.1080/15275922.2012.729005>
- Sahu, S. K., & Pandit, G. G. (2003). Estimation of octanol-water partition coefficients for polycyclic aromatic hydrocarbons using reverse-phase HPLC. *Journal of Liquid Chromatography & Related Technologies*, 26(1), 135–146. <https://doi.org/10.1081/JLC-120017158>
- Saltymakova, D., Desmond, D. S., Isleifson, D., Firoozy, N., Neusitzer, T. D., Xu, Z., Lemes, M., Barber, D. G., & Stern, G. A. (2020). Effect of dissolution, evaporation, and photooxidation on crude oil chemical composition, dielectric properties and its radar signature in the Arctic environment. *Marine Pollution Bulletin*, 151, 110629. <https://doi.org/10.1016/j.marpolbul.2019.110629>
- Samanta, S. K., Singh, O. V., & Jain, R. K. (2002). Polycyclic aromatic hydrocarbons: Environmental pollution and bioremediation. *Trends in Biotechnology*, 20(6), 243–248. [https://doi.org/10.1016/S0167-7799\(02\)01943-1](https://doi.org/10.1016/S0167-7799(02)01943-1)

- Sergy, G. A., & Blackall, P. J. (1987). Design and conclusions of the Baffin Island Oil Spill project. *ARCTIC*, 40(5), 1–9. <https://doi.org/10.14430/arctic1797>
- Shiu, W. Ying., Doucette, William., Gobas, F. A. P. C., Andren, Anders., & Mackay, Donald. (1988). Physical-chemical properties of chlorinated dibenzo-p-dioxins. *Environmental Science & Technology*, 22(6), 651–658. <https://doi.org/10.1021/es00171a006>
- Thomas, D. J., Tracey, B., Marshall, H., & Norstrom, R. J. (1992). Arctic terrestrial ecosystem contamination. *Science of The Total Environment*, 122(1–2), 135–164. [https://doi.org/10.1016/0048-9697\(92\)90247-P](https://doi.org/10.1016/0048-9697(92)90247-P)
- Tongo, I., Ogbeide, O., & Ezemonye, L. (2017). Human health risk assessment of polycyclic aromatic hydrocarbons (PAHs) in smoked fish species from markets in Southern Nigeria. *Toxicology Reports*, 4, 55–61. <https://doi.org/10.1016/j.toxrep.2016.12.006>
- Wang, Z., Fingas, M., Owens, E. H., Sigouin, L., & Brown, C. E. (2001). Long-term fate and persistence of the spilled Metula oil in a marine salt marsh environment: Degradation of petroleum biomarkers. *J. Chromatogr. A*, 16.
- Wu, W. Z., Schramm, K. W., Henkelmann, B., Xu, Y., Yediler, A., & Kettrup, A. (1997). PCDD, PCBs, HCHs and HCB in sediments and soils of Ya-Er Lake area in China: Results on residual levels and correlation to the organic carbon and the particle size. *Chemosphere*, 34(1), 191–202.
- Yeager, K. M., Santschi, P. H., Rifai, H. S., Suarez, M. P., Brinkmeyer, R., Hung, C.-C., Schindler, K. J., Andres, M. J., & Weaver, E. A. (2007). Dioxin chronology and fluxes in sediments of the Houston ship channel, Texas: Influences of non-steady-state sediment transport and total organic carbon. *Environmental Science & Technology*, 41(15), 5291–5298. <https://doi.org/10.1021/es062917p>

- Yin, F., John, G. F., Hayworth, J. S., & Clement, T. P. (2015). Long-term monitoring data to describe the fate of polycyclic aromatic hydrocarbons in Deepwater Horizon oil submerged off Alabama's beaches. *Science of The Total Environment*, 508, 46–56.
<https://doi.org/10.1016/j.scitotenv.2014.10.105>
- Yunker, M. B., Backus, S. M., Graf Pannatier, E., Jeffries, D. S., & Macdonald, R. W. (2002). Sources and significance of alkane and PAH hydrocarbons in Canadian Arctic rivers. *Estuarine, Coastal and Shelf Science*, 55(1), 1–31.
<https://doi.org/10.1006/ecss.2001.0880>

Supplementary Information (SI)

Section S1

Differences in hydrocarbon extraction techniques

Masses of samples being extracted depended on whether they were oiled or control sediments. 0.4 g of oiled samples and 2 g of control samples were administered for extraction. The mass of SRM added for extraction was 0.5 g. For sulfur removal, copper was rinsed twice, with each acetone and hexane. Nitrogen evaporators were not used. Instead, samples were left to evaporate inside a fume hood. Both fractions collected from the extraction process were collected into a single 125 mL flat-bottom boiling flask. All samples, blanks, and SRM were reduced to a pre-injection volume of 1.5 mL in iso-octane.

Section S2

Total Inorganic Carbon (TIC) and Total Carbon (TC) Analyses

TIC measurements were performed with a Carbon/Sulfur Analyzer (Helios, Eltra™). Sample powder was carefully weighed in a 50 mL flask, followed by the injection of 0.2 M HCl. The sample acidification was enhanced with heating to 70 °C and magnet stirring. The CO₂ generated from the sample was transferred to an IR cell for TIC measurement. Calibration standards were treated and analyzed the same as unknown samples to calculate % TIC. The quality of analysis was monitored by QC standards.

TC testing was performed on a different instrument. Sample powder was weighed into a Sn cup, wrapped, and analyzed for total carbon (in %) by a Costech™ 4010 Elemental Analyzer (EA) coupled to a Thermo Finnigan™ Delta V Plus isotope-ratio mass-spectrometer (IRMS) via an open-split interface (ConFlo IV, Thermo Finnigan™). In the EA, the sample Sn cup was dropped into the oxidation column (1020 °C), containing chromium oxide and silvered cobaltic oxide. With the O₂ supply, the sample was combusted with a strong flash. The produced CO₂ and other gaseous products passed through the reduction column (pure Cu wires), followed by the water trap (Mg(ClO₄)₂) to remove the moisture. The CO₂ from the sample was then separated from other gas products by passing through the GC column (55 °C) before being transferred to the IRMS for measurement through the open split. Calibration standards were treated and analyzed same as the unknown samples to calculate %TC. The quality of analysis was monitored by QC standards.

Table 2.S1. List of intertidal and supratidal sediment sample types acquired at respective stations and coordinates from the BIOS site during the 2019 CCGS Amundsen expedition. A surface (0-2cm) and subsurface (5-10cm) sample was collected for each entry.

Sample I.D	Location	Latitude, Longitude	Sediment Type	Sample Type
GICB-NHR1	BIOS: Z-Lagoon, Bay 102	72.488337, -79.7409	intertidal	Control
GICB-NHR2	BIOS: Z-Lagoon, Bay 102	72.488337, -79.7409	intertidal	Control
GICB-NHR3	BIOS: Z-Lagoon, Bay 102	72.488337, -79.7409	intertidal	Control
B11-I-1	BIOS: Bay 11	72.465032, -79.829518	intertidal	Oil
B11-I-2	BIOS: Bay 11	72.464883, -79.829210	intertidal	Oil
B11-I-3	BIOS: Bay 11	72.464704, -79.829119	intertidal	Oil
B11-I-4	BIOS: Bay 11	72.464542, -79.829124	intertidal	Oil
B11-I-5	BIOS: Bay 11	72.464365, -79.829052	intertidal	Oil
B11-I-6	BIOS: Bay 11	72.464237, -79.829027	intertidal	Oil
B11-I-8	BIOS: Bay 11	72.463898, -79.828980	intertidal	Oil
B11-I-9	BIOS: Bay 11	72.463782, -79.829038	intertidal	Oil
MI-I-1	Milne Inlet, Ragged Island	72.484866, -80.004129	intertidal	Control
MI-I-2	Milne Inlet, Ragged Island	72.484892, -80.004924	intertidal	Control
MI-I-3	Milne Inlet, Ragged Island	72.484905, -80.005943	intertidal	Control
IMC-c1	BIOS: Z-Lagoon, Bay 106	72.474104, -79.782194	supratidal	Oil
IMC-c2	BIOS: Z-Lagoon, Bay 106	72.474104, -79.782194	supratidal	Oil
IMC-c3	BIOS: Z-Lagoon, Bay 106	72.474104, -79.782194	supratidal	Oil
IMC-e1	BIOS: Z-Lagoon, Bay 106	72.474104, -79.782128	supratidal	Oil
IMC-e2	BIOS: Z-Lagoon, Bay 106	72.474104, -79.782128	supratidal	Oil
IMC-e3	BIOS: Z-Lagoon, Bay 106	72.474104, -79.782128	supratidal	Oil
IME-c1	BIOS: Z-Lagoon, Bay 106	72.474114, -79.782314	supratidal	Oil
IME-c2	BIOS: Z-Lagoon, Bay 106	72.474114, -79.782314	supratidal	Oil
IME-c3	BIOS: Z-Lagoon, Bay 106	72.474114, -79.782314	supratidal	Oil
IME-e1	BIOS: Z-Lagoon, Bay 106	72.474091, -79.782479	supratidal	Oil
IME-e2	BIOS: Z-Lagoon, Bay 106	72.474091, -79.782479	supratidal	Oil
IME-e3	BIOS: Z-Lagoon, Bay 106	72.474091, -79.782479	supratidal	Oil
GICB-NI11	BIOS: Z-Lagoon, Bay 106	72.474061, -79.781737	supratidal	Control
GICB-NI12	BIOS: Z-Lagoon, Bay 106	72.474061, -79.781737	supratidal	Control
GICB-NI2R1	BIOS: Z-Lagoon, Bay 106	72.474054, -79.781648	supratidal	Control
GICB-NI2R2	BIOS: Z-Lagoon, Bay 106	72.474054, -79.781648	supratidal	Control
B11-BS-1	BIOS: Bay 11	72.463782, -79.829038	supratidal	Oil
B11-BS-2	BIOS: Bay 11	72.463973, -79.828404	supratidal	Oil
T1R1	BIOS: Z-Lagoon, Crude Oil Point	72.482083, -79.755547	supratidal	Oil
T1R2	BIOS: Z-Lagoon, Crude Oil Point	72.482083, -79.755547	supratidal	Oil
T2R1	BIOS: Z-Lagoon, Crude Oil Point	72.482087, -79.756100	supratidal	Oil
T2R2	BIOS: Z-Lagoon, Crude Oil Point	72.482087, -79.756100	supratidal	Oil
TCR1	BIOS: Z-Lagoon, Crude Oil Point	72.482098, -79.756145	supratidal	Control
TCR2	BIOS: Z-Lagoon, Crude Oil Point	72.482098, -79.756145	supratidal	Control
MI-BS-1	Milne Inlet, Ragged Island	72.484922, -80.004945	supratidal	Control
MI-BS-2	Milne Inlet, Ragged Island	72.484941, -80.005885	supratidal	Control
MI-BS-3	Milne Inlet, Ragged Island	72.484396, -80.01001	supratidal	Control
RB1	Cornwallis Island, Resolute Bay	74.682228, -94.854522	Intertidal	Control
TB3	Cornwallis Island, Resolute Bay	74.749561, -95.092101	Intertidal	Control

Table 2.S2. PAH Surrogates Standard Mixture (D, 98%) (ES-5164) (CIL, 2016).

Compound	Purity	Target Concentration (µg/mL)	Concentration by Gravimetry ± Uncertainty (k=2) (µg/mL)	Analyzed Concentration ± Uncertainty (k=2) (µg/mL)
Naphthalene (D₈, 99%)	100%	200	200 ± 87.0	200.9 ± 8.3
Benz[a]anthracene (D₁₂, 98%)	99.2%	200	200 ± 86.4	200.5 ± 10.4
Phenanthrene (D₁₀, 98%)	99.9%	200	200 ± 86.9	197.9 ± 8.6
Fluoranthene (D₁₀, 98%)	98.6%	200	200 ± 85.8	196.9 ± 8.6
Benzo[b]fluoranthene (D₁₂, 98%)	100%	200	200 ± 87.0	190.7 ± 8.7
Benzo[a]pyrene (D₁₂, 98%)	98.9%	200	200 ± 86.1	197.9 ± 10.4
Benzo[g,h,i]perylene (D₁₂, 98%)	99.3%	200	200 ± 86.4	201.2 ± 10.4
Indeno[1,2,3-cd]pyrene (D₁₂, 98%)	100%	200	200 ± 87.0	207.1 ± 13.8
Dibenz[a,h]anthracene (D₁₄, 97%)	99.5%	200	200 ± 86.6	191.6 ± 9.2
Acenaphthylene (D₈, 98%)	100%	200	200 ± 87.0	190.1 ± 8.0
Acenaphthene (D₁₀, 99%)	100%	200	200 ± 87.0	194.6 ± 8.3
Fluorene (D₁₀, 98%)	99.2%	200	200 ± 86.3	200.7 ± 8.6
Pyrene (D₁₀, 98%)	99.2%	200	200 ± 86.3	203.9 ± 9.0
Benzo[k]fluoranthene (D₁₂, 98%)	100%	200	200 ± 87.0	199.3 ± 9.8
Perylene (D₁₂, 98%)	100%	200	200 ± 87.0	197.0 ± 8.9
Chrysene (D₁₂, 98%)	99.7%	200	200 ± 86.8	194.7 ± 8.1

Table 2.S3. A list of the PAHs analyzed, and their attributed abbreviations.

Naphthalene (Naph)	1,2,6-Trimethylphenanthrene (126-TMPhen)
2-Methylnaphthalene (2-MNaph)	1,2,8-Trimethylphenanthrene (128-TMPhen)
1-Methylnaphthalene (1-MNaph)	1-Methylfluoranthene (1-MFlant)
1,6-Dimethylnaphthalene (16-DMNaph)	Benzo[e]phenanthrene (B[e]Phen)
Acenaphthene (Ace)	Benzo[a]anthracene (B[a]Ant)
Acenaphthylene (Acy)	Chrysene (Chry)
2,3,5-Trimethylnaphthalene (235-TMNaph)	Triphenylene (Trip)
Fluorene (Fluor)	1-Methylchrysene (1-MChry)
Dibenzothiophene (DBThio)	6-Ethylchrysene (6-EChry)
Anthracene (Ant)	Benzo[b]fluoranthene (B[b]Flant)
Phenanthrene (Phen)	Benzo[j]fluoranthene (B[j]Flant)
2-Methyldibenzothiophene (2-MDBThio)	Benzo[k]fluoranthene (B[k]Flant)
2-Methylphenanthrene (2-MPhen)	Benzo[a]pyrene (B[a]P)
2,8-Dimethyldibenzothiophene (28-DMDBThio)	Benzo[e]pyrene (B[e]P)
2,4,7-Trimethyldibenzothiophene (247-TMDBThio)	Perylene (Perl)
2,4-Dimethylphenanthrene (24-DMPhen)	Dibenz[a,h]anthracene (DB[ah]Ant)
Fluoranthene (Flant)	Indeno[1,2,3-c,d]pyrene (I[123-cd]Pyr)
Pyrene (Pyr)	Benzo[g,h,i]perylene (B[ghi]Perl)

Table 2.S4. GCMS Parameters for analyses using the Agilent 7010B Triple Quadrupole GCMS (QQQ-MS). The column was trimmed on occasion for maintenance purposes.

Parameter	Value
Column length (m)	56-60
Column internal diameter (μm)	250
column film thickness (μm)	0.1
Initial oven temperature ($^{\circ}\text{C}$)	40
Initial isotherm (min)	1.5
Target temperature 1 ($^{\circ}\text{C}$)	140
Ramp rate 1 ($^{\circ}\text{C}/\text{min}$)	30
Target temperature 2 ($^{\circ}\text{C}$)	250
Ramp rate 2 ($^{\circ}\text{C}/\text{min}$)	3
Target temperature 3 ($^{\circ}\text{C}$)	320
Ramp rate 3 ($^{\circ}\text{C}/\text{min}$)	2
Electron energy (eV)	70
Ion source temperature ($^{\circ}\text{C}$)	280
Mass range (m/z)	50-300

Table 2.S5. Ion transitions of all PAHs, alkylated PAHs, and deuterated PAHs included in the analyses.

Compound	Precursor Ion	Product Ion	Compound	Precursor Ion	Product Ion
D8 Naphthalene	136	136	1,2,6-Trimethylphenanthrene	220	220
	136	108		220	205
	108	108		220	189
Naphthalene	128	128	1,2,8-Trimethylphenanthrene	220	220
	128	127		220	205
	127	127		220	189
2-Methylnaphthalene	142	142	1-Methylfluoranthene	216	216
	142	141		216	215
	142	115		216	213
2-Fluorobiphenyl	172	172	Benzo[e]phenanthrene	228	228
	172	171		228	227
	172	170		228	226
1-Methylnaphthalene	142	142	D12 Benz[a]anthracene	240	240
	142	141		240	236
	142	115		120	120
1,6-Dimethylnaphthalene	156	156	Benz[a]anthracene	228	228
	156	141		228	226
	141	141		226	226
D10 Acenaphthene	164	164	D12 Chrysene	240	240
	164	162		240	236
	164	160		236	236
D8 Acenaphthylene	160	160	Chrysene	228	228
	160	158		228	226
	158	158		228	228
Acenaphthene	154	154	Triphenylene	228	226
	154	153		226	226
Acenaphthylene	153	153	6-Ethylchrysene	256	256
	152	152		256	241
	152	151		256	239
2,3,5-Trimethylnaphthalene	170	170	1-Methylchrysene	242	242
	170	155		242	241
	170	153		242	239
D10 Fluorene	176	176	D12 Benzo[b]fluoranthene	264	264
	176	174		264	260
	174	174		132	132
Fluorene	166	166	D12 Benzo[k]fluoranthene	264	264
	166	165		264	260
	166	164		126	126
Dibenzothiophene	185	185	Benzo[b]fluoranthene	202	200
	184	184		252	252
	184	139		252	250
D10 Phenanthrene	188	188	Benzo[k]fluoranthene	126	126
	188	184		252	252
	188	160		252	250
Anthracene	178	178	Benzo[j]fluoranthene	126	126
	178	176		252	252

	178	152		252	250
Phenanthrene	178	178		250	250
	176	176	D12 Benzo[a]pyrene	264	264
	152	152		264	260
2-Methyldibenzothiophene	198	198		260	260
	198	197	Benzo[a]pyrene	253	253
	197	197		252	252
2-Methylphenanthrene	192	192		252	250
	192	191	Benzo[e]pyrene	252	252
	192	189		252	250
2,8-Dimethyldibenzothiophene	212	212		250	250
	212	211	D12 Perylene	264	264
	212	197		264	260
2,4,7-Trimethyldibenzothiophene	226	226		260	260
	226	225	Perylene	252	252
	226	211		252	250
2,4-Dimethylphenanthrene	206	206		250	250
	206	191	D14 Dibenz[a,h]anthracene	292	292
	206	189		292	288
D10 Fluoranthene	212	212		146	146
	212	210	D12 Indeno[1,2,3-c,d]pyrene	288	288
	212	208		288	284
Fluoranthene	202	202		144	144
	202	201	Dibenz[a,h]anthracene	278	278
	202	200		138	138
D10 Pyrene	212	212	Indeno[1,2,3-c,d]pyrene	276	276
	212	210		276	274
	212	208	D12 Benzo[g,h,i]perylene	288	288
Pyrene	202	202		288	284
	202	201		287	287
	202	200	Benzo[g,h,i]perylene	276	276
				276	274
				138	138

Table 2.S6. Low-end limits of quantitation for all PAHs included in the analysis conducted on the Agilent 7010B Triple Quadrupole GCMS (QQQ-MS).

Compound Name	Limit of Quantitation (ng/mL)
Naphthalene	0.59
2-Methylnaphthalene	0.60
1-Methylnaphthalene	0.60
1,6-Dimethylnaphthalene	0.65
Acenaphthene	0.55
Acenaphthylene	0.70
2,3,5-Trimethylnaphthalene	0.61
Fluorene	0.71
Dibenzothiophene	0.69
Anthracene	0.82
Phenanthrene	0.81
2-Methyldibenzothiophene	0.68
2-Methylphenanthrene	0.71
2,8-Dimethyldibenzothiophene	0.67
2,4,7-Trimethyldibenzothiophene	0.65
2,4-Dimethylphenanthrene	0.65
Fluoranthene	0.61
Pyrene	0.53
1,2,6-Trimethylphenanthrene	0.54
1,2,8-Trimethylphenanthrene	0.58
1-Methylfluoranthene	0.58
Benzo[e]phenanthrene	0.71
Benz[a]anthracene	0.84
Chrysene	0.76
Triphenylene	0.76
1-Methylchrysene	0.84
6-Ethylchrysene	0.82
Benzo[b]fluoranthene	0.60
Benzo[j]fluoranthene	0.98
Benzo[k]fluoranthene	0.95
Benzo[a]pyrene	0.73
Benzo[e]pyrene	0.72
Perylene	0.78
Dibenz[a,h]anthracene	0.83
Indeno[1,2,3-c,d]pyrene	0.87
Benzo[g,h,i]perylene	0.73

References

Cambridge Isotope Laboratories. Certificate of analysis, PAH surrogate standard mixture, catalogue no. ES-5164. 2016.

Chapter 3: The long-term fate of saturates and biomarkers within crude oil spilled during the Baffin Island Oil Spill (BIOS) Project

Blake E. Hunnie^a, Lars Schreiber^b, Charles W. Greer^{b,c}, Gary A. Stern^a

hunnieb@myumanitoba.ca, lars.schreiber@cnrc-nrc.gc.ca, Charles.greer@cnrc-nrc.gc.ca,
gary.stern@umanitoba.ca

^aUniversity of Manitoba, 125 Dysart Rd Winnipeg, MB R3T 2N2

^bNational Research Council Canada, 6100 Royalmount Ave Montreal, QC H4P 2R2

^cMcGill University, Department of Natural Resource Sciences, 21111 Lakeshore Rd Ste-Anne-de-Bellevue, QC, H9X 3V9

Corresponding Author:

Gary Stern (Gary.stern@umanitoba.ca) University of Manitoba, 125 Dysart Rd, Winnipeg, MB, Canada. R3T 2N2

Contributions of authors

Blake Hunnie: Methodology, Validation, Formal Analysis, Investigation, Resources, Data Curation, Writing – Original Draft, Writing – Review & Editing, Visualization, Project Administration

Lars Schreiber: Conceptualization, Methodology, Investigation, Resources, Data Curation, Visualization, Supervision, Project Administration

Charles Greer: Funding acquisition, Writing – Review & Editing, Conceptualization, Methodology, Resources,

Gary Stern: Conceptualization, Methodology, Formal Analysis, Resources, Writing – Original Draft, Supervision, Project Administration

Abstract

The Baffin Island Oil Spill (BIOS) Project is a long-term monitoring field study conducted in the early 1980s, seeking to examine the physical and chemical fate of crude oil released into a pristine Arctic setting. During the present study, sites of the BIOS Project were revisited in 2019 for the collection of oiled intertidal and backshore sediments. These samples were analyzed for several groups of petroleum hydrocarbons including n-alkanes, hopanes and steranes, alkylbenzenes, and alkylcycloalkanes using Gas Chromatography Mass Spectrometry. The analyzed suites of n-alkanes and hopanes and steranes are present in concentrations from 1.77 to 1210 mg/kg, and 0.00 to 11.7 mg/kg within individual samples, respectively. Representative medium-chain (nC18) and long-chain (nC30) n-Alkanes demonstrate extensive degradation, exhibiting up to 98 % and 77 % loss since the penultimate revisitation of the BIOS site in 2001, respectively.

Keywords: Arctic, Baffin Island Oil Spill (BIOS) Project, weathering, saturates, biomarkers, long-term monitoring

Introduction

The Arctic is warming at an accelerated rate, unlike any other region on Earth (Arctic Monitoring and Assessment Programme, 2017; Serreze et al., 2007; Steele et al., 2008). The extent of pan-Arctic sea ice cover has reduced at a rate of roughly 9% per decade, or 100,000km² per year (Serreze et al., 2007). A reduction in sea ice induces exacerbated heat flux between the Arctic ocean surface and the open atmosphere, leading to increased warming (Perovich et al., 2007; Steele et al., 2008). Melt seasons last up to 20 days longer compared to those observed 30 years ago, as a direct result of the disproportional warming within the Arctic (Arctic Monitoring and Assessment Programme, 2017; Markus et al., 2009). In addition to well-established routes for ship traffic within the Arctic such as the Northwest and Northeast Passages (Eguíluz et al., 2016; Melia et al., 2016), new routes have been hypothesized and modelled as ongoing sea ice loss measurements are being recorded (Smith & Stephenson, 2013). As such, previously unavailable opportunities for Arctic oil exploration have recently become possible and increasingly attractive (Arctic Monitoring and Assessment Programme, 2010b; Hasle et al., 2009), as an estimated 90 billion undiscovered barrels of oil (~6 % of the world's known reserves) are located within the Arctic (Bird et al., 2008). Both the total cargo (tonnes), and frequency of ships navigating across the Arctic have surged in the past decade (Eguíluz et al., 2016; Gunnarsson, 2021; Silber & Adams, 2019). Along with an increasing interest in oil exploration and exploitation within the Arctic, the risks of a heavy or crude oil spill in an Arctic marine setting are of special concern.

Advances in Arctic marine oil spill research by the late 1970's had culminated to where large-scale field studies became quintessential to produce meaningful, novel discoveries (Sergy & Blackall, 1987). Laboratory and mesocosm experiments were insufficient in practicality, as

they fundamentally lack the complexities of a natural ecosystem (Chikere et al., 2011; M. Reed et al., 1999; Sergy & Blackall, 1987). Also, pertinent information surrounding the efficacy of oil clean-up measures (E. H. Owens, Robson, et al., 1987; H. Owens, 1984), and the outcomes associated with a spill of a stranded crude oil within the Arctic over time was limited (Sergy & Blackall, 1987). As such, the rationale behind contaminating an untouched Arctic setting to better understand the long-term fate and behaviour of crude oil within the Arctic led to the conception of the Baffin Island Oil Spill (BIOS) Project at Cape Hatt, Baffin Island, Canadian Arctic, in 1979 (Figure 3.1)(Sergy & Blackall, 1987). The key elements of the BIOS project involved the natural attenuation of released crude oil within an Arctic setting, and the examination of oil spill countermeasures in both nearshore and shoreline experiments (E. H. Owens, Robson, et al., 1987; Sergy & Blackall, 1987). A series of pre-spill studies were conducted to determine the background concentrations of various hydrocarbons within sediments (Cretney et al., 1987b), water (Cretney et al., 1987a), and in the tissues of marine organisms (Cretney, 1987) present at the BIOS site, as this data is rarely available when examining accidental oil spills. In all three cases, the concentrations of petroleum hydrocarbons were found in the sub to low $\mu\text{g/g}$ and $\mu\text{g/L}$ ranges. In other regions of the Arctic, baseline concentrations of total petroleum hydrocarbons (TPH), and various hydrocarbon groups such as PAHs and n-alkanes have been recorded at sub to low $\mu\text{g/g}$ values, whereas other locations such as Baffin Bay, and coastal zones surrounding Iceland and Greenland harbor media containing much higher hydrocarbon concentrations, in the realm of sub to low $\mu\text{g/kg}$ (Foster et al., 2015; Jörundsdóttir et al., 2014; Mosbech et al., 2007). Consequently, Cape Hatt was determined to be representative of any pristine Arctic setting, and was thus deemed a suitable area to conduct the BIOS Project (Cretney, 1987; Cretney et al., 1987a, 1987b).

The nearshore component of the BIOS Project involved a surface release of 15m³ of a medium-weight Venezuelan Lagomedio crude oil slick on the waters of a protected beach identified as Bay 11 (72.46, -79.829) in 1981 (Figure 1) (E. H. Owens et al., 1994; E. H. Owens, Harper, et al., 1987; Sergy & Blackall, 1987). Without any intervention, the spilled crude oil was carried by wind and wave action onto the intertidal sediments of Bay 11 (Sergy & Blackall, 1987). Studies of oil spill countermeasures were carried out during the shoreline portion of the BIOS Project from 1980 to 1983 at various bays within the well-sheltered Z-lagoon (Figure 3.1) (E. H. Owens, Robson, et al., 1987). The areas of particular interest to the present study are Crude Oil Point (72.482, -79.756) and Bay 106 (72.474, -79.782), which were the sites of supratidal oiled control plots established in 1980 and 1982, respectively (Figure 3.1) (E. H. Owens, Robson, et al., 1987; H. Owens, 1984). The experimental sites of the BIOS project have been revisited on several occasions. Detailed accounts of oil distribution mapping, oil volumes, TPH analyses, and oil composition have been published from short time periods post-spill to up to twenty years later (Humphrey et al., 1992a; E. Owens et al., 2002; H. Owens, 1984; Prince et al., 2002; Zhendi. Wang et al., 1995). Since then, a single return to the BIOS site took place in 2019, nearly forty years after the initial sets of experiments, and which forms the basis of the present study. Information regarding potentially toxic oil residues such as polycyclic aromatic hydrocarbons (PAHs), and an examination of microbial degradation and general weathering patterns within backshore sediments collected during the 2019 BIOS site revisit are discussed elsewhere (Hunnie *et al.*, 2023; Schreiber & Hunnie *et al.*, Under Review). In contrast, the present study provides a closer look at the fate of saturates and biomarkers of with crude oil associated with intertidal and backshore sediments of the BIOS Project.

Crude oil does not represent a sole chemical species, but is rather made up of thousands of distinct compounds. Different types of crude oil exist as well, all with different compositions and proportions of their respective compounds (Fakher et al., 2020; Sugiura et al., 1997). The primary constituents of crude oil hydrocarbons can be broken down into four categories: saturates, aromatics, resins, and asphaltenes (Fakher et al., 2020; Leahy & Colwell, 1990; Sugiura et al., 1997). The chemical structures of resins and asphaltenes are challenging to distinguish and identify due to their sizes and complexities (Acevedo et al., 2007; Akmaz et al., 2011; Demirbas & Taylan, 2016; Groenzin & Mullins, 1999; Harayama et al., 1999). However, many compounds within the saturates and aromatics have structures that are readily identifiable (Saltymakova et al., 2020). The aromatic fraction of crude oil is largely composed of PAHs and alkylbenzenes (Francis, 1948; Haritash & Kaushik, 2009; Jesus et al., 2022; Sinninghe Damste et al., 1988). Saturates are made up of linear n-alkanes, branched alkanes, and cycloalkanes, together making up the largest proportion of hydrocarbons within crude oil (Wentzel et al., 2007; Wilkes et al., 2003). n-Alkanes are of particular interest when considering the long-term fate of crude oil due to their recalcitrance as a consequence of their inherent inertness, in addition to their high relative abundance in the composition of crude oil (Wentzel et al., 2007). Despite their lack of reactive centres, certain physiochemical properties of n-alkanes such as chain length affect their susceptibility to degrade over time (Alvarez et al., 2009; Rocha et al., 2011; Wardroper et al., 1984). Cycloalkanes also make up a large component of the saturate fraction in crude oil (Kissin, 1990). In general, increased structural complexity (cyclic versus linear) and increased degrees of substitution of alkanes leads to higher recalcitrance. Therefore, cycloalkanes are an important component of the saturated fraction of crude oil to monitor (Alvarez et al., 2009; Johnson et al., 2012; Rocha et al., 2011). As it pertains to the saturates, this

work focuses mainly on concentrations of linear n-alkanes and alkylcycloalkanes, but also includes data for two very important branched alkanes, pristane and phytane, which can be used to estimate the extents of various weathering processes (M. Blumer & Sass, 1972; Kristensen et al., 2015; Ward et al., 2018). A final class of compounds found within crude oil are referred to as biomarkers, and primarily include hopanes, steranes and terpanes. These compounds are very resistant to degradation, and thus serve as useful tools when normalizing concentration data of other compound groups such as n-alkanes (Bragg et al., 1993; Vergeynst, Greer, et al., 2019; Z. Wang et al., 1999). In particular, $17\alpha(H),21\beta(H)$ hopane is commonly used as an internal biomarker to account for variation in degradation between samples, when available (Bragg et al., 1993; Liu et al., 2022; Prince et al., 2002; Vergeynst, Greer, et al., 2019). This study analyzed a collection of hopanes and steranes, and reports concentrations of other compound groups that have been normalized to $17\alpha(H),21\beta(H)$ hopane.

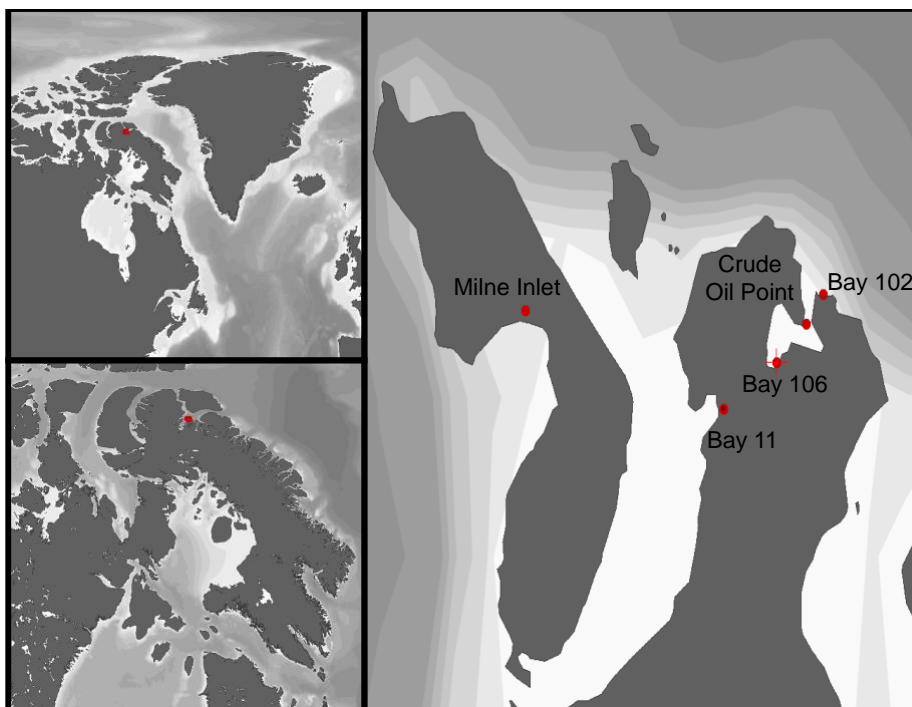


Figure 3.1. Locations of the sampling stations from the 2019 revisit of the BIOS site during the CCGS Amundsen expedition, created in Ocean Data View (Schlitzer, 2023). For the purposes of this study, Bay 102 and Milne Inlet were considered as control sites.

The BIOS project is truly a unique and valuable tool for progressing Arctic oil spill research. No other such study exists on similar temporal and geographic scales in its domain. Furthermore, obtaining legislative approval for a novel study looking at similar issues would be highly unlikely in current times, increasing the value of continuing ongoing studies such as the BIOS project. This work serves to build on the results and knowledge obtained from the original BIOS project and the number of revisitations, as well as the general understanding of long-term hydrocarbon weathering. In light of the advances made, a number of gaps in the collective knowledge of Arctic oil spills are apparent. This study aims to uncover the fate of various crude oil residues within Arctic beach sediments over the course of roughly forty years. Secondly, this is among the first works that provide quantitative results of individual crude oil hydrocarbon concentrations at the BIOS site. Thirdly, this is the first examination of alkylbenzenes and

alkylcycloalkanes within BIOS sediments. The efforts herein strive to develop the collective understanding of the long-term effects of natural attenuation of n-alkanes, alkylbenzenes, alkylcycloalkanes, hopanes and steranes within Arctic sediments. The results herein compliment data presented within Schreiber and Hunnie *et al.* (under review), which provide an assessment of the microbiological communities present at the BIOS site, and their capacities to degrade the measured hydrocarbons. Doing so can add important information to the ongoing evidence to influence decision makers away from considering future oil exploration and exploitation within the global Arctic.

Materials and Methods

Sample Collection

Samples were collected from the five sampling sites associated with the BIOS Project (Figure 3.1). A grand total of 86 samples including oiled sediments and controls, and both from the surface (0-2cm) and the subsurface (5-10cm) were acquired over the span of two days during the third leg of the 2019 CCGS Amundsen Expedition (Table 3.S1; for more details on sampling see Hunnie *et al.*, 2023). All samples were sheltered from solar radiation until they could be stored on the CCGS Amundsen at 4°C, then were kept frozen at -20°C during transport to and storage at the Centre for Earth Observation Science (CEOS) at the University of Manitoba (Hunnie *et al.*, 2023). Sample nomenclature was mainly selected based on the classifications of the experimental plots assigned during the original BIOS project (Hunnie *et al.*, 2023). An overview of the collected oiled samples can be found in Table 3.1.

Table 3.1. Locations and nomenclature of oiled surface (0-2cm) and subsurface (5-10cm) beach sediment samples collected from the BIOS site during the 2019 CCGS Amundsen Expedition.

Site	Sample I.D.	No. replicates	Sample location characteristics
Bay 11	B11-BS	2	backshore area
	B11-I	8	intertidal zone ^a
Z-Lagoon, Bay 106	IMC-c	3	above high-water swash, below high storm swash line ^b
	IMC-e	3	
	IME-c	3	
	IME-e	3	
Z-Lagoon, Crude Oil Point	T1	2	backshore, above high-water mark ^b
	T2	2	

^aLocations described by E. H. Owens, Harper et al. (1987).

^bPlot positions described by Owens (1984).

Sample Processing

Hydrocarbon fractionation extractions were performed on all samples, adopting the methods outlined in Asihene (2019). In most cases, extraction batches consisted of 11 unique samples, two laboratory duplicates, two laboratory blanks, and one Standard Reference Material (SRM), for a total of 16 extractions. To examine the recoveries of n-alkanes of varying sizes throughout the extraction process, all samples were spiked with 10-30 μL Chiron AS perdeuterated n-alkane solution (seven compounds, prepared to 5.0 $\mu\text{g}/\text{mL}$ in iso-octane; Table 3.S2) (Aslund, 2019b). In order to quantify the hydrocarbons of interest in each sample, 150 μL 2-fluorobiphenyl (prepared to 2.0 $\mu\text{g}/\text{mL}$ in iso-octane) was added as an internal standard. A sample of the crude oil initially applied during the original BIOS experiments was graciously sent to CEOS by Environment and Climate Change Canada (Hunnie *et al.*, 2023). Subsamples of this technical mixture were spiked with the same Chiron AS perdeuterated n-alkane solution and 2-fluorobiphenyl.

Consistency during the sample preparation phase was monitored by comparing the concentrations of n-alkanes, hopanes and steranes between laboratory duplicates. The congruity between laboratory duplicates regarding n-alkane, hopane and sterane concentrations was 72 % and 82 %, respectively. To account for laboratory contamination, a pre-washed sand baked for eight hours at 550 °C was used as the laboratory blanks, then had had their respective hydrocarbon concentrations subtracted from the rest of the samples. The SRMs used for this experiment were NIST 1941b (Gonzalez & Watters, 2015) and NIST 1944 (Gonzalez & Choquette, 2017). Both SRMs were chosen, based on their extensive suites of certified mass fractions for PAHs, the results of which are outlined in Hunnie et al. (2023). NIST 1944 had no officially stated data for n-alkanes or hopanes and steranes but were analyzed to monitor the consistency of these compounds between extraction batches. The average uniformity of hopane and sterane concentrations within NIST 1941b and NIST 1944 across all batches was 86 % and 93 %, respectively.

n-Alkane analysis

A suite of n-alkanes from nC11-nC35 were analyzed using the LECO Pegasus multidimensional gas chromatography high-resolution time of flight mass spectrometry (GCxGC-HR-TOF-MS, LECO) instrument, which operates in a full-scan mode. Instrumental parameters followed those outlined in Saltymakova *et al.* (2020) and Desmond *et al.* (2021), with slight adjustments (Table 3.S3). A full list of the compounds included in this work, along with their quantitation limits can be found in Table 3.S4. A mixture of standards for identification and quantitation of n-alkanes was prepared, which included nC11-nC18 n-alkanes (SPEX CertiPrep, 2019), nC15-nC35 odd n-alkanes (Burton, N.D.a), and nC16-nC36 even n-alkanes (Burton,

N.D.b) (prepared to 5.0 $\mu\text{g/mL}$ in iso-octane). A separate series of calibration standards was prepared to identify and quantify pristane and phytane (Aslund, 2019a). Weekly instrument tunes were conducted to ensure proper function of the analytical assembly. The software used for qualitative and quantitative analyses of n-alkanes was LECO ChromaTOF (ver. 5.10). Nine-point calibration curves ranging from 8.8 – 2250 ng/mL were constructed. Due to the presence of n-alkanes nC15-nC18 in two of the standards included in our mixture, these four compounds exhibited concentrations of 17.6 – 4500 ng/mL within their respective calibration set. The corresponding r values for every compound within the calibration curves were ≥ 0.99 , except for pristane, octadecane, and docosane, which had r values of 0.98. Despite extracting small amounts of sediments, many samples had to be diluted further upon storing them in GC vials, as concentrations of various n-alkanes greatly exceeded the respective upper quantitation limits. A low-end signal-to-noise (S/N) ratio limit of 5.0 was assigned to the quantitation of each compound. As such, if the peak S/N for a particular n-alkane fell below the limit, the retention time was examined to determine whether a distinguishable signal was present on its chromatogram. Analytical consistency was assessed by analyzing laboratory and instrument duplicates, which proved to be in agreement by 72 and 89 %, respectively. Additionally, the average recovery of the included perdeuterated n-alkanes was 100%.

Alkylbenzene and alkylcycloalkane analysis

A standard mixture of nine alkylcycloalkanes (prepared to 5.0 $\mu\text{g/mL}$ in iso-octane) (Knott, 2019) and 16 alkylbenzenes (prepared to 5.0 $\mu\text{g/mL}$ in iso-octane) (Kalouzskaya, 2017) was prepared for identification and quantitation, *via* the Agilent 7010B Triple Quadrupole GC/MS device operating in Multiple Reaction Monitoring (MRM) mode. A list of the

compounds analyzed, their respective limits of quantitation, and ion transitions can be found in Table 3.S5. An Rxi-PAH column (59.5 m x 250 μm x 0.1 μm) was attached to the back inlet, which was equipped with a split (10:1) liner, and exhibited a split flow of 11 mL/min. The electron ionization energy and the gain factor were set to 70 eV and 5.0, respectively. Helium was used as the carrier gas, and nitrogen as the collision gas, at flow rates of 1.1 mL/min and 1.5 mL/min, respectively. The oven parameters for this method include an initial temperature of 40 $^{\circ}\text{C}$ held for 1.5 minutes, followed by a 30 $^{\circ}\text{C}/\text{min}$ ramp to 140 $^{\circ}\text{C}$, then to 190 $^{\circ}\text{C}$ at 3 $^{\circ}\text{C}/\text{min}$, and to a final temperature of 290 $^{\circ}\text{C}$ at a rate of 10 $^{\circ}\text{C}/\text{min}$ where it was then held for 10 minutes. The total runtime was 41.5 minutes. A post-run time of 5 minutes at 300 $^{\circ}\text{C}$ occurred after each run. Routine tunes were validated to assess the functionality of the instrumental components, and air-water checks were executed before every analysis to monitor for leaks. The software used to identify and quantify these compounds were the Agilent MassHunter Qualitative Analysis B.07.00 and the Agilent MassHunter Quantitative Analysis (for QQQ), respectively. An eight-point calibration curve ranging from 2.2 – 281.3 ng/mL with $1/x$ R^2 values ≥ 0.98 was prepared for the quantitation of these two groups of hydrocarbons, with a low-end peak S/N limit of 5.0. Laboratory and instrument duplicates were included in each batch of analyzed samples. With regards to the alkylbenzenes and alkylcycloalkanes, the laboratory duplicates demonstrated 87.2 and 80.8 % reproducibility, respectively, and respective 93.8 and 93.4 % reproducibility within the instrument duplicates.

Hopane and sterane analysis

A collection of 11 biomarkers (hopanes and steranes) based on the Chiron S-4492-10-IO standard mixture (prepared to 10.0 $\mu\text{g}/\text{mL}$ in iso-octane) was chosen for analysis on the Agilent

7010B Triple Quadrupole GC/MS instrument in MRM mode. The instrument settings for the MRM analysis are similar to those mentioned in Saltymakova *et al.* (2020), with minor changes (Table 3.S6). Tunes and air-water leak checks were conducted as described previously. The same two pieces of software used for the alkylbenzenes and alkylcycloalkanes were utilized for the characterization of the hopanes and steranes. A 10-point calibration curve with concentrations ranging from 2.0 – 1000.0 ng/mL with $1/x R^2$ values of ≥ 0.95 was applied for quantitation of the hopanes and steranes included within the analysis. In certain cases, individual compound concentrations exceeded those denoted in the calibration curve. As such, a second, five-point curve from 250.0 – 2500.0 ng/mL with $1/x R^2$ values of ≥ 0.96 was generated to properly quantify these aforementioned compounds. The names, limits of quantitation, and ion transitions for the hopanes and steranes are reported in Table 3.S7. Similarly, to the preceding analyses, a low-end peak S/N limit of 5.0 was applied to all hopanes and steranes. Laboratory and Instrument duplicates were included in every batch of analyzed samples, and exhibited 82.2 and 93.0 % precisions, respectively.

Principal Components Analysis (PCA)

PCAs were conducted to examine any potential relationships between individual hydrocarbons within the n-alkanes, alkylbenzenes, and alkylcycloalkanes. The mean values of individual compound concentrations were calculated from respective replicates, then imported into RStudio (ver. 2022.12.0+353, RStudio Posit Software PBC, 2020). The RMarkdown files including the code used to conduct the individual PCAs, as well as the associated figures produced to share the PCA results can be found [here](#).

Results and Discussion

General compound group comparison

Relative proportions of the analyzed compound groups (i.e. alkylbenzenes, alkylcycloalkanes, hopanes and steranes, pristane and phytane, nC11-nC15 alkanes, nC16-nC26 alkanes, nC27-nC35 alkanes, PAHs) in oiled samples and the technical mixture are presented in Figure 3.2. The PAH data is presented to provide a more comprehensive depiction of the overall crude oil composition; a full detailed discussion on the presence and potential toxicity of PAHs within the BIOS sediments has been published previously (Hunnie *et al.* (2023)). For the sake of transparency, when mentioning the n-alkanes as their own hydrocarbon group in this manuscript, the branched alkanes pristane and phytane are included as well. Of the compound groups analyzed, the n-alkanes were the predominant species detected, with an average proportion of 91%. In contrast, the group contributing the least to the total proportion of hydrocarbons was the alkylbenzenes, with an average proportion of <1% (Figure 2). Despite there being no recorded average hopane or sterane concentrations within the subsurface B11-BS, some were detected but were measured below the concentration of those within the laboratory blanks from their respective batches (Figure 3.2).

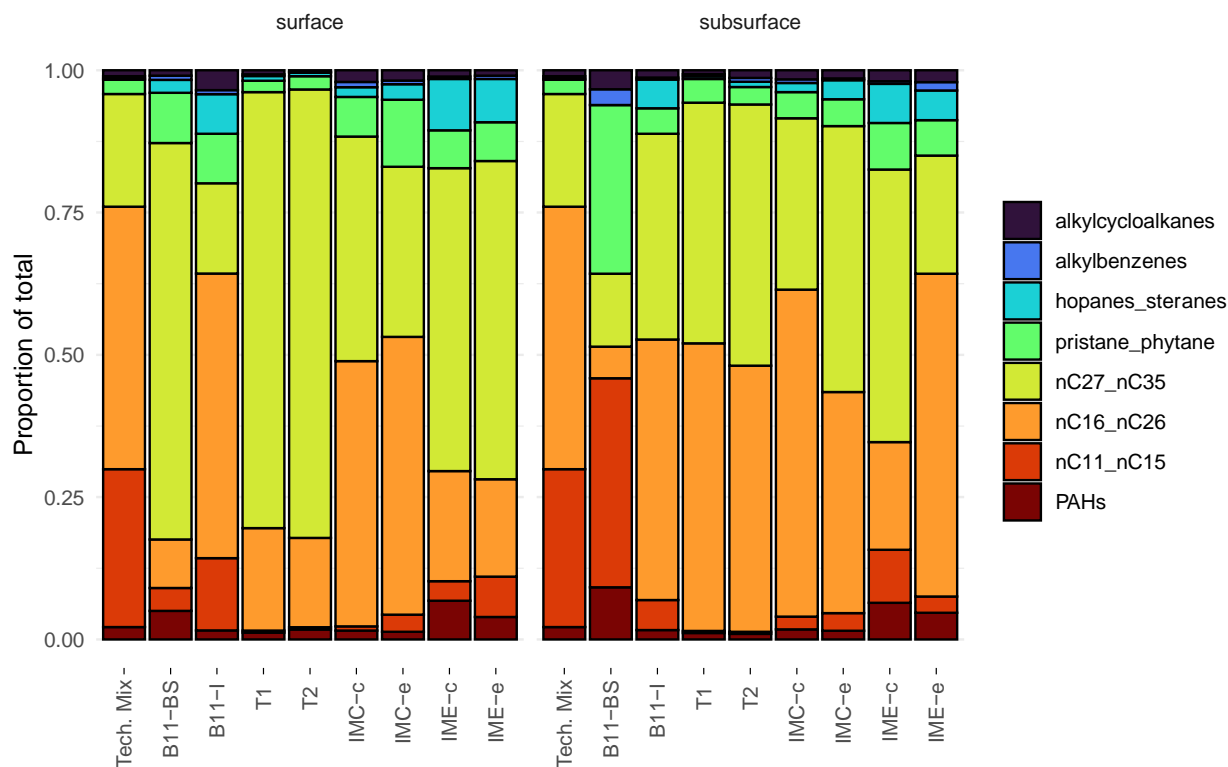


Figure 3.2. Relative proportions of PAHs, alkanes (which are divided into subcategories nC11-nC15, nC16-nC26, nC27-nC35, and pristane-phytane), hopanes and steranes, alkylbenzenes, and alkylcycloalkanes measured within the oil residues from the samples collected during the 2019 revisit of the BIOS site. In this figure, “Tech. Mix” refers to the technical mixture

Total mean concentrations of each compound group

Extensive depletion of the hydrocarbon groups within the samples collected during the 2019 revisit of the BIOS site was observed. Across all compound groups, Bay 11 consistently demonstrated the highest extents of depletion, followed by Bay 106, and then finally Crude Oil Point (Table 3.2). Interestingly, a one-way analysis of means not assuming equal variances reveals a statistically significant difference in total PAH concentrations between surface and subsurface sediments collected from the intertidal zone at Bay 11 ($p = .045$); however, no statistically significant differences were detected with regards to the total mean concentrations of n-alkanes ($p = .42$), hopanes and steranes ($p = .78$), alkylbenzenes ($p = .69$),

nor alkylcycloalkanes ($p = .39$). Although it is difficult to tease apart any one potential cause of the observed difference between the PAHs and other compound groups with respect to the sample depth, the analyzed PAHs cover a wide range of molecular weights (MW) (128 – 278 g mol^{-1}) and structures, and could therefore exhibit preferential dissolution and volatilization of the lighter MW PAHs within the surface sediments, relative to the subsurface sediments. Additionally, the aromatic compounds are the only ones in this dataset that are sensitive to photooxidation (Dabestani & Ivanov, 1999; Garrett et al., 1998; Larson et al., 1979; Yu et al., 1997), which could be another driver of the significant difference observed between the surface and subsurface PAH concentrations.

The overall concentrations of crude oil residues within the sediments at Crude Oil Point were the most unchanged across the revisited sites of BIOS Project (Table 3.2). The relative proportions of each hydrocarbon group analyzed within the Crude Oil Point samples also most closely resembled those of the technical mixture, with the exception of short chain n-alkanes (Figure 2). In particular, this is observed for the crude oil plot T1, more so than for the crude oil-water emulsion plot T2, although they are proportionally similar (Figure 3.2). Additionally, a one-way analysis of means not assuming equal variances suggests that there are no statistically significant differences between sample depth (surface vs. subsurface) and oil type (crude oil vs. oil-water emulsion) with respect to the total mean concentrations of PAHs ($p = .15$), n-alkanes ($p = .29$), hopanes and steranes ($p = .29$), alkylbenzenes ($p = .13$), and alkylcycloalkanes ($p = .10$).

Bay 106 was the site to test post-oiling sediment mixing as a countermeasure (E. H. Owens, Robson, et al., 1987). After incurring thirty seven years of weathering, a one-way analysis of means not assuming equal variances determined that there were no statistically significant differences between sample depth, oil type, nor mixing (tilled vs. not tilled) as

regarding the total mean concentrations of PAHs ($p = .053$), n-alkanes ($p = .12$), hopanes and steranes ($p = .27$), alkylbenzenes ($p = .22$), and alkylcycloalkanes ($p = .079$) within the sediments from Bay 106. As such, when considering the long-term degradation of crude oil within Arctic sediments, it appears that tilling the sediments did not have an impact on the total concentrations of hydrocarbon groups.

Table 3.2. Total mean concentrations of detected PAHs, n-alkanes, hopanes and steranes, alkylbenzenes, and alkylcycloalkanes within oiled sediments from the BIOS site revisited in 2019, and the technical mixture.

Sample I.D.	ΣPAHs		Σn-alkanes		Σhopanes and steranes		Σalkylbenzenes		Σalkylcycloalkanes	
	[mean] (mg/kg)	(std. dev)	[mean] (mg/kg)	(std. dev)	[mean] (mg/kg)	(std. dev)	[mean] (mg/kg)	(std. dev)	[mean] (mg/kg)	(std. dev)
Technical Mixture	3240	47.7	144000	11000	284	16.6	618	203	1570	584
B11-BS 0-2	0.935	0.400	16.9	11.7	0.418	0.332	0.138	0.0100	0.179	0.0634
B11-BS 5-10	0.192	0.0561	1.77	0.208	0.00	0.00	0.0577	0.0134	0.0699	0.00162
B11-I 0-2	0.0486	0.0329	2.67	1.91	0.213	0.213	0.0213	0.0282	0.108	0.142
B11-I 5-10	0.0831	0.0317	4.58	5.74	0.253	0.327	0.0171	0.0141	0.0643	0.0518
T1 0-2	7.12	1.63	572	21.8	4.82	6.81	1.86	2.54	4.19	5.47
T1 5-10	14.0	1.80	1210	177	5.74	5.74	4.80	4.76	8.43	8.17
T2 0-2	13.1	0.167	736	462	4.68	4.68	1.08	1.01	2.14	1.82
T2 5-10	12.3	1.90	1210	332	11.7	2.48	8.60	6.52	16.9	12.8
IMC-c 0-2	7.99	5.58	482	327	8.78	5.97	4.68	3.35	10.6	7.11
IMC-c 5-10	4.27	1.60	225	136	3.83	2.66	1.49	1.22	3.84	2.95
IMC-e 0-2	0.429	0.430	29.9	34.7	0.870	1.03	0.212	0.244	0.577	0.723
IMC-e 5-10	0.914	1.04	55.3	71.4	1.98	2.45	0.173	0.200	0.860	1.07
IME-c 0-2	3.66	5.11	44.5	48.0	4.86	6.30	0.226	0.314	0.599	0.792
IME-c 5-10	1.47	1.23	19.3	15.7	1.57	1.16	0.102	0.0362	0.444	0.134
IME-e 0-2	0.532	0.250	11.7	3.60	1.02	0.537	0.0808	0.0238	0.128	0.0466
IME-e 5-10	5.08	3.43	93.9	62.5	5.66	3.70	1.60	1.62	2.27	2.30

Since n-alkanes made up the vast majority of the crude oil composition within all the samples from the BIOS Project (Figure 3.2, Table 3.2), this group of hydrocarbons was subdivided into the four categories as described above (Table 3.3). When considering the relative abundances of the n-alkane subgroups within the technical mixture, the compounds of medium chain-length were present in the highest total amount, but this group also includes the highest number of compounds. Short chain n-alkanes (nC11-nC15) were in fact present in higher concentrations than medium length n-alkanes (nC16-nC26), there were just fewer compounds within this subcategory (Table 3.3). It is expected that the short chain n-alkanes would likely volatilize quickly into the atmosphere, therefore the varying environmental conditions at each site would not influence this process. A *post-hoc* analysis of the values between sites and the respective n-alkane groups was performed, using the Holm-Sidak method ($\alpha = .05$). Regarding the short chain alkanes, there were no statistically significant differences detected between Bay 11 and Crude Oil Point ($p = 1$), Bay 11 and Bay 106 ($p = .99$), nor between Crude Oil Point and Bay 106 ($p = 0.98$), which supports the above claim. When considering the medium chain n-alkanes, there were no significant differences between the values from Bay 11 and Bay 106 ($p = .33$) however, there were statistically significant differences between Bay 11 and Crude Oil Point ($p < .001$) and between Crude Oil Point and Bay 106 ($p < .001$). A two-way ANOVA determined that there were no statistically significant differences between sample depth ($p = .33$) across the four subcategories of alkanes ($p = .47$). As such, the driving factor of these observed differences would largely be attributed to tidal action, which can cause both physical removal from the sediments into water, and provide an influx of hydrocarbon-degrading bacteria. The trends observed for the long chain n-alkanes (nC27-nC35) were identical to the medium chain n-alkanes between the sites ($p = .48$, $p < .001$, $p < .001$, respectively). Finally, there were no

significant differences across any of the site combinations in respect to pristane and phytane ($p = .90$, $p = .95$, $p = .93$, respectively). Although extensive weathering of these two compounds did occur at each site (Table 3.3), the losses appear to be proportionally uniform among the hydrocarbon compositions of samples across sites, based on total amounts of hydrocarbons.

Table 3.3. Total mean concentrations of alkane subcategories nC11-nC15, nC16-nC26, nC27-nC35, and pristane & phytane within oiled sediments from the BIOS site revisited in 2019, and the technical mixture.

Sample I.D.	Σ nC11-nC15		Σ nC16-nC26		Σ nC27-nC35		pristane & phytane	
	[mean] (mg/kg)	(std. dev)	[mean] (mg/kg)	(std. dev)	[mean] (mg/kg)	(std. dev)	[mean] (mg/kg)	(std. dev)
Technical Mixture	41600	1760	69000	1240	29700	719	3780	390
B11-BS 0-2	0.743	0.866	1.58	1.31	12.9	9.46	1.64	0.207
B11-BS 5-10	0.767	0.651	0.116	0.0280	0.267	0.267	0.620	0.153
B11-I 0-2	0.389	0.443	1.53	1.05	0.485	0.547	0.266	0.0636
B11-I 5-10	0.263	0.185	2.29	2.48	1.80	3.19	0.224	0.0485
T1 0-2	2.05	0.434	106	13.7	452	9.38	11.8	3.07
T1 5-10	4.54	0.820	627	91.7	524	67.3	51.7	11.0
T2 0-2	3.23	0.301	119	69.8	597	385	17.7	4.82
T2 5-10	4.48	1.16	587	264	576	67.7	38.2	8.43
IMC-c 0-2	3.75	1.63	239	159	203	146	35.8	7.18
IMC-c 5-10	5.28	2.29	137	91.7	71.8	37.3	11.0	1.27
IMC-e 0-2	0.967	0.904	15.6	20.0	9.57	12.7	3.77	0.443
IMC-e 5-10	1.82	1.06	23.0	30.2	27.7	36.7	2.79	0.372
IME-c 0-2	1.85	0.881	10.4	13.7	28.7	29.1	3.58	0.926
IME-c 5-10	2.13	0.566	4.32	1.52	10.9	12.4	1.87	0.254
IME-e 0-2	0.952	0.429	2.30	0.358	7.51	3.25	0.913	0.130
IME-e 5-10	3.09	1.89	61.5	52.3	22.5	13.9	6.76	1.48

n-Alkane composition

The composition of the analyzed n-alkanes within the technical mixture, mean control samples, and oiled samples are shown in Figure 3.3 (for associated data see Table 3.S9). These profiles highlight the differences in the relative percentages of individual n-alkanes amongst samples from both within a single site, and across sites. The n-alkane compositions of the Bay 11 samples appear erratic (Figure 3.3), mainly due to the limited detection of various compounds when processing the available data. Many compounds that were detected were present in very low concentrations, and some were below their respective limits of quantitation (Table 3.S4) and thus could not be accurately quantified, therefore those compounds were listed as “not detected.” Overall, the compositions of n-alkanes differed considerably between sites (Figure 3.3), and between the BIOS samples and the technical mixture (Figure 3.3A). The relative proportions of individual alkylbenzenes and alkylcycloalkanes are presented in Figures 3.S1-3.S2 and Tables 3.S10-3.S11, respectively.

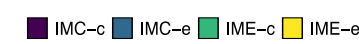
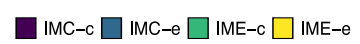
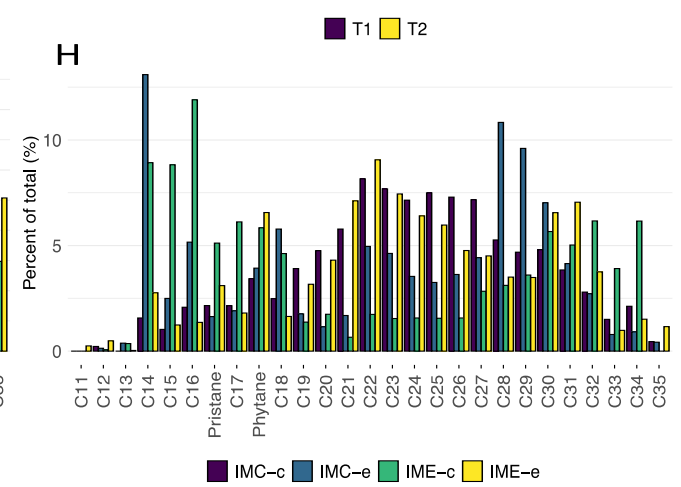
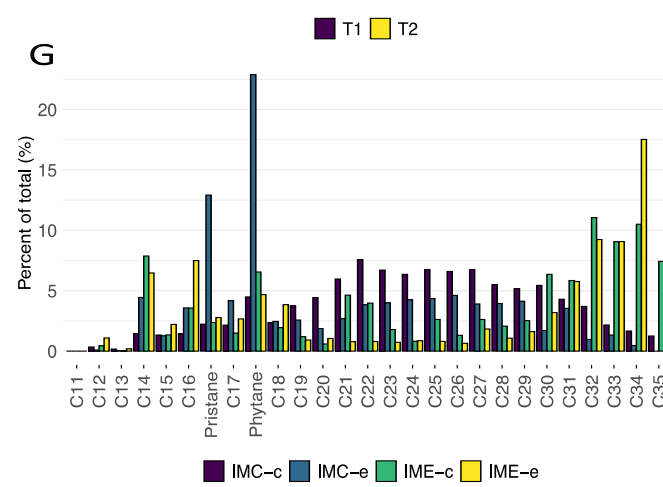
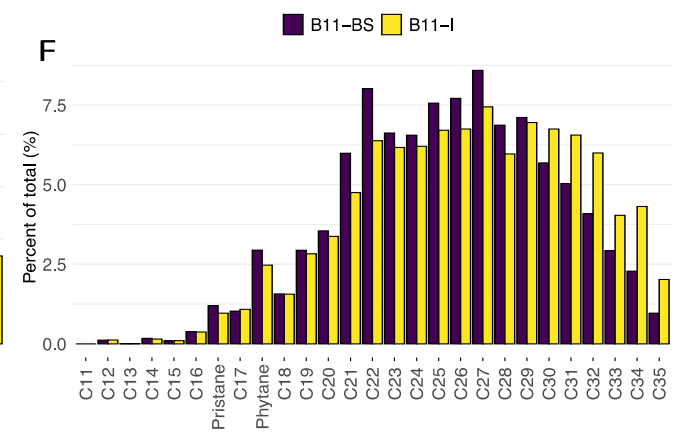
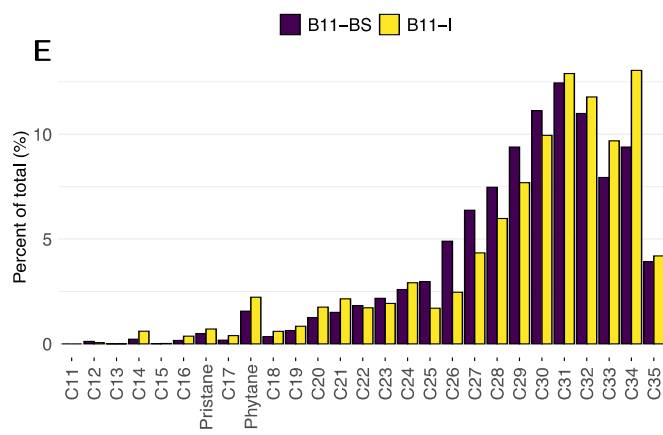
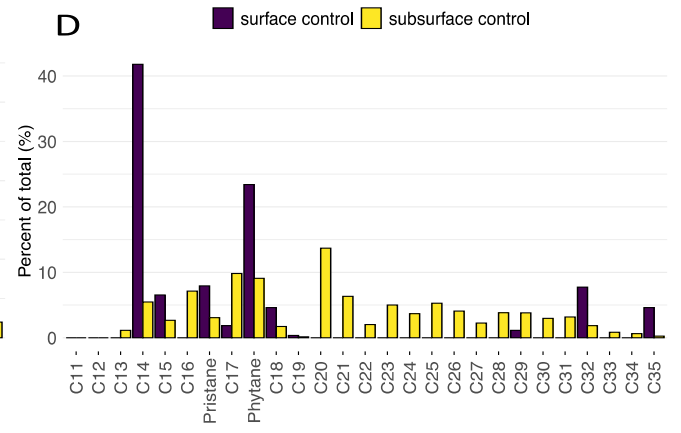
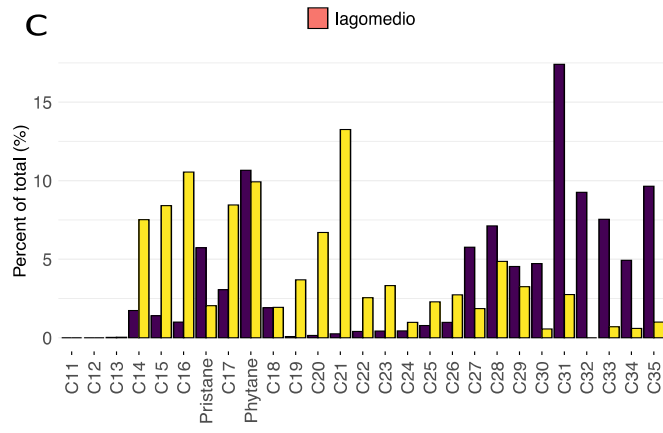
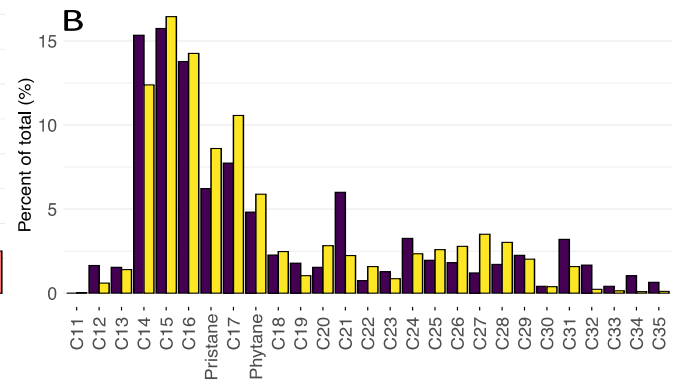
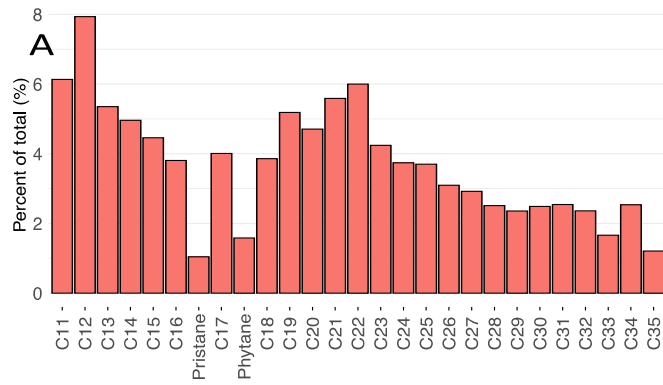


Figure 3.3. Composition of n-alkanes, represented by the percentage (%) towards the total measured concentration of alkanes present within each sample. (A) = technical mixture, (B) = mean surface and subsurface control sample values, (C) = Bay 11 surface sediments, (D) = Bay 11 subsurface sediments, (E) = Crude Oil Point surface sediments, (F) = Crude Oil Point subsurface sediments, (G) = Bay 106 surface sediments, (H) = Bay 106 subsurface sediments.

Principal component analysis of n-alkanes

n-Alkane compositions were analyzed by principal component analysis (PCA; Figure 3.4). A separate PCA was carried out for alkylbenzenes and alkylcycloalkanes. However, as these compound groups contributed relatively little to the total concentration of crude oil residues (Figure 3.2), results of these analyses are presented as part of the supplementary information (Figures 3.S3-3.S4). Principal components of the n-alkane composition data (PC) 1 and 2 account for 37.62 and 31.56 % of the total variance, respectively (Figure 3.4). The top and bottom quadrants are well-separated by longer versus shorter-chained n-alkanes, with a clockwise behaviour of increasing carbon constituents starting from the bottom-left quadrant, up to the top-left quadrant (Figure 3.4). The component scores are likewise fairly evenly distributed across the axes, with a heavier emphasis of variation between PC1, rather than PC2, especially for the samples from Bay 106. As this plot only encompasses 69.18% of the cumulative variance, PC3 was investigated, as it contributes 10.1 % towards the total variance. However, PC3 appears to have a negligible impact on the distribution of samples from both Crude Oil Point and Bay 106, whereas B11-I 0-2 and B11-BS 5-10 shared roughly equal, but opposite positions on the PC3 axis.

The intertidal samples collected from Bay 11 appear to be mainly characterized by n-alkanes of carbon chain length nC14-nC21 (Figure 3.4). Roughly 71 % of the n-alkane composition found within B11-BS 0-2 is made up of nC27-nC35, positioning itself far to the left

on the PC1 axis (Figure 3.4). The n-alkane composition of the backshore subsurface sample, B11-BS 5-10 is almost entirely made up of nC14, nC15, pristane, and phytane. Hence, it shows a strong, positive correlation to these particular compounds (Figure 3.4).

The four samples from Crude Oil Point appear in two distinct clusters, differentiated by sample depth. However, there appears to be no correlation observed between these two clusters, as they are positioned orthogonally to one another on the PCA plot (Figure 3.4). The surface samples are mainly characterized by the n-alkanes of \geq nC30, and suggest a strong, negative correlation with n-alkanes with chain lengths of nC18-nC21. The subsurface samples from Crude Oil Point show relatively high proportions of n-alkanes of chain length nC21-nC29 and also negligible proportions of alkanes nC11-nC16, hence the strong, negative correlation with the bottom-left quadrant (Figure 3.4).

The n-alkane composition of the IME-e 0-2 sample is mostly made up of shorter-chained alkanes such as nC14, nC16, pristane, and phytane, as well as the long-chain alkanes nC32-nC35, providing this sample with the lowest value captured by PC1 (Figure 3.4). The two IME-c samples also follow this general trend, but to lesser extents. In an opposite fashion, the surface and subsurface IMC-c and IMC-e samples have a more even distribution of the entire suite of the analyzed n-alkanes, with a heavier contribution from the medium-chained alkanes nC18-nC30 (Figure 3.4). The discrepancies between the concentrations of n-alkanes within the provided range lead to their differences within PC2.

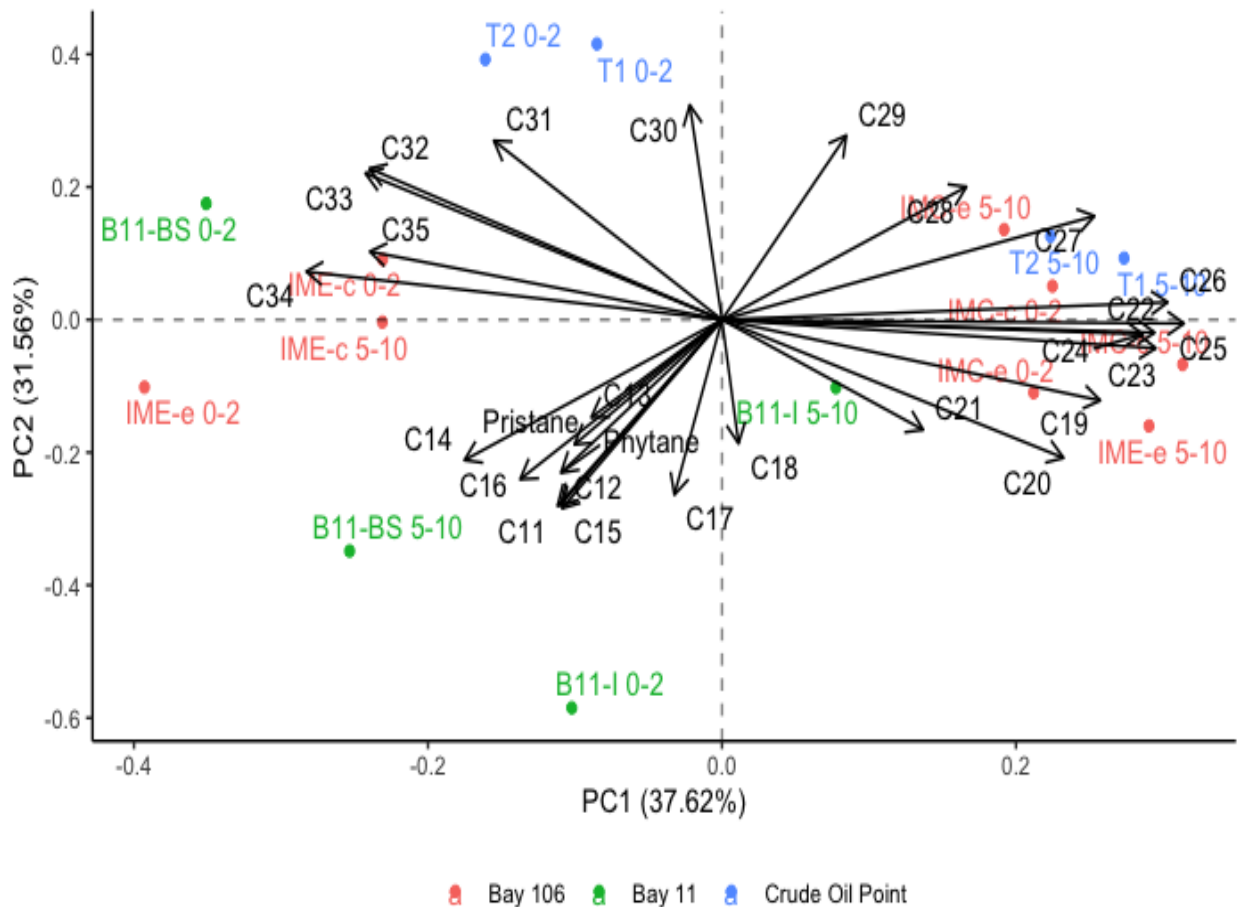


Figure 3.4. Principal Components Analysis (PCA) made up of component loadings (labelled vectors) and component scores (labelled dots) of the n-alkanes present within the oiled sediments from the BIOS site, separated by sampling stations.

Percent Residual Comparison between 2001 and 2019 data

When possible, an attempt is made to compare relevant findings between results from the present study and previous revisitations of the BIOS site. Unfortunately, little data regarding the concentrations of individual hydrocarbons from previous studies encompassed within the BIOS project is available. As a result, the potential to expose temporal variations in the composition of the applied crude oil, apart from comparing directly with the technical mixture is limited (Schreiber & Hunnie *et al.*, Under Review).

Some insight towards the percent loss of specific hydrocarbons are available associated with resampling of the BIOS site in 2001 (Prince *et al.* (2002)). This 2001 data presented the percent losses of octadecane (nC18), phytane, and triacontane (nC30), relative to their respective concentrations found within the technical mixture (see Figure 4 in Prince *et al.* (2002)). In order to account for physical removal of the oil from each sample, the concentrations of each compound were normalized to 17 α (H)21 β (H)hopane (Dutta & Harayama, 2000; Prince *et al.*, 1994, 2002; Venosa *et al.*, 1997, 2002). The extent of further depletion of these compounds was determined by comparing the associated hopane-normalized concentrations from the 2019 samples to those of the technical mixture (Figure 3.5), which was calculated as follows (adapted from (Prince *et al.*, 2002)):

$$\%Residual = 100 - \left(\left(\frac{[X_{Tech.mix}]}{[H_{Tech.mix}]} \right) - \left(\frac{[X_{Sample}]}{[H_{Sample}]} \right) / \left(\frac{[X_{Tech.mix}]}{[H_{Tech.mix}]} \right) \right) * 100$$

Where:

[X] = concentration of analyte X

[H] = concentration of 17 α (H)21 β (H)hopane

Tech.mix = technical mixture

Samples that were considered “fresh,” with little depletion of hydrocarbons between the initial releases of oil until collection in 2001 have undergone extensive degradation in the past eighteen years (Figure 3.5). In particular, the subsurface Bay 11 sample labelled as “B11-I 5-10” demonstrates an additional 79, 90, and 78 % loss in nC18, phytane, and nC30, respectively since 2001. Similarly, the two surface plots from Crude Oil Point, T1 and T2 displayed essentially negligible traces of alkane depletion between 1980 and 2001, but have since exhibited nearly 99 and 98 % losses of nC18, 84 and 85 % losses of phytane, and 26 and 43 % depletion of nC30,

respectively (Figure 3.5). There was relatively little change in the percent residual nC18 within the samples from Bay 106 (IMC-c 0-2 & IMC-c 5-10) compared to what is observed for phytane and nC30.

The compound that experienced the highest extent of degradation between 2001 and 2019 was phytane (Figure 3.5). Overall, the mean percent depletions of nC18, phytane, and nC30 from 2001 to 2019 are 46, 57, and 38 %, respectively. Although phytane is less prone to degradation by most weathering processes than nC18, there was a comparative mean 79 versus 49 % residual phytane to nC18 in the 2001 samples (Figure 3.5).

A significant enrichment of putative microbial oil degraders has been observed in oiled sediments of Crude Oil Point (Schreiber and Hunnie *et al.*, Under Review). This suggests that despite a lack of interaction with the marine interface, the T1 and T2 plots are still subjected to microbial degradation to a certain extent. It is well understood that phytane is resistant to biodegradation, but not to the same capacity as other compounds such as 17 α (H)21 β (H)hopane (Prince *et al.*, 1994; Venosa *et al.*, 1997, 2002). Over time, it is possible that the extensive biodegradation of shorter chained n-alkanes led to a more recent preferential biodegradation of phytane, compared to longer chain n-alkanes such as nC30. The degradation of n-alkanes by photooxidation occurs to a much lesser extent than compared to the degradation of PAHs (Bacosa *et al.*, 2015). It has been mentioned that n-alkanes are not sensitive to ultraviolet waves by themselves, but can be broken down when in the presence of both sunlight and various photochemical products of PAH degradation which act as photosensitizers (Bacosa *et al.*, 2015). It is not expected that nC30 would readily volatilize; however, it is possible that limited extents of volatilization occurred to phytane within each of the samples.

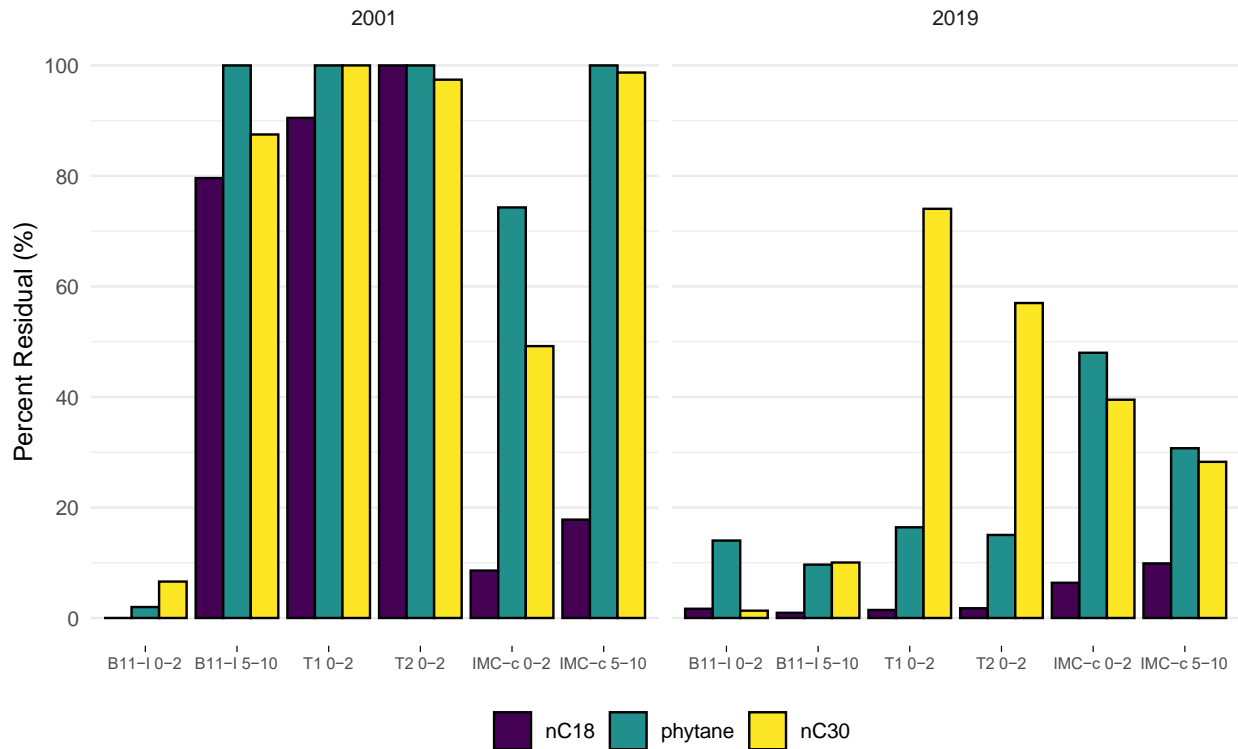


Figure 3.5. Percent residual of n-alkanes octadecane (nC18) and triacontane (nC30), and the isoprenoid alkane phytane within oiled samples collected during the 2001 and 2019 revisitations of the BIOS site. The 2001 data is adapted from Prince et al. (2002), and is included for direct comparison purposes.

There is a slight, noticeable increase in the percent residual of nC18 and phytane from 2001 to 2019 within the surface samples from Bay 11 (Figure 3.5). This could be due the heterogeneity in the manner that the crude oil encroached and remained in the intertidal sediments at Bay 11, which could be affected by the location and number of replicates acquired to produce the mean values shared in Prince et al. (2002). Another possible explanation of this discrepancy is that with the evolution of analytical techniques over the past roughly twenty years; improved instrumental sensitivities could contribute to this observation.

Weathering ratios

The values presented in Table 3.4 with regards to the “T=0” sample are meant to be commensurate of the n-alkane composition within a sample collected from any sampling station at the BIOS site upon initial application, as the composition should be identical across locations when first released. Based on the results denoting the total petroleum hydrocarbon (TPH) values for the year of crude oil application at Bay 11, Crude Oil Point, and Bay 106 provided in Owens (1984), the concentrations of individual hydrocarbons within the T=0 samples were estimated as follows:

$$[X_{i_{T=0}}] = \left(\frac{\sum_{i=1}^n Y_{i_{T=0}}}{n} \right) * \left(\frac{[X_{i_{Tech.mix}}]}{\sum_{i=1}^n [X_{i_{Tech.mix}}]} \right)$$

Where:

$[X_{i_{T=0}}]$ = concentration of compound i within a T=0 sample

$Y_{i_{T=0}}$ = TPH values for each replicate of a T=0 sample

$[X_{i_{Tech.mix}}]$ = concentration of compound i within the technical mixture

All concentration values used in the calculations of the following ratios were normalized to the concentration of 17 α (H)21 β (H)hopane, in order to account for physical removal of crude oil by tidal action from the sampling station (Prince et al., 1994; Venosa et al., 1997, 2002). The nC17/Pristane and Pristane/Phytane ratios are commonly used when assessing the impacts of biodegradation among weathered crude oil samples (B. Blumer & Sass, 1972; Boehm, 1981, 1983; Johnston et al., 2007). The Saturated Hydrocarbon Weathering Ratio (SHWR) has been used for decades as an indicator of general weathering of short-chain n-alkanes to slightly larger-chain n-alkanes (Boehm, 1981, 1983; H. Owens, 1984; Zhendi. Wang et al., 1995) and is calculated as follows:

$$SHWR = \frac{\sum n\text{-alkanes:C11-C25}}{\sum n\text{-alkanes:C17-C25}}$$

Typically, the SHWR would include decane (nC10) in the numerator of the equation however, in this case, decane was not included within the analyzed suite of n-alkanes. Two additional ratios were included for the purposes of comparing the weathering of short chain (nC11-nC15) and medium chain (nC16-nC26) n-alkanes to large chain (nC27-nC35) n-alkanes. These last two ratios were included as no others included data from the large chain n-alkanes, which are widely understood to be more recalcitrant than their shorter-chained counterparts. The results of these five weathering ratios are included for the general T=0 sample, and all comparable samples to those acquired in previous revisitations of the BIOS site (H. Owens, 1984) are presented in Table 3.4.

Much work has been done to understand the patterns of biodegradation concerning n-alkanes. In general, there tends to be preferential biodegradation of short chain n-alkanes versus longer chain n-alkanes, and the linear compounds are typically consumed before branched alkanes (Bacosa et al., 2015; Prince, 2002). Not unexpectedly, the T=0 sample exhibits the highest value for the nC17/Pristane, and Pristane/Phytane ratios, as little to no biodegradation had the opportunity to occur (Table 3.4).

When considering the nC17/Pristane ratio, the expectation would be to observe a decrease between the T=0 sample and the those collected in 2019, as preferential biodegradation of nC17 would occur relative to pristane due to their structural differences. When examining the differences in the nC17/Pristane ratio between sites, the Bay 11 samples most closely resemble the T=0 value of 3.85 with an average value of 3.20. This is hypothesized to be a result of

extensive physical removal and dissolution by tidal action, rather than the majority of losses being exhibited by biodegradation (Table 3.4). The Crude Oil Point and Bay 106 samples share much more similar nC17/Pristane results, with averages of 0.740 and 0.684, respectively. These two mean values are much lower than the T=0 sample, suggesting that extensive biodegradation has taken place at each of these sites. Of note, all the oiled samples collected from Crude Oil Point and Bay 106 display higher nC17/Pristane values within the subsurface sediments, relative to the surface, except in the case of IME-e (Table 3.4). A two-sample t-test assuming equal variances (two-sample F-test $p = .25$) indicates that there were significant differences between the nC17/Pristane ratios within the surface and subsurface sediments between Crude Oil Point and Bay 106 (two-tailed $p = .029$). This result corroborates earlier data regarding higher microbial biomass within surface samples, relative to their subsurface counterparts (Schreiber & Hunnie *et al.*, Under Review). However, based on the method used to determine microbial biomass, the differences between surface and subsurface samples fell within a single order of magnitude (Schreiber & Hunnie *et al.*, Under Review).

The Pristane/Phytane ratio values appear more consistent across both temporal and spatial scales than what is observed for the nC17/Pristane ratio (Table 3.4). The lowest average Pristane/Phytane value comes from Crude Oil Point. A two-sample t-test assuming equal variances (two-sample F-test $p = 0.42$) illustrated no significant differences between the surface and subsurface samples across Bay 11, Crude Oil Point, and Bay 106 (two-tailed $p = 0.40$).

The value of the SHWR in the T=0 sample is not the highest across the dataset (Table 3.4). Two samples from Bay 106, IME-c 5-10 and IME-e 0-2 have greater SHWR values. This is largely due to disproportionately high signals representing tetradecane (nC14) and hexadecane (nC16) across each of their triplicates, in comparison to the n-alkanes ranging from nC17 –

nC25. Although these results are puzzling, they are consistent across replicates and were analyzed in separate batches, ruling out instrumental error. The remaining 12 samples reveal lower SHWR than the T=0 sample, demonstrating the propensity for the smaller-chain n-alkanes to preferentially degrade when compared to slightly longer-chained ones. This is consistent with the expected outcomes of biodegradation and evaporation. Exposing these incongruous results can be of value, as the degradation of an incredibly complex contaminant such as crude oil may not always follow such rigid expectations. A two-sample t-test assuming equal variances (two-sample F-test $p = .48$) denotes no significant differences between surface and subsurface Pristane/Phytane ratios (two-tailed $p = .72$).

The results concerning the nC11-nC15/nC27-nC35 ratio tend to follow previously reported expectations in terms of natural attenuation trends in crude oil. When considering the samples collected in 2019, the Bay 11 sediments exhibit the highest mean value for this ratio, at 0.47. Since the Bay 11 samples were collected from the intertidal zone, regular tidal action during open-water seasons would contribute to a large removal of crude oil through physical loss and dissolution. Although the large chain n-alkanes are much less likely to dissolve than short chain n-alkanes, they would still be largely removed through physical loss, hence the largest nC11-nC15/nC27-nC35 ratio value. The site with the second highest mean value of this ratio was Bay 106 with a result of 0.098, the site with supratidal plots that were occasionally subject to storm-water inundation. Finally, the sediments from Crude Oil Point exhibited the lowest average nC11-nC15/nC27-nC35 ratio value, which was 0.007. This result is over an entire order of magnitude less than what is observed at Bay 106, and nearly two orders of magnitude lower than the values from Bay 11 (Table 3.4). Since the plots at Crude Oil Point have no interaction with the marine interface, the capacity for the sediments to be washed out is limited to spring and

summer meltwater, in addition to rain events. As such, the main sources of degradation pertaining especially to the short-chain n-alkanes are volatilization and biodegradation, which occur to lesser extents as the number of carbon atoms increase in compounds such as n-alkanes. A two-sample t-test assuming unequal variances (two-sample F-test $p = 0.0018$) denotes no significant differences between surface and subsurface nC11-nC15/nC27-nC35 ratios (two-tailed $p = 0.55$).

The final weathering ratio being examined here was the nC16-nC26/nC27-nC35 ratio. There were two BIOS samples collected in 2019 that denote higher values of this ratio than within the T=0 sample, which are B11-I 0-2 and IME-e 5-10 (Table 3.4). In the case of the Bay 11 sample, there were ubiquitously low S/N ratios acquired from the GCMS analyses concerning the n-alkanes nC30, nC32, nC33, nC34, and nC35, leading to non-detectable values across most of the eleven replicates collected. Conversely, nC16, nC17, nC20, and nC21 were among the most abundant n-alkanes detected within the surface samples from Bay 11 (Figure 3.3). The n-alkane composition of the Bay 106 sample, IME-e 5-10, is mainly characterized by medium-chained alkanes, as opposed to long-chain ones (Figure 3.3), compared to what is observed in the T=0 sample. The preferential biodegradation of long-chained n-alkanes over medium-chained ones has been observed in long-term monitoring studies of crude oil spills conducted in more temperate environments, depending on the subsurface soil conditions (Bekins et al., 2005). Not unsurprisingly, the sediments of Bay 11 demonstrate the highest mean nC16-nC26/nC27-nC35 value, followed by Bay 106, and Crude Oil Point. These values were measured at 2.21, 1.169, and 0.662, respectively. A two-sample t-test assuming equal variances (two-sample F-test $p = .21$) denotes no significant differences between surface and subsurface nC16-nC26/nC27-nC35 ratios (two-tailed $p = .53$) across the collection of samples collected in 2019.

Notably, the values for each abovementioned ratio within the surface samples from Bay 11 have been greater than those in the respective subsurface sediments (Table 3.4), which is in agreement with the proposed effects of exposure to the marine interface. These results suggest that increased levels of alkane biodegradation occur in the subsurface sediments, while physical removal appears to dominate of crude oil loss within the surface samples.

Table 3.4. Diagnostic ratios of n-alkane weathering in crude oil.

Sample	nC17/ Pristane	Pristane/ Phytane	SHWR	nC11-nC15/ nC27-nC35	nC16-nC26/ nC27-nC35
T=0	3.85	0.658	1.80	1.40	2.33
B11-I 0-2	3.41	0.467	1.57	0.801	3.15
B11-I 5-10	3.00	0.395	1.23	0.146	1.27
T1 0-2	0.354	0.316	1.04	0.00454	0.235
T1 5-10	0.868	0.404	1.02	0.00866	1.20
T2 0-2	0.579	0.294	1.05	0.00541	0.199
T2 5-10	1.16	0.388	1.02	0.00777	1.02
IMC-c 0-2	0.528	0.428	1.03	0.0185	1.18
IMC-c 5-10	1.08	0.626	1.08	0.0735	1.91
IMC-e 0-2	0.463	0.619	1.11	0.101	1.63
IMC-e 5-10	0.647	0.580	1.13	0.0657	0.832
IME-c 0-2	0.369	0.318	1.29	0.0644	0.364
IME-c 5-10	0.777	0.644	2.12	0.195	0.395
IME-e 0-2	0.960	0.578	2.11	0.127	0.305
IME-e 5-10	0.656	0.390	1.07	0.137	2.73

Conclusion

The Arctic is one of the world's most fragile ecosystems, being disproportionately impacted by the effects of climate change (Arctic Monitoring and Assessment Programme, 2017; Serreze et al., 2007). As warming trends continue to decrease the overall extent of sea ice; additional open, navigable waters become attractive options for shipping traffic and oil exploration within the Arctic (Smith & Stephenson, 2013). As such, crude oil spills are bound to

occur, and will do so with increasing frequency (Arctic Monitoring and Assessment Programme, 2010b; Hasle et al., 2009). To mitigate the deleterious impacts of crude oil within the Arctic environment, it is crucial to understand the short and long-term patterns of degradation for some of the most common and abundant groups of hydrocarbons present within these contaminants. This work serves to expose the extents of crude oil degradation within an initially remote, pristine Arctic setting. Ultimately, when subject to natural remediation processes for nearly forty years, both the total concentrations and compositions of hydrocarbon groups including n-alkanes, alkylbenzenes, and alkylcycloalkanes change drastically. These effects can be largely ascribed to both environmental and experimental factors. However, oil residues are still present in significant quantities, and have not yet degraded back to baseline levels. Much work has been done to understand the temporal effects of hydrocarbon degradation processes, both in laboratory experiments and cold, marine environments (Góngora et al., 2022; Péquin et al., 2022). However, studies such as those encompassed within the BIOS project are incredibly one-of-a-kind opportunities to take part in. Examining the long-term fate and degradation of crude oil in a true Arctic setting provides information that cannot be obtained elsewhere, as the Arctic is such a unique and extreme environment (Sergy & Blackall, 1987). Additionally, given the fundamental lack of infrastructure capable of mitigating the recalcitrance of crude oil in the Arctic, human-based remediation tactics are largely impractical on both logistical and economical bases. As such, long-term monitoring studies such as the BIOS project are of utmost importance to continue for the foreseeable future.

References

- Acevedo, S., Castro, A., Negrin, J. G., Fernández, A., Escobar, G., Piscitelli, V., Delolme, F., & Dessalces, G. (2007). Relations between asphaltene structures and their physical and chemical properties: The rosary-type structure. *Energy & Fuels*, *21*(4), 2165–2175. <https://doi.org/10.1021/ef070089v>
- Akmaz, S., Iscan, O., Gurkaynak, M. A., & Yasar, M. (2011). The structural characterization of saturate, aromatic, resin, and asphaltene fractions of batiraman crude oil. *Petroleum Science and Technology*, *29*(2), 160–171. <https://doi.org/10.1080/10916460903330361>
- Alvarez, L. A., Exton, D. A., Timmis, K. N., Suggett, D. J., & McGenity, T. J. (2009). Characterization of marine isoprene-degrading communities. *Environmental Microbiology*, *11*(12), 3280–3291. <https://doi.org/10.1111/j.1462-2920.2009.02069.x>
- Arctic Monitoring and Assessment Programme. (2010). *AMAP assessment 2007: Oil and gas activities in the Arctic - effects and potential effects. 1* (R. Shearer, Ed.). AMAP.
- Arctic Monitoring and Assessment Programme. (2017). *Snow, water, ice and permafrost in the Arctic—Summary for policy-makers*. Arctic Monitoring and Assessment Programme (AMAP).
- Asihene, W. (2019). *Sources and geochemical controls on hydrocarbons in Arctic sediments, Kivalliq Region, Nunavut*.
- Aslund, A. (2019a). *N-alkanes C10-C40 (all + pristane/phytane) product information sheet* (pp. 1–2) [Reference Material]. Chiron AS.
- Aslund, A. (2019b). *Perdeuterated n-alkane solution product information sheet* [Reference Material]. Chiron AS.

- Bacosa, H. P., Erdner, D. L., & Liu, Z. (2015). Differentiating the roles of photooxidation and biodegradation in the weathering of light Louisiana sweet crude oil in surface water from the Deepwater Horizon site. *Marine Pollution Bulletin*, 95(1), 265–272.
<https://doi.org/10.1016/j.marpolbul.2015.04.005>
- Bekins, B. A., Hostettler, F. D., Herkelrath, W. N., Delin, G. N., Warren, E., & Essaid, H. I. (2005). Progression of methanogenic degradation of crude oil in the subsurface. *Environmental Geosciences*, 12(2), 139–152. <https://doi.org/10.1306/eg.11160404036>
- Bird, K., Charpentier, R., Gautier, D., Houseknecht, D., Klett, T., Pitman, J., Moore, T., Schenk, C., Tennyson, M., & Wandrey, C. (2008). *Circum-Arctic resource appraisal: Estimates of undiscovered oil and gas north of the Arctic circle* (Fact Sheet, p. 4) [Fact Sheet]. U.S. Geological Survey (USGS).
- Blumer, B., & Sass, J. (1972). *II. Chemistry* (The West Falmouth oil spill, p. 129) [Technical Report].
- Blumer, M., & Sass, J. (1972). Oil pollution: Persistence and degradation of spilled fuel oil. *Science*, 176(4039), 1120–1122.
- Boehm, P. D. (1981). *Chemistry:2 Hydrocarbon chemistry—1980 study results. (BIOS) Baffin Island Oil Spill working report* (p. 184) [Working Report].
- Boehm, P. D. (1983). *Chemistry: 2. Analytical biogeochemistry—1982 Study results* (p. 231).
- Bragg, J. R., Prince, R. C., Harner, E. J., & Atlas, R. M. (1993). Bioremediation effectiveness following the Exxon Valdez spill. *International Oil Spill Conference Proceedings*, 1993(1), 435–447. <https://doi.org/10.7901/2169-3358-1993-1-435>
- Burton, J. (N.D.a). *C15 through C35 alk mix* (pp. 1–2) [Certified Reference Material]. SPEX CertiPrep.

- Burton, J. (N.D.b). *Even alk (C16-C36)* (pp. 1–2) [Certified Reference Material]. SPEX CertiPrep.
- Chikere, C. B., Okpokwasili, G. C., & Chikere, B. O. (2011). Monitoring of microbial hydrocarbon remediation in the soil. *3 Biotech, 1*(3), 117–138.
<https://doi.org/10.1007/s13205-011-0014-8>
- Cretney, W. J. (1987). Hydrocarbon biogeochemical setting of the Baffin Island Oil Spill experimental sites. III. Biota. *ARCTIC, 40*, 9.
- Cretney, W. J., Green, D. R., Fowler, B. R., Humphrey, B., Fiest, D. L., & Boehm, P. D. (1987a). Hydrocarbon biogeochemical setting of the Baffin Island Oil Spill experimental sites. II. Water. *Arctic, 40*, 66–70.
- Cretney, W. J., Green, D. R., Fowler, B. R., Humphrey, B., Fiest, D. L., & Boehm, P. D. (1987b). Hydrocarbon biogeochemical setting of the Baffin Island Oil Spill experimental sites. I. Sediments. *ARCTIC, 40*(5), 51–65. <https://doi.org/10.14430/arctic1802>
- Demirbas, A., & Taylan, O. (2016). Removing of resins from crude oils. *Petroleum Science and Technology, 34*(8), 771–777. <https://doi.org/10.1080/10916466.2016.1163397>
- Desmond, D. S., Saltymakova, D., Smith, A., Wolfe, T., Snyder, N., Polcwiartek, K., Bautista, M., Lemes, M., Hubert, C. R. J., Barber, D. G., Isleifson, D., & Stern, G. A. (2021). Photooxidation and biodegradation potential of a light crude oil in first-year sea ice. *Marine Pollution Bulletin, 165*, 112154. <https://doi.org/10.1016/j.marpolbul.2021.112154>
- Dutta, T. K., & Harayama, S. (2000). Fate of crude oil by the combination of photooxidation and biodegradation. *Environmental Science & Technology, 34*(8), 1500–1505.
<https://doi.org/10.1021/es991063o>

- Eguíluz, V. M., Fernández-Gracia, J., Irigoien, X., & Duarte, C. M. (2016). A quantitative assessment of Arctic shipping in 2010–2014. *Scientific Reports*, *6*(1), 30682. <https://doi.org/10.1038/srep30682>
- Fakher, S., Ahdaya, M., Elturki, M., & Imqam, A. (2020). Critical review of asphaltene properties and factors impacting its stability in crude oil. *Journal of Petroleum Exploration and Production Technology*, *10*(3), 1183–1200. <https://doi.org/10.1007/s13202-019-00811-5>
- Foster, K. L., Stern, G. A., Carrie, J., Bailey, J. N. L., Outridge, P. M., Sanei, H., & Macdonald, R. W. (2015). Spatial, temporal, and source variations of hydrocarbons in marine sediments from Baffin Bay, Eastern Canadian Arctic. *Science of the Total Environment*, *506*(507), 430–443.
- Góngora, E., Chen, Y.-J., Ellis, M., Okshevsky, M., & Whyte, L. (2022). Hydrocarbon bioremediation on Arctic shorelines: Historic perspective and roadway to the future. *Environmental Pollution*, *305*, 119247. <https://doi.org/10.1016/j.envpol.2022.119247>
- Gonzalez, C., & Choquette, S. (2017). *Certificate of analysis—Standard reference material 1944*. National Institute of Standards & Technology.
- Gonzalez, C., & Watters, R. (2015). *Certificate of analysis—Standard reference material 1941b*. National Institute of Standards & Technology.
- Groenzin, H., & Mullins, O. C. (1999). Asphaltene molecular size and structure. *The Journal of Physical Chemistry A*, *103*(50), 11237–11245. <https://doi.org/10.1021/jp992609w>
- Gunnarsson, B. (2021). Recent ship traffic and developing shipping trends on the Northern Sea Route—Policy implications for future arctic shipping. *Marine Policy*, *124*, 104369. <https://doi.org/10.1016/j.marpol.2020.104369>

- Harayama, S., Kishira, H., Kasai, Y., & Shutsubo, K. (1999). Petroleum biodegradation in marine environments. *Journal of Molecular Microbiology and Biotechnology*, *1*(1), 63–70.
- Hasle, J. R., Kjellén, U., & Haugerud, O. (2009). Decision on oil and gas exploration in an Arctic area: Case study from the Norwegian Barents Sea. *Safety Science*, *47*(6), 832–842. <https://doi.org/10.1016/j.ssci.2008.10.019>
- Humphrey, B., Owens, E. H., & Sergy, G. A. (1992). *The fate and persistence of stranded crude oil: A 9-year overview from the BIOS project, Baffin Island, N.W.T., Canada* (pp. 1–60). Environment Canada.
- Hunnie, B. E., Schreiber, L., Greer, C. W., & Stern, G. A. (2023). The recalcitrance and potential toxicity of polycyclic aromatic hydrocarbons within crude oil residues in beach sediments at the BIOS site, nearly forty years later. *Environmental Research*, *222*, 115329. <https://doi.org/10.1016/j.envres.2023.115329>
- Johnson, R. J., West, C. E., Swaih, A. M., Folwell, B. D., Smith, B. E., Rowland, S. J., & Whitby, C. (2012). Aerobic biotransformation of alkyl branched aromatic alkanolic naphthenic acids via two different pathways by a new isolate of Mycobacterium: Isolation and characterization of an aromatic NA degrading Mycobacterium spp. *Environmental Microbiology*, *14*(4), 872–882. <https://doi.org/10.1111/j.1462-2920.2011.02649.x>
- Johnston, C. D., Bastow, T. P., & Innes, N. L. (2007). The use of biodegradation signatures and biomarkers to differentiate spills of petroleum hydrocarbon liquids in the subsurface and estimate natural mass loss. *European Journal of Soil Biology*, *43*(5–6), 328–334. <https://doi.org/10.1016/j.ejsobi.2007.03.008>

- Jörundsdóttir, H. Ó., Jensen, S., Hylland, K., Holth, T. F., Gunnlaugsdóttir, H., Svavarsson, J., Ólafsdóttir, Á., El-Taliawy, H., Rigét, F., Strand, J., Nyberg, E., Bignert, A., Hoydal, K. S., & Halldórsson, H. P. (2014). Pristine Arctic: Background mapping of PAHs, PAH metabolites and inorganic trace elements in the North-Atlantic Arctic and sub-Arctic coastal environment. *Science of The Total Environment*, *493*, 719–728.
<https://doi.org/10.1016/j.scitotenv.2014.06.030>
- Kalouzkaya, O. (2017). *Gravimetric certificate - Alkylbenzene mixture* (p. 2) [Product Information Sheet]. Chiron AS.
- Kissin, Y. V. (1990). Catagenesis of light cycloalkanes in petroleum. *Organic Geochemistry*, *15*(6), 575–594.
- Knott, K. (2019). *Reference material—Alkylcycloalkane mixture 1* (p. 2) [Product Information Sheet]. Chiron AS.
- Kristensen, M., Johnsen, A. R., & Christensen, J. H. (2015). Marine biodegradation of crude oil in temperate and Arctic water samples. *Journal of Hazardous Materials*, *300*, 75–83.
<https://doi.org/10.1016/j.jhazmat.2015.06.046>
- Leahy, J. G., & Colwell, R. R. (1990). Microbial degradation of hydrocarbons in the environment. *Microbiological Reviews*, *54*(3), 305–315.
- Liu, H., Yang, G., Jia, H., & Sun, B. (2022). Crude oil degradation by a novel strain *Pseudomonas aeruginosa* AQNU-1 isolated from an oil-contaminated lake wetland. *Processes*, *10*(2), 307. <https://doi.org/10.3390/pr10020307>
- Markus, T., Stroeve, J. C., & Miller, J. (2009). Recent changes in Arctic sea ice melt onset, freezeup, and melt season length. *Journal of Geophysical Research: Oceans*, *114*(C12).
<https://doi.org/10.1029/2009JC005436>

- Melia, N., Haines, K., & Hawkins, E. (2016). Sea ice decline and 21st century trans-Arctic shipping routes. *Geophysical Research Letters*, *43*(18), 9720–9728.
<https://doi.org/10.1002/2016GL069315>
- Mosbech, A., Hansen, A., Asmund, G., Dahllof, I., Groth Peterson, D., & Strand, J. (2007). *A chemical and biological study of the impact of a suspected oil seep at the coast of Maarrat, Nuussuaq, Greenland* (pp. 1–61) [Technical Report]. National Environmental Research Institute.
- Owens, E. H., Harper, J. R., Robson, W., & Boehm, P. D. (1987). Fate and persistence of crude oil stranded on a sheltered beach. *ARCTIC*, *40*(5), 109–123.
<https://doi.org/10.14430/arctic1807>
- Owens, E. H., Humphrey, B., & Sergy, G. A. (1994). Natural cleaning of oiled coarse sediment shorelines in Arctic and Atlantic Canada. *Spill Science & Technology Bulletin*, *1*(1), 37–52. [https://doi.org/10.1016/1353-2561\(94\)90006-X](https://doi.org/10.1016/1353-2561(94)90006-X)
- Owens, E. H., Robson, W., & Foget, C. R. (1987). A field evaluation of selected beach-cleaning techniques. *ARCTIC*, *40*(5), 244–257. <https://doi.org/10.14430/arctic1818>
- Owens, E., Sergy, G. A., & Prince, R. (2002). The fate of stranded oil at the BIOS site twenty years after the experiment. *Environment Canada Arctic and Marine Oil Spill Program Technical Seminar (AMOP) Proceedings*, *25*, 1–11.
- Owens, H. (1984). *Shoreline countermeasures—1983 Results. Baffin Island Oil Spill project working report 83-4* (pp. 1–115) [Working Report]. Environmental Protection Service, Environment Canada, Ottawa.

- Péquin, B., Cai, Q., Lee, K., & Greer, C. W. (2022). Natural attenuation of oil in marine environments: A review. *Marine Pollution Bulletin*, 176, 113464.
<https://doi.org/10.1016/j.marpolbul.2022.113464>
- Perovich, D. K., Light, B., Eicken, H., Jones, K. F., Runciman, K., & Nghiem, S. V. (2007). Increasing solar heating of the Arctic Ocean and adjacent seas, 1979–2005: Attribution and role in the ice-albedo feedback. *Geophysical Research Letters*, 34(19).
<https://doi.org/10.1029/2007GL031480>
- Prince, R. C. (2002). Biodegradation of petroleum and other hydrocarbons. In *Encyclopedia of Environmental Microbiology* (pp. 2402–2416).
- Prince, R. C., Elmendorf, D. L., Lute, J. R., Hsu, C. S., Haith, C. E., Senius, J. D., Dechert, G. J., Douglas, G. S., & Butler, E. L. (1994). 17.alpha.(H)-21.beta.(H)-hopane as a conserved internal marker for estimating the biodegradation of crude oil. *Environmental Science & Technology*, 28(1), 142–145. <https://doi.org/10.1021/es00050a019>
- Prince, R. C., Owens, E. H., & Sergy, G. A. (2002). Weathering of an Arctic oil spill over 20 years: The BIOS experiment revisited. *Marine Pollution Bulletin*, 44(11), 1236–1242.
[https://doi.org/10.1016/S0025-326X\(02\)00214-X](https://doi.org/10.1016/S0025-326X(02)00214-X)
- Reed, M., Johansen, Ø., Brandvik, P. J., Daling, P., Lewis, A., Fiocco, R., Mackay, D., & Prentki, R. (1999). Oil spill modeling towards the close of the 20th century: Overview of the state of the art. *Spill Science & Technology Bulletin*, 5(1), 3–16.
[https://doi.org/10.1016/S1353-2561\(98\)00029-2](https://doi.org/10.1016/S1353-2561(98)00029-2)
- Rocha, C. A., Pedregosa, A. M., & Laborda, F. (2011). Biosurfactant-mediated biodegradation of straight and methyl-branched alkanes by *Pseudomonas aeruginosa* ATCC 55925. *AMB Express*, 1(1), 9. <https://doi.org/10.1186/2191-0855-1-9>

- RStudio Team. (2020). RStudio: Integrated development for R. RStudio, PBC, Boston, MA <http://www.rstudio.com/>*
- Saltymakova, D., Desmond, D. S., Isleifson, D., Firoozy, N., Neusitzer, T. D., Xu, Z., Lemes, M., Barber, D. G., & Stern, G. A. (2020). Effect of dissolution, evaporation, and photooxidation on crude oil chemical composition, dielectric properties and its radar signature in the Arctic environment. *Marine Pollution Bulletin*, *151*, 110629. <https://doi.org/10.1016/j.marpolbul.2019.110629>
- Schlitzer, R. (2023). Ocean Data View. [Idv.awi.de](http://idv.awi.de).
- Sergy, G. A., & Blackall, P. J. (1987). Design and conclusions of the Baffin Island Oil Spill project. *ARCTIC*, *40*(5), 1–9. <https://doi.org/10.14430/arctic1797>
- Serreze, M. C., Holland, M. M., & Stroeve, J. (2007). Perspectives on the Arctic's shrinking sea-ice cover. *Science*, *315*(5818), 1533–1536. <https://doi.org/10.1126/science.1139426>
- Silber, G. K., & Adams, J. D. (2019). Vessel operations in the Arctic, 2015–2017. *Frontiers in Marine Science*, *6*, 573. <https://doi.org/10.3389/fmars.2019.00573>
- Smith, L. C., & Stephenson, S. R. (2013). New Trans-Arctic shipping routes navigable by midcentury. *Proceedings of the National Academy of Sciences*, *110*(13). <https://doi.org/10.1073/pnas.1214212110>
- SPEX CertiPrep. (2019). *C-11 through C-18 organics* (pp. 1–8) [Safety Data Sheet]. SPEX CertiPrep.
- Steele, M., Ermold, W., & Zhang, J. (2008). Arctic Ocean surface warming trends over the past 100 years. *Geophysical Research Letters*, *35*(2). <https://doi.org/10.1029/2007GL031651>

- Sugiura, K., Ishihara, M., Shimauchi, T., & Harayama, S. (1997). Physicochemical properties and biodegradability of crude oil. *Environmental Science & Technology*, *31*(1), 45–51. <https://doi.org/10.1021/es950961r>
- Venosa, A. D., Lee, K., Suidan, M. T., Garcia-Blanco, S., Cobanli, S., Moteleb, M., Haines, J. R., Tremblay, G., & Hazelwood, M. (2002). Bioremediation and biorestitution of a crude oil-contaminated freshwater wetland on the St. Lawrence River. *Bioremediation Journal*, *6*(3), 261–281. <https://doi.org/10.1080/10889860290777602>
- Venosa, A. D., Suidan, M. T., King, D., & Wrenn, B. A. (1997). Use of hopane as a conservative biomarker for monitoring the bioremediation effectiveness of crude oil contaminating a sandy beach. *Journal of Industrial Microbiology and Biotechnology*, *18*(2–3), 131–139. <https://doi.org/10.1038/sj.jim.2900304>
- Vergeynst, L., Greer, C. W., Mosbech, A., Gustavson, K., Meire, L., Poulsen, K. G., & Christensen, J. H. (2019). Biodegradation, photo-oxidation, and dissolution of petroleum compounds in an Arctic fjord during summer. *Environmental Science & Technology*, *53*(21), 12197–12206. <https://doi.org/10.1021/acs.est.9b03336>
- Wang, Z., Fingas, M., & Page, D. S. (1999). Oil spill identification. *Journal of Chromatography A*, *843*, 369–411.
- Wang, Zhendi., Fingas, Merv., & Sergy, Gary. (1995). Chemical characterization of crude oil residues from an Arctic beach by GC/MS and GC/FID. *Environmental Science & Technology*, *29*(10), 2622–2631. <https://doi.org/10.1021/es00010a025>
- Ward, C. P., Sharpless, C. M., Valentine, D. L., French-McCay, D. P., Aeppli, C., White, H. K., Rodgers, R. P., Gosselin, K. M., Nelson, R. K., & Reddy, C. M. (2018). Partial photochemical oxidation was a dominant fate of *Deepwater Horizon* surface oil.

Environmental Science & Technology, 52(4), 1797–1805.

<https://doi.org/10.1021/acs.est.7b05948>

Wardroper, A. M. K., Hoffmann, C. F., Maxwell, J. R., Barwise, A. J. G., Goodwin, N. S., & Park, P. J. D. (1984). Crude oil biodegradation under simulated and natural conditions—II. Aromatic steroid hydrocarbons. *Organic Geochemistry*, 6, 605–617.

[https://doi.org/10.1016/0146-6380\(84\)90083-4](https://doi.org/10.1016/0146-6380(84)90083-4)

Wentzel, A., Ellingsen, T. E., Kotlar, H.-K., Zotchev, S. B., & Throne-Holst, M. (2007).

Bacterial metabolism of long-chain n-alkanes. *Applied Microbiology and Biotechnology*, 76(6), 1209–1221. <https://doi.org/10.1007/s00253-007-1119-1>

Wilkes, H., Kühner, S., Bolm, C., Fischer, T., Classen, A., Widdel, F., & Rabus, R. (2003).

Formation of n-alkane- and cycloalkane-derived organic acids during anaerobic growth of a denitrifying bacterium with crude oil. *Organic Geochemistry*, 34(9), 1313–1323.

[https://doi.org/10.1016/S0146-6380\(03\)00099-8](https://doi.org/10.1016/S0146-6380(03)00099-8)

Supplemental Information

Table 3.S1. List of intertidal and supratidal sediment sample types acquired at respective stations and coordinates from the BIOS site during the 2019 CCGS Amundsen expedition. A surface (0-2cm) and subsurface (5-10cm) sample was collected for each entry.

Sample I.D	Location	Sediment Type	Sample Type	Latitude, Longitude
B11-I-1	BIOS: Bay 11	intertidal	Oil	72.465032, -79.829518
B11-I-2	BIOS: Bay 11	intertidal	Oil	72.464883, -79.829210
B11-I-3	BIOS: Bay 11	intertidal	Oil	72.464704, -79.829119
B11-I-4	BIOS: Bay 11	intertidal	Oil	72.464542, -79.829124
B11-I-5	BIOS: Bay 11	intertidal	Oil	72.464365, -79.829052
B11-I-6	BIOS: Bay 11	intertidal	Oil	72.464237, -79.829027
B11-I-8	BIOS: Bay 11	intertidal	Oil	72.463898, -79.828980
B11-I-9	BIOS: Bay 11	intertidal	Oil	72.463782, -79.829038
B11-BS-1	BIOS: Bay 11	supratidal	Oil	72.463782, -79.829038
B11-BS-2	BIOS: Bay 11	supratidal	Oil	72.463973, -79.828404
GICB-NHR1	BIOS: Z-Lagoon, Bay 102	intertidal	Control	72.488337, -79.7409
GICB-NHR2	BIOS: Z-Lagoon, Bay 102	intertidal	Control	72.488337, -79.7409
GICB-NHR3	BIOS: Z-Lagoon, Bay 102	intertidal	Control	72.488337, -79.7409
IMC-c1	BIOS: Z-Lagoon, Bay 106	supratidal	Oil	72.474104, -79.782194
IMC-c2	BIOS: Z-Lagoon, Bay 106	supratidal	Oil	72.474104, -79.782194
IMC-c3	BIOS: Z-Lagoon, Bay 106	supratidal	Oil	72.474104, -79.782194
IMC-e1	BIOS: Z-Lagoon, Bay 106	supratidal	Oil	72.474104, -79.782128
IMC-e2	BIOS: Z-Lagoon, Bay 106	supratidal	Oil	72.474104, -79.782128
IMC-e3	BIOS: Z-Lagoon, Bay 106	supratidal	Oil	72.474104, -79.782128
IME-c1	BIOS: Z-Lagoon, Bay 106	supratidal	Oil	72.474114, -79.782314
IME-c2	BIOS: Z-Lagoon, Bay 106	supratidal	Oil	72.474114, -79.782314
IME-c3	BIOS: Z-Lagoon, Bay 106	supratidal	Oil	72.474114, -79.782314
IME-e1	BIOS: Z-Lagoon, Bay 106	supratidal	Oil	72.474091, -79.782479
IME-e2	BIOS: Z-Lagoon, Bay 106	supratidal	Oil	72.474091, -79.782479
IME-e3	BIOS: Z-Lagoon, Bay 106	supratidal	Oil	72.474091, -79.782479
GICB-NI11	BIOS: Z-Lagoon, Bay 106	supratidal	Control	72.474061, -79.781737
GICB-NI12	BIOS: Z-Lagoon, Bay 106	supratidal	Control	72.474061, -79.781737
GICB-NI2R1	BIOS: Z-Lagoon, Bay 106	supratidal	Control	72.474054, -79.781648
GICB-NI2R2	BIOS: Z-Lagoon, Bay 106	supratidal	Control	72.474054, -79.781648
T1R1	BIOS: Z-Lagoon, Crude Oil Point	supratidal	Oil	72.482083, -79.755547
T1R2	BIOS: Z-Lagoon, Crude Oil Point	supratidal	Oil	72.482083, -79.755547
T2R1	BIOS: Z-Lagoon, Crude Oil Point	supratidal	Oil	72.482087, -79.756100
T2R2	BIOS: Z-Lagoon, Crude Oil Point	supratidal	Oil	72.482087, -79.756100
TCR1	BIOS: Z-Lagoon, Crude Oil Point	supratidal	Control	72.482098, -79.756145
TCR2	BIOS: Z-Lagoon, Crude Oil Point	supratidal	Control	72.482098, -79.756145
RB1	Cornwallis Island, Resolute Bay	Intertidal	Control	74.682228, -94.854522
TB3	Cornwallis Island, Resolute Bay	Intertidal	Control	74.749561, -95.092101
MI-I-1	Milne Inlet, Ragged Island	intertidal	Control	72.484866, -80.004129
MI-I-2	Milne Inlet, Ragged Island	intertidal	Control	72.484892, -80.004924
MI-I-3	Milne Inlet, Ragged Island	intertidal	Control	72.484905, -80.005943

MI-BS-1	Milne Inlet, Ragged Island	supratidal	Control	72.484922, -80.004945
MI-BS-2	Milne Inlet, Ragged Island	supratidal	Control	72.484941, -80.005885
MI-BS-3	Milne Inlet, Ragged Island	supratidal	Control	72.484396, -80.01001

Table 3.S2. Perdeuterated n-alkane standard solution, acquired from Chiron AS (Aslund, 2019b).

Compound	Product code	Batch	CAS	Isotopic purity	Gravimetric concentration
n-Dodecane-d26 (C12)	1019.12	1837	[16416-30-1]	98.3 atom%D	1.0 mg/mL
n-Hexadecane-d34 (C16)	1020.16	1838	[15716-08-2]	98.4 atom%D	1.0 mg/mL
n-Eicosane-d42 (C20)	1021.20	1972	[62369-67-9]	99.2 atom%D	1.0 mg/mL
n-Tetracosane-d50 (C24)	1022.24	1894	[16416-32-3]	98.2 atom%D	1.0 mg/mL
n-Octacosane-d58 (C28)	1309.28	2433	[16416-33-4]	98.8 atom%D	1.0 mg/mL
n-Dotriacontane-d66 (C32)	1308.32	2432	[62369-68-0]	99.2 atom%D	1.0 mg/mL
n-Hexatriacontane-d74 (C36)	1310.36	2481	[16416-34-5]	98.0 atom%D	1.0 mg/mL

Table 3.S3. GCMS Parameters for n-alkane analyses using the LECO Pegasus multidimensional gas chromatography high-resolution time of flight mass spectrometry (GCxGC-HR-TOF-MS, LECO) instrument.

Parameter	Value
Column length (m)	59.5
Column internal diameter (μm)	250
column film thickness (μm)	0.1
Initial oven temperature ($^{\circ}\text{C}$)	80
Initial isotherm (min)	1.5
Target temperature 1 ($^{\circ}\text{C}$)	120
Ramp rate 1 ($^{\circ}\text{C}/\text{min}$)	20
Target temperature 2 ($^{\circ}\text{C}$)	250
Ramp rate 2 ($^{\circ}\text{C}/\text{min}$)	3
Target temperature 3 ($^{\circ}\text{C}$)	300
Ramp rate 3 ($^{\circ}\text{C}/\text{min}$)	2
Final isotherm (min)	21.5
Electron energy (eV)	70
Ion source temperature ($^{\circ}\text{C}$)	250
Mass range (m/z)	50-310

Table 3.S4. List of all analyzed n-alkanes and branched alkanes, along with their associated limits of quantitation.

Compound	Limit of Quantitation (ng/mL)						
	Batch 0	Batch 1	Batch 2	Batch 3	Batch 4	Batch 5	Batch 6
Undecane	76.03	147.19	131.94	123.23	123.23	123.23	123.23
Dodecane	15.65	90.47	146.61	98.51	98.51	98.51	98.51
Tridecane	17.23	43.89	63.29	90.43	90.43	90.43	90.43
Tetradecane	18.27	17.54	83.41	57.62	57.62	57.62	57.62
Pentadecane	34.55	56.98	94.33	62.59	62.59	62.59	62.59
Hexadecane	38.74	55.04	107.44	61.64	61.64	61.64	61.64
Pristane	86.62	86.62	86.62	14.04	14.04	14.04	14.04
Heptadecane	43.42	34.12	97.51	112.41	112.41	112.41	112.41
Phytane	303.18	303.18	303.18	100.87	100.87	100.87	100.87
Octadecane	47.49	58.69	105.22	111.76	111.76	111.76	111.76
Nonadecane	29.58	41.57	106.51	100.23	100.23	100.23	100.23
Icosane	29.84	49.49	99.62	99.01	99.01	99.01	99.01
Heneicosane	33.57	50.42	159.6	99.27	99.27	99.27	99.27
Docosane	35.41	93.45	99.6	66.41	66.41	66.41	66.41
Tricosane	36.93	32.79	107.49	104.35	104.35	104.35	104.35
Tetracosane	37.25	57.27	193.02	181.12	181.12	181.12	181.12
Pentacosane	40.29	66.61	46.85	47.7	47.7	47.7	47.7
Hexacosane	40.89	49.88	103.91	168.06	168.06	168.06	168.06
Heptacosane	41.77	46.73	62.72	91.4	91.4	91.4	91.4
Octacosane	44.02	154.63	177.08	183.43	183.43	183.43	183.43
Nonacosane	43.51	88.84	103.59	172.83	172.83	172.83	172.83
triacontane	43.07	79.81	305.59	158.8	158.8	158.8	158.8
Hentriacontane	39.39	81.79	172.62	157.97	157.97	157.97	157.97
Dotriacontane	41.56	138	327.27	91.47	91.47	91.47	91.47
Trtriacontane	34.01	163	127.34	83.55	83.55	83.55	83.55
Tetratriacontane	33.75	294.32	301.9	574.99	574.99	574.99	574.99
Pentatriacontane	27.42	51.08	170.84	127.74	127.74	127.74	127.74

Table 3.S5. List of all analyzed alkylbenzenes and alkylcycloalkanes, their respective limits of quantitation, and MRM ion transitions.

Compound	Limit of Quantitation (ng/mL)	Transition 1	Transition 2	Transition 3
n-Butylbenzene	2.61	134 -> 91	92 -> 92	91 -> 91
n-Pentylbenzene	2.57	148 -> 91	92 -> 92	91 -> 91
n-Hexylbenzene	2.4	162 -> 91	92 -> 92	91 -> 91
n-Heptylbenzene	2.5	176 -> 91	92 -> 92	91 -> 91
n-Octylbenzene	2.68	190 -> 91	92 -> 92	91 -> 91
n-Nonylbenzene	2.79	202 -> 91	92 -> 92	91 -> 91
n-Decylbenzene	3.01	218 -> 91	92 -> 92	91 -> 91
n-Undecylbenzene	2.73	232 -> 91	92 -> 92	91 -> 91
n-Dodecylbenzene	3.07	246 -> 91	92 -> 92	91 -> 91
n-Tridecylbenzene	3.27	260 -> 91	92 -> 92	91 -> 91
n-Tetradecylbenzene	3.29	274 -> 91	92 -> 92	91 -> 91
n-Pentadecylbenzene	3.32	288 -> 91	92 -> 92	91 -> 91
n-Hexadecylbenzene	3.69	302 -> 91	92 -> 92	91 -> 91
n-Heptadecylbenzene	8.26	316 -> 91	92 -> 92	91 -> 91
n-Octadecylbenzene	2.66	330 -> 91	92 -> 92	91 -> 91
n-Nonadecylbenzene	3.78	344 -> 91	92 -> 92	91 -> 91
n-Hexylcyclohexane	3.27	83 -> 83	82 -> 82	55 -> 55
n-Heptylcyclohexane	2.52	83 -> 83	82 -> 82	55 -> 55
n-Octylcyclohexane	2.68	83 -> 83	82 -> 82	55 -> 55
n-Nonylcyclohexane	2.67	83 -> 83	82 -> 82	55 -> 55
n-Decylcyclohexane	2.82	83 -> 83	82 -> 82	55 -> 55
n-Undecylcyclohexane	2.67	83 -> 83	82 -> 82	55 -> 55
n-Dodecylcyclohexane	2.82	83 -> 83	82 -> 82	55 -> 55
n-Tridecylcyclohexane	2.99	83 -> 83	82 -> 82	55 -> 55
n-Tetradecylcyclohexane	3.11	83 -> 83	82 -> 82	55 -> 55

Table 3.S6. GCMS Parameters for biomarker analyses using the Agilent 7010B Triple Quadrupole GCMS (QQQ-MS).

Instrumental Parameter	Value
Column length (m)	60
Column internal diameter (μm)	250
column film thickness (μm)	0.1
Initial oven temperature ($^{\circ}\text{C}$)	60
Initial isotherm (min)	1
Target temperature 1 ($^{\circ}\text{C}$)	260
Ramp rate 1 ($^{\circ}\text{C}/\text{min}$)	32
Target temperature 2 ($^{\circ}\text{C}$)	320
Ramp rate 2 ($^{\circ}\text{C}/\text{min}$)	4
Electron energy (eV)	70
Ion gain	5
Ion source temperature ($^{\circ}\text{C}$)	250

Table 3.S7. List of all analyzed biomarkers, their respective limits of quantitation, and MRM ion transitions.

Compound	Limit of Quantitation (ng/mL)	Transition 1	Transition 2	Transition 3
aaa20S-Cholestane	1.09	372 -> 372	372 -> 357	372 -> 217
aaa20R-Cholestane	1.11	372 -> 372	372 -> 357	372 -> 217
abb20R 24S-Methylcholestane	0.99	386 -> 386	386 -> 371	386 -> 217
aaa20R 24R-Ethylcholestane	1.18	400 -> 400	400 -> 385	400 -> 217
17a(H)-22,29,30-Trisnorhopane	1.13	370 -> 370	370 -> 191	370 -> 95
abb20R 24R-Ethylcholestane	1.42	400 -> 400	400 -> 385	400 -> 217
17a(H),21b(H)-30-Norhopane	1.10	398 -> 191	398 -> 177	398 -> 95
17a(H),21b(H)-Hopane	1.17	412 -> 412	412 -> 191	412 -> 95
17b(H),21a(H)-Hopane	1.29	412 -> 412	412 -> 191	412 -> 95
17a(H),21b(H)-22R-Homohopane	1.14	426 -> 426	426 -> 191	426 -> 95
17a(H),21b(H)-22S-Homohopane	1.41	426 -> 426	426 -> 191	426 -> 95

Table 3.S8. List of all analyzed polycyclic aromatic hydrocarbons, their respective limits of quantitation, and MRM ion transitions.

Compound	Precursor Ion	Product Ion	Compound	Precursor Ion	Product Ion
Naphthalene	128	128	1,2,6-Trimethylphenanthrene	220	220
	128	127		220	205
	127	127		220	189
2-Methylnaphthalene	142	142	1,2,8-Trimethylphenanthrene	220	220
	142	141		220	205
	142	115		220	189
1-Methylnaphthalene	142	142	1-Methylfluoranthene	216	216
	142	141		216	215
	142	115		216	213
1,6-Dimethylnaphthalene	156	156	Benzo[e]phenanthrene	228	228
	156	141		228	227
	141	141		228	226
Acenaphthene	154	154	Benz[a]anthracene	228	228
	154	153		228	226
Acenaphthylene	153	153	Chrysene	226	226
	152	152		228	228
	152	151		228	226
2,3,5-Trimethylnaphthalene	170	170	Triphenylene	228	228
	170	155		228	226
	170	153		226	226
Fluorene	166	166	6-Ethylchrysene	256	256
	166	165		256	241
	166	164		256	239
Dibenzothiophene	185	185	1-Methylchrysene	242	242
	184	184		242	241
	184	139		242	239
Anthracene	178	178	Benzo[b]fluoranthene	252	252
	178	176		252	250
	178	152		126	126
Phenanthrene	178	178	Benzo[k]fluoranthene	252	252
	176	176		252	250
	152	152		126	126
2-Methyldibenzothiophene	198	198	Benzo[j]fluoranthene	252	252
	198	197		252	250
	197	197		250	250
2-Methylphenanthrene	192	192	Benzo[a]pyrene	253	253
	192	191		252	252

	192	189		252	250
2,8-Dimethyldibenzothiophene	212	212	Benzo[e]pyrene	252	252
	212	211		252	250
	212	197		250	250
2,4,7-Trimethyldibenzothiophene	226	226	Perylene	252	252
	226	225		252	250
	226	211		250	250
2,4-Dimethylphenanthrene	206	206	Dibenz[a,h]anthracene	278	278
	206	191		138	138
	206	189	Indeno[1,2,3-c,d]pyrene	276	276
Fluoranthene	202	202		276	274
	202	201	Benzo[g,h,i]perylene	276	276
	202	200		276	274
Pyrene	202	202		138	138
	202	201			
	202	200			

Table 3.S9. Mean concentrations (mg/kg) of individual, analyzed n-alkanes and branched alkanes within the technical mixture, oiled sediments, and control sediments from the 2019 revisit of BIOS site.

Sample id	Undecane	Dodecane	Tridecane	Tetradecane
NI-11 0-2	0	11.2875752	35.8241483	494.857214
NI-11 5-10	0	0	46.3731343	442.014925
N12 0-2	0	100.110135	100.464444	910.474295
N12 5-10	9.30611222	44.7227978	129.15339	1134.15483
GICB-NH 0-2	0	47.3041417	0	38.7391818
GICB-NH 5-10	0	0	0	28.6575074
TC 0-2	0	19.8357363	80.0894558	842.653788
TC 5-10	0	28.427098	48.2102615	483.729895
MI-BS 0-2	0	115.992038	251.038406	1114.26041
MI-BS 5-10	0	175.80774	278.539972	1103.58105
MI-I 0-2	0	84.6580189	48.9976415	376.46993
MI-I 5-10	0	23.9965139	39.2486725	298.814231
RB1 0-2	0	0	0	179.433118
RB1 5-10	0	0	0	138.314215
TB3 0-2	0	0	0	34.6286142
TB3 5-10	0	0	0	0
IMC-c 0-2	0	874.789719	96.8866655	1637.31443
IMC-c 5-10	0	544.250201	0	2462.99701
IMC-e 0-2	0	65.3225806	36.9379653	443.885086
IMC-e 5-10	0	215.095238	92.1904762	1045.21206
IME-c 0-2	0	435.782978	12.0186598	1202.23673
IME-c 5-10	0	7.25186104	32.4896509	1409.7612
IME-e 0-2	0	141.873558	14.2760181	549.224316
IME-e 5-10	249.882075	603.253426	55.2189781	1611.21605
B11-BS 0-2	0	0	7.88372093	568.255814
B11-BS 5-10	0	0	0	652.777094
B11-I 0-2	0	0	1.63228293	173.372559
B11-I 5-10	0	0	16.8935644	152.953391
T1 0-2	0	661.922678	35.3361239	1269.54494
T1 5-10	0	1356.33874	103.841912	2009.92679
T2 0-2	0	709.558824	42.2794118	2280.78504
T2 5-10	0	1414.65015	54.3841464	1780.20686
	Pentadecane	Hexadecane	Pristane	Heptadecane
NI-11 0-2	179.511523	302.269539	74.0455912	79.7119239
NI-11 5-10	332.686567	340.365672	260.820896	155.507463

N12 0-2	810.889958	727.823161	328.776052	285.501742
N12 5-10	1555.57649	1571.6473	728.997297	809.762733
GICB-NH 0-2	68.346199	65.5412412	45.8128449	80.6574994
GICB-NH 5-10	76.5428537	63.0178872	47.823971	85.2515225
TC 0-2	931.050939	826.168443	256.534084	372.297973
TC 5-10	620.863574	561.660078	460.441098	369.097218
MI-BS 0-2	1340.61162	671.045854	249.149501	430.329387
MI-BS 5-10	1381.42822	980.856862	464.382857	607.503489
MI-I 0-2	594.095296	409.456649	179.851461	269.938116
MI-I 5-10	399.411075	266.775626	98.1813729	173.112066
RB1 0-2	0	61.0367976	52.4664346	78.5504724
RB1 5-10	54.605985	41.6857855	27.7481297	76.9451372
TB3 0-2	0	44.6485543	46.3459621	0
TB3 5-10	0	37.675986	66.650025	72.2516226
IMC-c 0-2	1141.79866	2763.70177	10728.5323	5665.08005
IMC-c 5-10	2270.87027	3922.11749	4224.94099	4544.65475
IMC-e 0-2	421.294045	493.291563	1440.55407	666.996951
IMC-e 5-10	467.200004	580.467421	1025.8666	663.449434
IME-c 0-2	196.54813	654.5352	865.041046	319.461974
IME-c 5-10	679.887366	1042.24655	734.243681	570.365658
IME-e 0-2	246.196599	707.145215	334.327025	320.890525
IME-e 5-10	568.833625	723.320401	1899.14312	1246.39834
B11-BS 0-2	167.27557	327.255814	657.888489	228.209334
B11-BS 5-10	114.333457	0	156.735	36.7674419
B11-I 0-2	213.698478	282.292277	84.6390849	288.716369
B11-I 5-10	92.9073839	165.005938	63.3386347	189.879273
T1 0-2	82.8658207	954.773794	2837.98942	1003.61741
T1 5-10	1070.33278	4762.67146	14866.4852	12910.3363
T2 0-2	195.275735	1779.80117	4011.02322	2323.9262
T2 5-10	1228.58295	4166.15247	10695.422	12391.5859
	Phytane	Octadecane	Nonadecane	Icosane
NI-11 0-2	39.6117235	81.3727455	13.9854709	27.9784569
NI-11 5-10	159	70.8880597	18.6492537	14.9701493
N12 0-2	227.098012	128.071625	40.3329757	37.7753018
N12 5-10	416.272672	255.029031	74.2657054	60.2839454
GICB-NH 0-2	66.0564669	8.83535921	26.5587166	10.3553678

MI-BS 5-10	16.7676728	13.1818565	0	0.93609586
MI-I 0-2	13.7954432	12.7135055	0	36.6274027
MI-I 5-10	0	1.07338992	0	0
RB1 0-2	667.742417	58.2247638	102.657882	157.018896
RB1 5-10	108.104738	68.8578554	102.209476	148.32419
TB3 0-2	61.4282154	0	0	61.8506979
TB3 5-10	73.8617074	50.5117324	0	43.505991
IMC-c 0-2	25710.3245	35284.4784	31229.1681	30711.4035
IMC-c 5-10	13110.6335	19427.6193	18413.1437	17323.1762
IMC-e 0-2	1436.59305	2162.40023	1945.86228	1927.59429
IMC-e 5-10	1731.34856	3187.81124	2317.10041	2706.64806
IME-c 0-2	4107.10057	1110.35891	681.419892	614.322446
IME-c 5-10	75.0682382	365.285044	292.27132	317.668978
IME-e 0-2	98.4159785	111.819457	116.893835	132.710294
IME-e 5-10	8669.70237	11426.4833	9113.44125	7242.01963
B11-BS 0-2	62.1947674	96.9075581	92.6430233	106.340698
B11-BS 5-10	0	0	0	0
B11-I 0-2	340.169874	49.6903318	47.905656	20.7861029
B11-I 5-10	81.1365567	130.773298	380.824534	384.080599
T1 0-2	8626.52165	10573.9227	12440.602	14829.7121
T1 5-10	74184.62	96510.4992	79156.3882	78276.908
T2 0-2	14615.0496	12641.9018	13164.2264	18038.986
T2 5-10	60635.5786	81885.4094	79188.8118	79139.3331
	Pentacosane	Hexacosane	Heptacosane	Octacosane
NI-11 0-2	5.61372746	7.13927856	14.4589178	10.746493
NI-11 5-10	2.79850746	0	16.738806	0
N12 0-2	7.71889653	0.35803393	19.4858508	9.32915235
N12 5-10	25.7830941	4.16457916	79.7579973	11.4679359
GICB-NH 0-2	10.8645677	0	0	27.278827
GICB-NH 5-10	16.2807215	20.2234943	7.00647088	16.4230961
TC 0-2	5.49975622	5.872745	15.2915214	6.88932228
TC 5-10	13.4740673	13.0740368	30.2236034	14.7075018
MI-BS 0-2	9.41821929	3.25336526	18.3804834	3.31710147
MI-BS 5-10	0.52223888	2.03899733	4.10946302	0.37231384
MI-I 0-2	0	0	2.81529573	24.4196872
MI-I 5-10	10.0524214	26.3318341	0	0
RB1 0-2	106.715564	161.225758	180.029836	147.516161

RB1 5-10	147.598504	209.902743	212.588529	183.134663
TB3 0-2	47.2058824	41.3733799	0	0
TB3 5-10	59.775337	49.1188218	99.6155766	91.669995
IMC-c 0-2	33586.3289	34263.1054	35401.5542	30722.7233
IMC-c 5-10	18327.1359	17715.1976	17116.1148	12406.4306
IMC-e 0-2	2294.31373	2223.25008	2287.90074	1726.99007
IMC-e 5-10	4085.82738	4444.99947	5331.03782	4442.87476
IME-c 0-2	826.749612	1013.81754	1633.22112	1530.39874
IME-c 5-10	361.015728	439.006144	775.365718	983.975614
IME-e 0-2	98.0704164	95.4038744	238.666365	148.526527
IME-e 5-10	6888.45357	5000.77024	4102.01267	2896.61572
B11-BS 0-2	171.224419	234.897674	655.874499	741.699381
B11-BS 5-10	0	0	0	0
B11-I 0-2	82.8341467	80.0468105	75.6261817	93.2543472
B11-I 5-10	381.145309	289.828187	181.265446	280.52857
T1 0-2	17022.6344	28004.9431	36570.0254	42729.8189
T1 5-10	90169.8954	91555.7166	102230.602	82207.4303
T2 0-2	14458.3206	19873.012	33932.5951	45374.3781
T2 5-10	87329.9948	85524.786	92392.1838	72388.489
	Nonacosane	Triacontane	Hentriacontane	Dotriacontane
NI-11 0-2	25.1002004	13.1137275	47.9008016	86.7835671
NI-11 5-10	28.8134328	0	14.5746269	36.1865672
N12 0-2	32.4570386	60.1313054	59.7946966	80.6626639
N12 5-10	153.062911	37.8957916	112.200466	17.3296593
GICB-NH 0-2	0	0	25.7628865	0
GICB-NH 5-10	0	0	0	0
TC 0-2	10.0670405	14.8829839	36.0848367	22.2879083
TC 5-10	44.3246643	70.6478744	25.7569696	3.92127554
MI-BS 0-2	25.0122816	21.3525346	14.3816245	0
MI-BS 5-10	5.89775561	1.10694653	5.51724138	18.5610973
MI-I 0-2	0	0	0	0
MI-I 5-10	0	0	0	0
RB1 0-2	0	0	0	182.051218
RB1 5-10	205.937656	0	0	0
TB3 0-2	87.3155533	0	85.0124626	0
TB3 5-10	0	0	67.7059411	0
IMC-c 0-2	28818.4754	32489.1627	24085.7289	22182.1943

IME-c 5-10	1271.5214	1828.68641	0
IME-e 0-2	1048.99176	2106.19164	1508.1945
IME-e 5-10	133.602941	629.688708	506.230857
B11-BS 0-2	1631.87093	1612.25581	2089.68372
B11-BS 5-10	0	0	91.3255814
B11-I 0-2	29.2018439	28.2997053	19.9292929
B11-I 5-10	159.007444	122.102978	50.578474
T1 0-2	45337.4349	53675.8814	21951.8731
T1 5-10	36070.2295	27103.4083	12725.3428
T2 0-2	72268.1839	79871.5364	40485.8826
T2 5-10	43182.5921	46237.9673	21778.2957

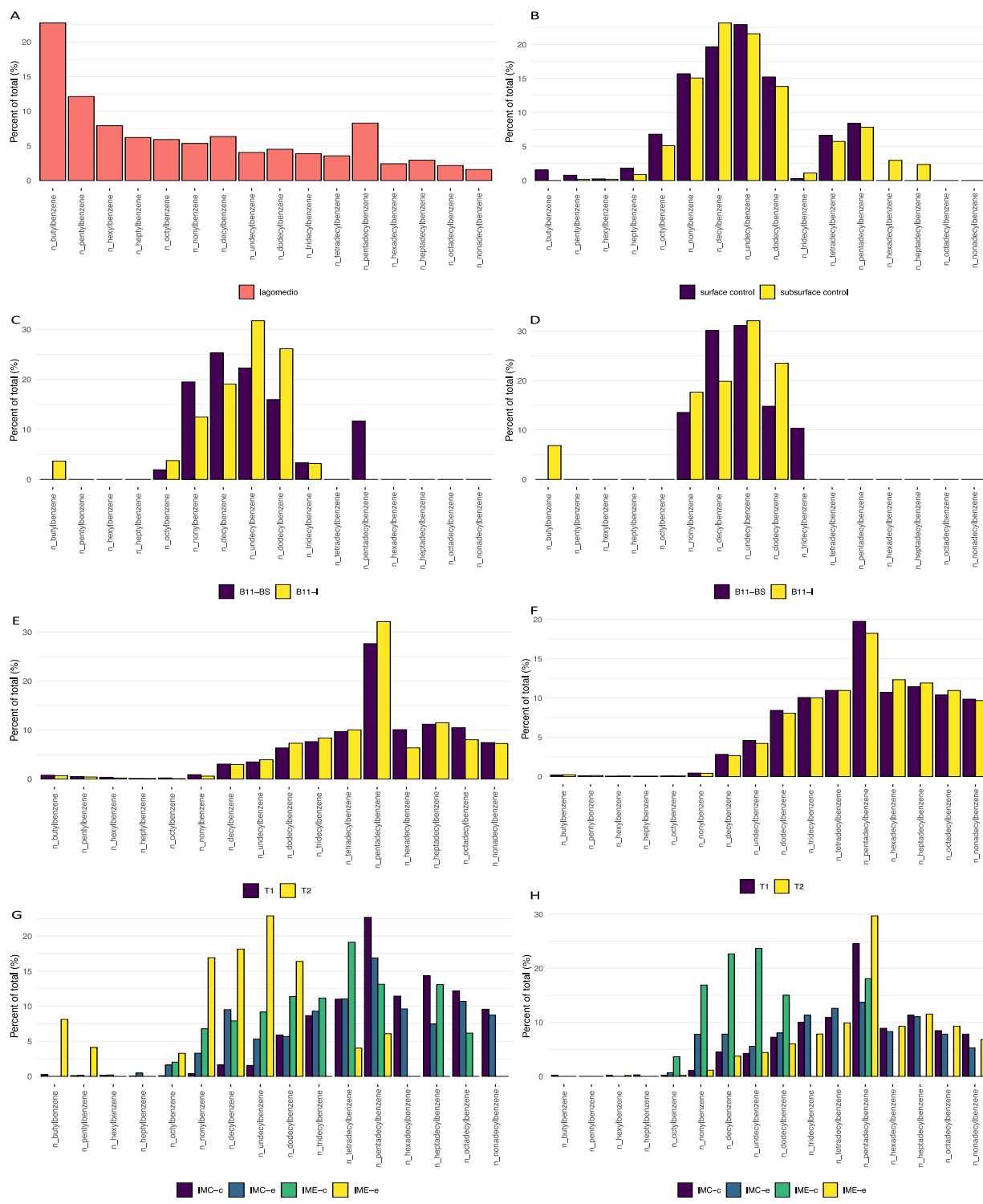


Figure 3.S1. Composition of alkylbenzenes, represented by the percentage (%) towards the total measured concentration of alkylbenzenes present within each sample. (A) = technical mixture, (B) = mean surface and subsurface control sample values, (C) = Bay 11 surface sediments, (D) = Bay 11 subsurface sediments, (E) = Crude Oil Point surface sediments, (F) = Crude Oil Point subsurface sediments, (G) = Bay 106 surface sediments, (H) = Bay 106 subsurface sediments.

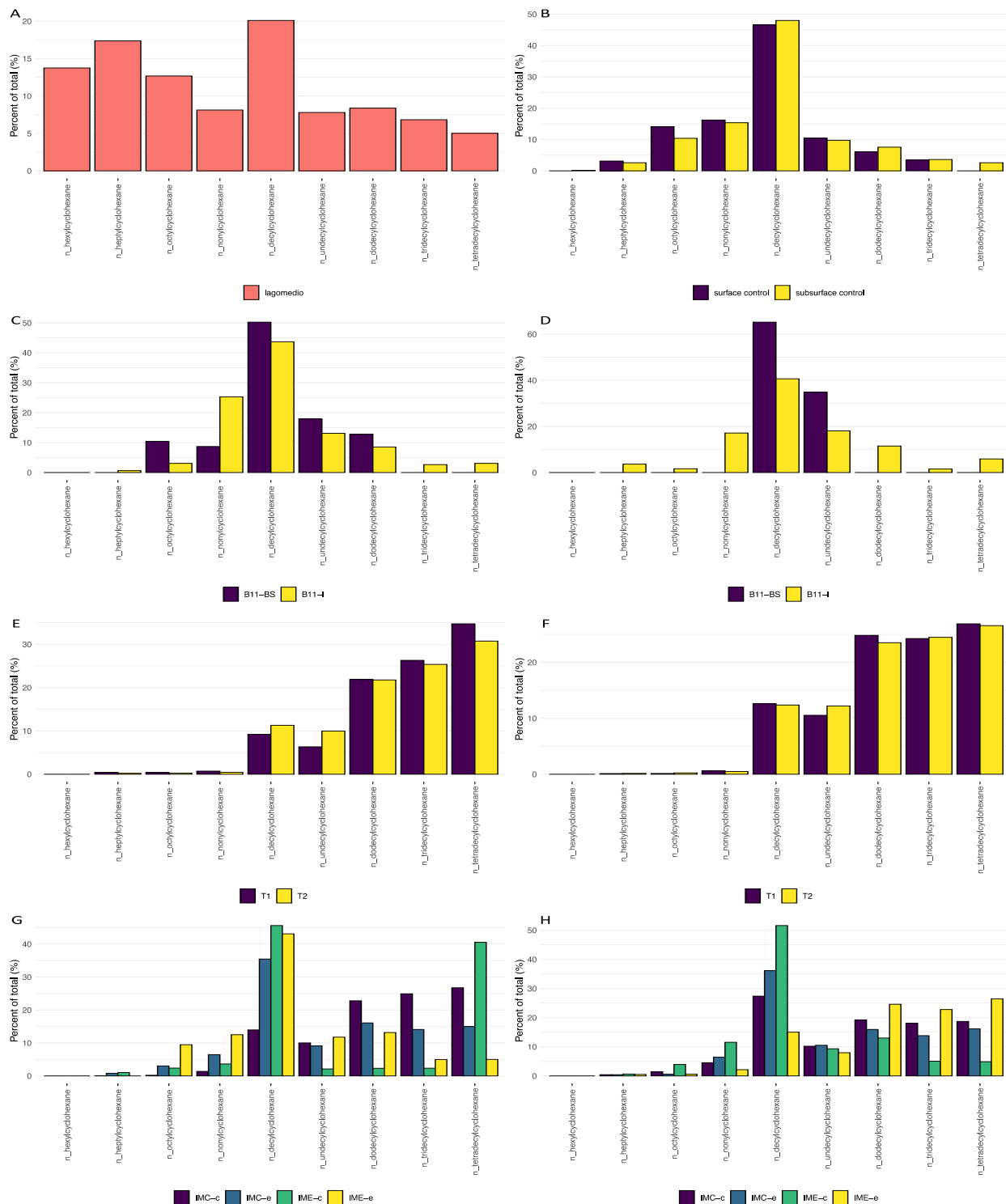


Figure 3.S2. Composition of alkylcycloalkanes, represented by the percentage (%) towards the total measured concentration of alkylcycloalkanes present within each sample. (A) = technical mixture, (B) = mean surface and subsurface control sample values, (C) = Bay 11 surface sediments, (D) = Bay 11 subsurface sediments, (E) = Crude Oil Point surface sediments, (F) = Crude Oil Point subsurface sediments, (G) = Bay 106 surface sediments, (H) = Bay 106 subsurface sediments.

Table 3.S10. Mean concentrations (mg/kg) of individual, analyzed alkylbenzenes within the technical mixture, oiled sediments, and control sediments from the 2019 revisit of BIOS site.

sample id	n-Butylbenzene	n-Pentylbenzene	n-Hexylbenzene	n-Heptylbenzene
GICB-N12 0-2	0.76	1.01	1.07	1.50
GICB-N12 5-10	0.00	0.00	0.00	2.42
GICB-NH 0-2	1.24	0.62	0.00	0.00
GICB-NH 5-10	0.00	0.00	0.00	0.00
NI-11 0-2	0.00	0.00	0.00	0.00
NI-11 5-10	0.00	0.00	0.00	0.00
IMC-c 0-2	12.13	4.81	5.36	2.59
IMC-c 5-10	3.07	0.00	2.27	4.12
IMC-e 0-2	0.00	0.28	0.44	1.00
IMC-e 5-10	0.00	0.00	0.00	0.00
IME-c 0-2	0.00	0.00	0.00	0.00
IME-c 5-10	0.00	0.00	0.00	0.00
IME-e 0-2	6.56	3.33	0.00	0.00
IME-e 5-10	0.00	0.00	2.50	0.00
B11-BS 0-2	0.00	0.00	0.00	0.00
B11-BS 5-10	0.00	0.00	0.00	0.00
B11-I 0-2	0.78	0.00	0.00	0.00
B11-I 5-10	1.17	0.00	0.00	0.00
T1 0-2	15.83	10.59	7.31	2.85
T1 5-10	23.21	11.04	6.62	5.61
T2 0-2	24.01	15.55	7.44	4.40
T2 5-10	25.92	14.85	8.26	5.84
TC 0-2	0.00	0.00	0.00	1.79
TC 5-10	0.00	0.00	0.00	0.00
MI-BS 0-2	0.00	0.00	0.00	1.22
MI-BS 5-10	0.00	0.95	0.94	2.74
MI-I 0-2	0.38	0.00	0.00	0.88
MI-I 5-10	0.00	0.00	0.00	0.00
RB1 0-2	0.00	0.00	0.00	0.00
RB1 5-10	0.00	0.00	0.00	0.00
TB3 0-2	0.00	0.00	0.00	0.00
TB3 5-10	0.00	0.00	0.00	0.00

	n-Octylbenzene	n-Nonylbenzene	n-Decylbenzene	n-Undecylbenzene
GICB-N12 0-2	3.84	10.18	13.32	12.77

GICB-N12 5-10	6.28	18.40	26.11	16.31
GICB-NH 0-2	0.69	2.62	3.29	3.26
GICB-NH 5-10	0.00	2.72	4.77	4.78
NI-11 0-2	1.10	4.29	7.85	5.65
NI-11 5-10	0.83	2.98	7.16	4.33
IMC-c 0-2	4.20	17.56	76.60	73.03
IMC-c 5-10	2.60	16.48	67.04	63.56
IMC-e 0-2	3.42	7.03	20.19	11.32
IMC-e 5-10	1.18	13.50	13.56	9.63
IME-c 0-2	4.57	15.33	17.85	20.69
IME-c 5-10	3.70	17.21	23.09	24.15
IME-e 0-2	2.66	13.67	14.66	18.49
IME-e 5-10	3.00	18.22	59.81	70.44
B11-BS 0-2	2.66	26.97	35.05	30.81
B11-BS 5-10	0.00	7.83	17.42	17.97
B11-I 0-2	0.80	2.65	4.06	6.75
B11-I 5-10	0.00	3.02	3.39	5.48
T1 0-2	4.65	18.16	62.18	71.05
T1 5-10	8.96	50.95	323.61	525.66
T2 0-2	2.81	21.40	108.83	143.17
T2 5-10	8.59	46.19	292.70	463.37
TC 0-2	3.88	8.87	10.38	9.73
TC 5-10	3.91	12.67	17.65	20.08
MI-BS 0-2	7.11	11.02	10.71	11.09
MI-BS 5-10	7.99	14.65	15.11	14.03
MI-I 0-2	2.60	3.08	3.17	5.38
MI-I 5-10	2.30	4.05	3.74	4.61
RB1 0-2	0.00	0.00	0.00	2.34
RB1 5-10	0.00	0.00	1.61	2.49
TB3 0-2	0.00	1.75	2.65	2.44
TB3 5-10	0.00	1.93	4.61	4.69

	n-Dodecylbenzene	n-Tridecylbenzene	n-Tetradecylbenzene	n-Pentadecylbenzene
GICB-N12 0-2	6.33	0.81	2.14	4.43
GICB-N12 5-10	7.95	0.00	2.37	5.23
GICB-NH 0-2	2.30	0.00	0.00	0.00

GICB-NH 5-10	3.27	0.00	1.05	1.68
NI-11 0-2	4.39	0.00	2.04	5.01
NI-11 5-10	3.38	0.00	2.05	2.48
IMC-c 0-2	276.55	406.23	515.67	1062.19
IMC-c 5-10	108.23	149.13	163.29	366.47
IMC-e 0-2	11.99	19.74	23.48	35.86
IMC-e 5-10	13.90	19.59	21.83	23.70
IME-c 0-2	25.70	25.23	43.16	29.66
IME-c 5-10	15.29	0.00	0.00	18.44
IME-e 0-2	13.24	0.00	3.25	4.91
IME-e 5-10	95.59	125.22	157.69	474.19
B11-BS 0-2	22.09	4.60	0.00	16.14
B11-BS 5-10	8.54	5.98	0.00	0.00
B11-I 0-2	5.56	0.67	0.00	0.00
B11-I 5-10	4.02	0.00	0.00	0.00
T1 0-2	129.24	155.43	196.88	561.98
T1 5-10	964.72	1152.31	1256.40	2262.17
T2 0-2	266.78	305.41	366.25	1173.22
T2 5-10	885.98	1099.47	1202.99	2002.47
TC 0-2	3.96	0.00	0.00	1.15
TC 5-10	8.69	0.00	2.22	3.19
MI-BS 0-2	4.48	0.41	0.00	1.30
MI-BS 5-10	5.09	0.00	0.63	2.05
MI-I 0-2	2.38	0.00	0.00	0.00
MI-I 5-10	2.56	0.00	0.00	1.42
RB1 0-2	2.55	0.00	2.67	2.02
RB1 5-10	2.98	1.90	2.71	2.29
TB3 0-2	2.93	0.00	2.08	2.30
TB3 5-10	4.37	0.00	2.45	2.23

	n- Hexadecylbenzene	n- Heptadecylbenzene	n- Octadecylbenzene	n- Nonadecylbenzene
GICB-N12 0-2	0.00	0.00	0.00	0.00
GICB-N12 5-10	1.29	0.00	0.00	0.00
GICB-NH 0-2	0.00	0.00	0.00	0.00
GICB-NH 5-10	0.00	0.00	0.00	0.00
NI-11 0-2	0.00	0.00	0.00	0.00
NI-11 5-10	0.00	0.00	0.00	0.00

IMC-c 0-2	535.82	671.50	570.94	448.82
IMC-c 5-10	132.59	168.97	126.34	116.57
IMC-e 0-2	20.39	15.85	22.70	18.48
IMC-e 5-10	14.35	19.09	13.54	9.13
IME-c 0-2	0.00	29.55	13.95	0.00
IME-c 5-10	0.00	0.00	0.00	0.00
IME-e 0-2	0.00	0.00	0.00	0.00
IME-e 5-10	148.03	184.00	148.51	108.65
B11-BS 0-2	0.00	0.00	0.00	0.00
B11-BS 5-10	0.00	0.00	0.00	0.00
B11-I 0-2	0.00	0.00	0.00	0.00
B11-I 5-10	0.00	0.00	0.00	0.00
T1 0-2	204.79	227.49	213.13	151.32
T1 5-10	1228.45	1310.54	1190.82	1128.29
T2 0-2	231.95	419.18	292.71	264.86
T2 5-10	1353.23	1307.90	1203.72	1062.28
TC 0-2	0.00	0.00	0.00	0.00
TC 5-10	2.74	0.00	0.00	0.00
MI-BS 0-2	0.00	0.00	0.00	0.00
MI-BS 5-10	1.00	0.00	0.00	0.00
MI-I 0-2	0.00	0.00	0.00	0.00
MI-I 5-10	0.00	0.00	0.00	0.00
RB1 0-2	0.00	0.00	0.00	0.00
RB1 5-10	3.67	4.08	0.00	0.00
TB3 0-2	0.00	0.00	0.00	0.00
TB3 5-10	0.00	0.00	0.00	0.00

Table 3.S11. Mean concentrations (mg/kg) of individual, analyzed alkylcycloalkanes within the technical mixture, oiled sediments, and control sediments from the 2019 revisit of BIOS site.

sample id	n-		
	n-Hexylcyclohexane	Heptylcyclohexane	n-Octylcyclohexane
GICB-N12 0-2	0	17.020161	65.7230467
GICB-N12 5-10	0	15.5083833	100.949668
GICB-NH 0-2	0	0.58101297	1.3875499
GICB-NH 5-10	0	0	0
NI-11 0-2	0	4.64068136	15.8660321
NI-11 5-10	0	6.93738806	16.1653731
IMC-c 0-2	0	6.82257342	20.0518552
IMC-c 5-10	0	15.5088875	55.2989354
IMC-e 0-2	0	4.55887097	17.4834446
IMC-e 5-10	0	3.71446078	5.00919118
IME-c 0-2	0	6.21688745	14.2144155
IME-c 5-10	0	2.89813896	17.3636915
IME-e 0-2	0	0	12.1363999
IME-e 5-10	0	11.4686918	13.0228256
B11-BS 0-2	0	0	18.5854709
B11-BS 5-10	0	0	0
B11-I 0-2	0	0.69422992	3.30044769
B11-I 5-10	0	2.35226852	1.04004342
T1 0-2	0	18.3516857	16.6700538
T1 5-10	0	25.7283659	32.5923301
T2 0-2	0	17.0319613	19.7756817
T2 5-10	0	27.6807178	44.8071535
TC 0-2	0	7.6812042	45.1313722
TC 5-10	0	7.07594589	43.6224303
MI-BS 0-2	0	34.7112088	140.760732
MI-BS 5-10	9.01924038	47.0865629	155.962582
MI-I 0-2	0	4.13037777	27.7442725
MI-I 5-10	0	5.94644569	28.2052194
RB1 0-2	0	0	2.12670313
RB1 5-10	0	0	0
TB3 0-2	0	0	0
TB3 5-10	0	0	0
	n-Nonylcyclohexane	n-Decylcyclohexane	n-Undecylcyclohexane

GICB-N12 0-2	77.8179819	148.88249	19.5808066
GICB-N12 5-10	120.263384	323.901646	52.8475044
GICB-NH 0-2	3.22267515	17.1120137	3.11484766
GICB-NH 5-10	2.9035551	20.1594188	4.15857956
NI-11 0-2	7.80975075	35.1455411	9.65418337
NI-11 5-10	14.6069963	71.5866418	11.5709701
IMC-c 0-2	144.383721	1479.84436	1060.99403
IMC-c 5-10	173.838372	1051.95439	391.09967
IMC-e 0-2	37.3529994	204.734647	52.5407936
IMC-e 5-10	55.4659438	310.658956	90.4212868
IME-c 0-2	21.7400772	273.056512	12.74884
IME-c 5-10	51.2901321	228.926468	41.385175
IME-e 0-2	16.0456311	55.3016056	15.084246
IME-e 5-10	48.4806429	340.09851	180.319123
B11-BS 0-2	15.5030797	89.6734614	31.9179307
B11-BS 5-10	0	45.522742	24.3288005
B11-I 0-2	27.242629	47.0275153	14.0925304
B11-I 5-10	11.0209395	26.1239543	11.6082812
T1 0-2	29.7794818	381.447862	262.617526
T1 5-10	145.795187	2915.06535	2435.91956
T2 0-2	34.8910846	915.038427	807.695655
T2 5-10	91.2470108	2291.98775	2258.54818
TC 0-2	55.5990157	133.791011	14.9697692
TC 5-10	59.8918209	166.939847	23.5030715
MI-BS 0-2	129.649068	172.684322	21.6499247
MI-BS 5-10	188.626047	246.054629	27.5989036
MI-I 0-2	38.2228935	84.4847315	11.6879223
MI-I 5-10	35.1367018	64.2390717	10.0619304
RB1 0-2	2.6395823	13.0136748	3.95601691
RB1 5-10	1.01296758	12.2640898	2.66805486
TB3 0-2	1.96211366	11.5670862	6.37492522
TB3 5-10	3.15089865	12.0785197	6.00778832
	n-Dodecylcyclohexane	n-Tridecylcyclohexane	n-Tetradecylcyclohexane
GICB-N12 0-2	10.4123187	1.22764207	0

GICB-N12 5-10	26.7294183	7.89551786	0
GICB-NH 0-2	2.06174503	0	0
GICB-NH 5-10	3.41110173	0	0
NI-11 0-2	6.58542084	0	0
NI-11 5-10	9.66067164	0	0
IMC-c 0-2	2417.26819	2642.53045	2837.82423
IMC-c 5-10	739.819801	696.102857	719.322021
IMC-e 0-2	92.7705349	81.4398139	86.461799
IMC-e 5-10	137.317857	118.844524	138.949643
IME-c 0-2	13.9317492	13.9949595	242.700092
IME-c 5-10	57.7362975	22.4312965	21.6249457
IME-e 0-2	16.8900995	6.378875	6.416375
IME-e 5-10	557.032791	515.843729	598.745554
B11-BS 0-2	22.8457933	0	0
B11-BS 5-10	0	0	0
B11-I 0-2	9.18926839	2.83667672	3.29004981
B11-I 5-10	7.3950695	0.98047059	3.78452233
T1 0-2	905.302809	1088.20288	1436.83433
T1 5-10	5738.5128	5605.4555	6212.2976
T2 0-2	1764.12032	2055.78014	2492.08833
T2 5-10	4355.35817	4535.38039	4922.57472
TC 0-2	8.94491442	0	0
TC 5-10	16.1107543	4.53747149	1.34417331
MI-BS 0-2	9.57221379	0	0
MI-BS 5-10	14.2650642	4.79602579	1.01595107
MI-I 0-2	3.71375948	1.16389647	0
MI-I 5-10	3.94463016	0	0
RB1 0-2	2.01011934	3.71188463	0
RB1 5-10	2.75117207	4.81309227	5.93663342
TB3 0-2	4.26483051	3.62923729	0
TB3 5-10	5.52468797	2.72171742	0

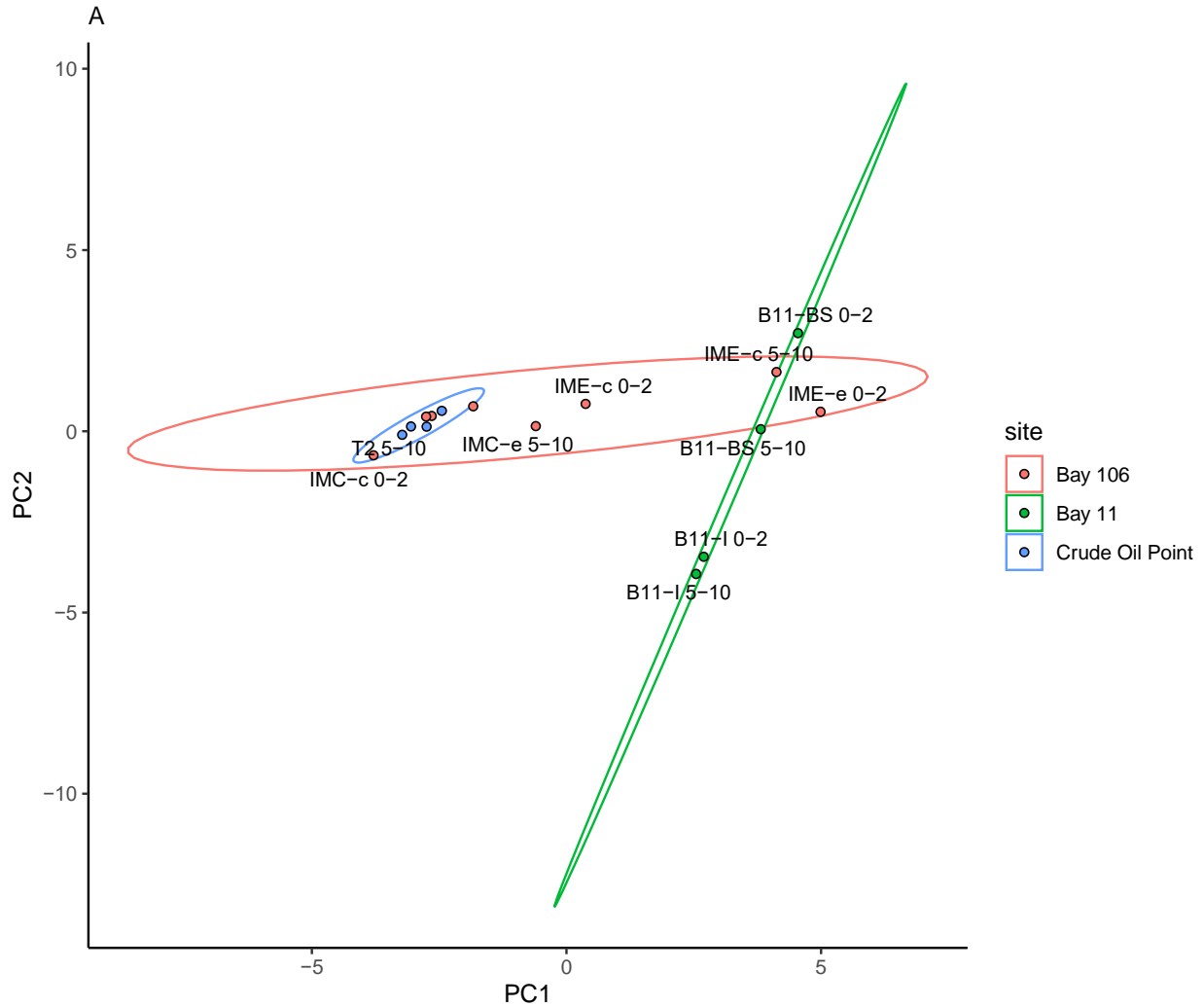


Figure 3.S3. Principal Components Analysis (PCA) made up of principal components (PCs) one and two, accounting for 65.4 and 16.7 % of the cumulative variance, respectively, of the alkylbenzenes present within the oiled sediments from the BIOS site, separated by sampling stations. The ellipses represent the 95 % confidence intervals for each respective site.

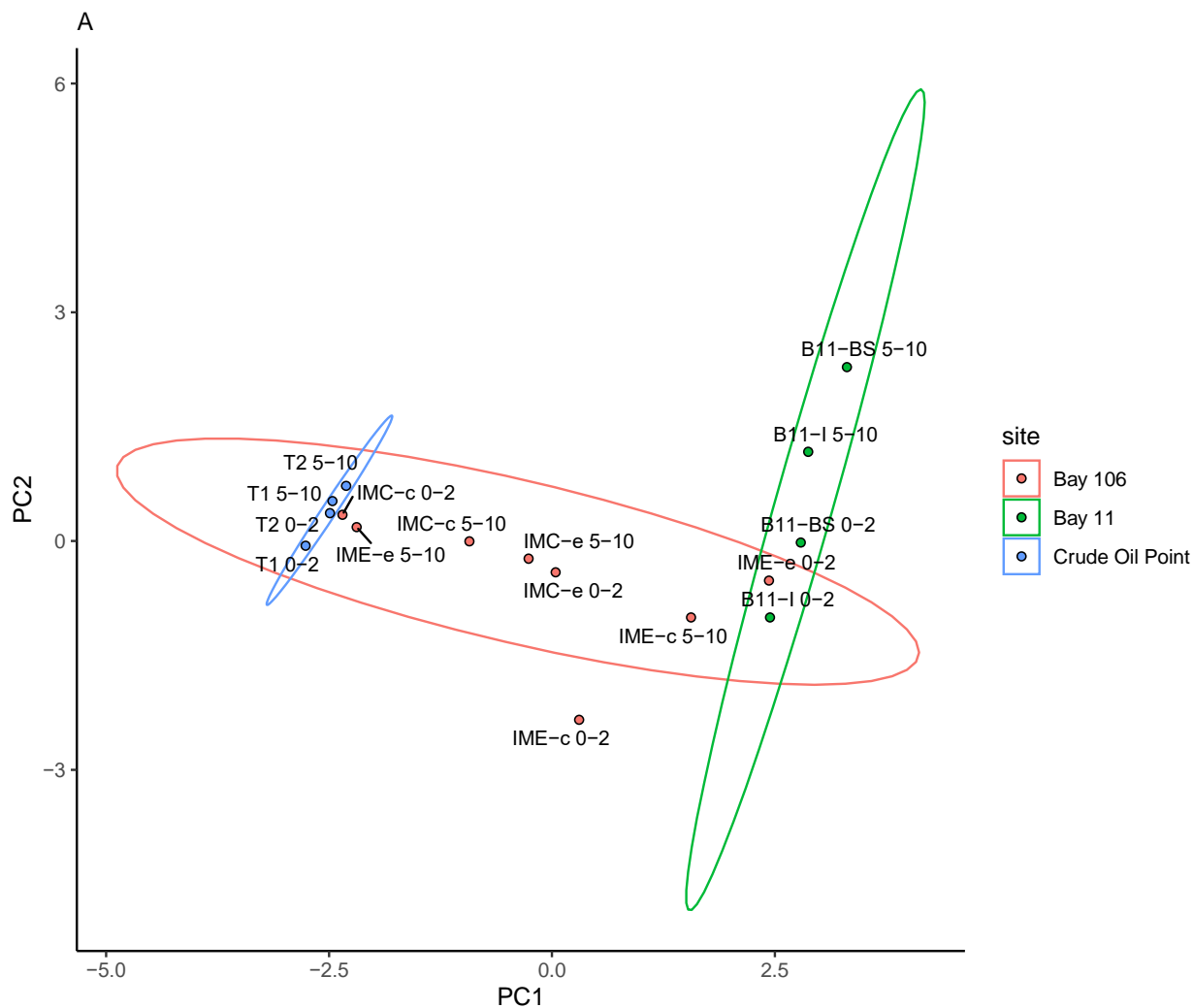


Figure 3.S4. Principal Components Analysis (PCA) made up of principal components (PCs) one and two, accounting for 64.9 and 13.1 % of the cumulative variance, respectively, of the alkylcycloalkanes present within the oiled sediments from the BIOS site, separated by sampling stations. The ellipses represent the 95 % confidence intervals for each respective site.

Chapter 4: Conclusion

Synthesis

The research performed herein serves to further the collective understanding pertaining to the recalcitrance and degradation of crude oil residues when released into a marine, Arctic environment. The various studies encompassed within the BIOS project were designed with the intention of having scientists return to monitor the long-term physical and chemical trends of crude oil when left subject to natural attenuation processes. To contribute to the legacy of the BIOS project in a meaningful manner, the beach sediment samples collected from the BIOS site during the 2019 CCGS Amundsen expedition were prepared to allow for chemical analysis, with the goal of determining the identities and concentrations of various petroleum hydrocarbons, thereby creating a chemical composition of the crude oil residues within the sediments from each sampling station at the BIOS site. Doing so provides an assessment of the chemical fate of the crude oil spilled in a remote Arctic setting, roughly four decades after initial release. This is an incredibly unique opportunity, as no other such study examining oil spills in sediments within such an extreme, cold environment have been performed to date. Additionally, there exist tremendous legislative barriers preventing the design of new field experiments of such caliber. As such, the need to progress such ongoing research projects are of paramount importance.

Ultimately, after roughly four decades, significant amounts of crude oil still remain within the beach sediments at the BIOS site. The hydrocarbon group contributing the most towards the total chemical compositions within the various samples were the linear and branched alkanes, accounting for 96 % of the total analyzed petroleum profile, on average. Despite only making up approximately 1.4 % of the total composition, many individual PAHs are present in potentially

toxic concentrations, as they exceed the dictated marine sediment quality guidelines set by the Canadian Council of Ministers of the Environment. There are serious implications involved with environmental health when considering that certain petroleum hydrocarbons are still present in potentially toxic concentrations, roughly four decades after being exposed to the open Arctic. With the increasing likelihood of crude oil spills within the Arctic, these outcomes should not be ignored.

Reflection

Research process

The return to the sites of the BIOS project occurred as part of a GENICE I initiative. The approach taken for the 2019 sampling regime was based on extensive research into previous reports and literature published from past studies conducted at the BIOS site. There were additional experimental oil plot studies conducted within the Z-lagoon (E. H. Owens & Robson, 1987) however, careful consideration and prioritization were necessary as the GENICE team was only permitted two full days for sample collection. This was largely due to the logistical complexities of keeping the CCGS Amundsen relatively nearby to allow other scientists to perform their research as we conducted our own. To acquire an accurate depiction of different environmental characteristics, we ensured to sample from locations that received different degrees of tidal inundation: The plots T1 and T2 from Crude Oil Point were setup in the backshore with no access to the marine interface, the plots IMC-c, IMC-e, IME-c, and IME-e at Bay 106 were positioned in the supratidal zone of the beach, but in a manner where spring water flows or storm events could introduce water to the sediments, and finally, Bay 11 incurred a stranded oil slick on the water surface, therefore we sampled from the intertidal area here.

The collected sediment samples were processed for analysis in manners performed previously by our lab group, based on standardized methods (Asihene, 2019). However, a preliminary set of samples were prepared to optimize the sample size needed to allow for detectable hydrocarbon concentrations upon analysis without potentially contaminating the analytical instruments. As such, only routine maintenance would be required throughout the course of sample analysis.

An important goal of ours was to report the concentrations of individual petroleum hydrocarbons from the sediments collected from the BIOS site. It was our belief that for the sake of continuity in long-term monitoring, having a tangible value to use as a comparison tool was essential. Unfortunately, previous work reporting on the chemical fate of the spilled crude oil at the BIOS site had not shared concentrations of individual compounds. Rather, Total Petroleum Hydrocarbon (TPH) values or percent depletion results were offered (Boehm, 1981, 1983; Humphrey, 1984; H. Owens, 1984; Prince et al., 2002). We acknowledge that the discipline of analytical chemistry has evolved significantly over the past few decades. Methods of analysis and technological capacities are constantly being improved upon, which allow for more selective and sensitive examinations. As a result, it is possible that previous reports sharing the concentrations of individual hydrocarbons would not accurately reflect what is in the crude oil residues however, it would allow for numerous additional comparisons to be made when considering the temporal effect of natural attenuation processes on hydrocarbons of differing sizes and chemical structure.

Expectations and Outcomes

Overall, we expected to observe a positive correlation between crude oil degradation and access to the marine interface. This theme emerged quite strongly. The lowest mean total concentrations of all the included hydrocarbon groups were observed in the Bay 11 sediments, followed by those in the Bay 106 samples, and the highest mean hydrocarbon concentrations were observed in the sediments of Crude Oil Point.

Additionally, it was expected that the percent residual of specific PAHs and alkanes would decrease between the penultimate revisitation of the BIOS site in 2001 and the most recent return in 2019. In certain cases, there had been little to no degradation observed between the initial releases of crude oil and the 2001 sampling regime (Prince et al., 2002). However, in nearly all available cases for direct comparisons, extensive losses of PAHs and alkanes occurred between 2001 and 2019. There were two cases where the results did not match with our expectations: The percent residuals of octadecane (nC18) and phytane within the surface sediments of Bay 11 were higher in the 2019 samples than they were in the 2001 samples. Although we cannot definitively attribute these outcomes to any specific process, it is believed that this could be in part due to the improvements in analytical instrumentation between the two sampling events, or the heterogeneity of oil encroached onto the Bay 11 sediments. Many of the hydrocarbon concentrations recorded within the Bay 11 sediments in the present study were similar to the lower limits of quantitation allowed by our instruments. It is possible that such low concentrations were not detectable and quantifiable in 2001, leading towards lower mean percent residual values.

Recommendations for Future Work

The remoteness of the study site, the environmental conditions, the experimental design and variables, and the legislative and logistical barriers of today all contribute to the complex and unique nature of the BIOS project, making it truly a one-of-a-kind study. No two oil spill field experiments will ever be identical. As such, comparing the results of these examinations can offer insight to the fate and behaviour of crude oil when subject to varying environmental, temporal, and experimental conditions; but ultimately can be difficult to accurately extrapolate expected outcomes to a separate study, as the effects of individual variables become more challenging to tease apart over time. As such, compiling a review of available literature concerning long-term monitoring projects related to crude oil spills could be of value.

As crude oil spill case studies offer a wealth of information pertinent to legislation surrounding oil exploration, we recommend an additional return to the BIOS site in the distant future. If a similar experimental approach to the 2019 revisitation were to take place, future research could strengthen temporal trends associated with crude oil recalcitrance and degradation. Now that we have contributed results pertaining to individual concentrations of many hydrocarbons detected within the BIOS sediments, future investigations of the chemical fate of the spilled crude oil can assist in creating a timeline suggesting the time needed for all 16 US EPA PAHs to weather under Arctic conditions until they are no longer present in potentially toxic concentrations. Additionally, simple, cost-effective toxicological experiments such as seedling germination tests using subtidal or terrestrial vegetation from the BIOS site could be performed to monitor the potentially toxic effects of the PAH concentrations recorded from the 2019 revisitation.

Two approaches could be taken to further improve upon the results presented herein. An additional form of chemical analysis, Liquid Chromatography Mass Spectrometry (LCMS) is an effective tool in separating, identifying, and quantifying high MW and polar petroleum hydrocarbons (Hewlett-Packard, 1998). Doing so would provide a more comprehensive understanding of the chemical compositions of the oiled sediments from the BIOS site. Also, three subtidal sediment cores were obtained from a subset of the sampling stations at the BIOS site during the 2019 sampling regime but were not included as part of this Master's project. If one were to process and analyze these samples, further information pertaining to the long-term chemical fate of crude oil within a subtidal Arctic beach setting could be shared.

Contributions and Wrap-up

The work completed herein serves to further the collective understanding as it pertains to the long-term fate of crude oil released into the Arctic marine ecosystem. Due to the unique environmental features of the Arctic, long-term examinations of crude oil degradation in lower latitudinal settings or in laboratory experiments are insufficient resources to extrapolate from. As such, the only reliable method to uncover the natural attenuation of crude oil spilled within the Arctic is to directly monitor such an event. The BIOS project has an important legacy to carry on, and I am honoured to have contributed to its most recent chapter. Our results demonstrate that when left subject to natural weathering processes for roughly forty years, crude oil will remain present in detectable and quantifiable concentrations within Arctic beach sediments. The largest driver contributing to the extents of weathering appears to be access to the tide, as it allows for numerous degradation mechanisms to take place, such as physical removal/washing out, dissolution, and biodegradation. Many of our findings support previous theories discussed

pertaining to the various patterns observed in the rate of degradation of particular hydrocarbon groups. However, the intricacies of several weathering processes working in tandem, along with additional experimental variables in an open, extreme environment make it difficult to confidently attribute cause to specific factors. As such, we offer suggestions based on the available knowledge in the field of oil spill chemistry and weathering. We recognize the limitations of being unable to prescribe direct answers to certain specific questions with regards to the behaviour of many individual petroleum hydrocarbons, however, circumventing the minutia of the obtained results would take efforts beyond the scope of a Master's project. Ultimately, we were able to offer an account of what is expected if and when crude oil is accidentally or intentionally spilled into the Arctic marine ecosystem, long after the release occurs. Doing so can assist policymakers with curating governance regimes that aim to mitigate and minimize any potential deleterious impacts that a crude oil spill incurs on its surroundings. With the ongoing and seemingly unending impacts of climate change, specifically in the Arctic, more human activity will give rise to more frequent petroleum spills (Dawson et al., 2018; Sergy & Blackall, 1987). Our world is not immune to our actions, so as a collective we need to understand the implications of the impacts we cause to the planet, both near and far.

References

- Asihene, W. (2019). *Sources and geochemical controls on hydrocarbons in Arctic sediments, Kivalliq region, Nunavut*.
- Boehm, P. D. (1981). *Chemistry:2 Hydrocarbon chemistry—1980 study results. (BIOS) Baffin Island Oil Spill working report* (p. 184) [Working Report].
- Boehm, P. D. (1983). *Chemistry: 2. Analytical biogeochemistry—1982 study results* (p. 231).
- Dawson, J., Pizzolato, L., Howell, S. E. L., Copland, L., & Johnston, M. E. (2018). Temporal and spatial patterns of ship traffic in the Canadian Arctic from 1990 to 2015. *ARCTIC*, 71(1), Article 1. <https://doi.org/10.14430/arctic4698>
- Hewlett-Packard. (1998). *Basics of LC/MS - A primer* (p. 24). Hewlett-Packard.
- Humphrey, B. (1984). *Chemistry I: Field sampling and measurements—1983 study results* (Baffin Island Oil Spill, p. 64) [Working Report]. Environmental Protection Service.
- Owens, E. H., & Robson, W. (1987). Experimental design and the retention of oil on Arctic test beaches. *ARCTIC*, 40(5), 230–243. <https://doi.org/10.14430/arctic1817>
- Owens, H. (1984). *Shoreline countermeasures—1983 Results. Baffin Island Oil Spill project working report 83-4* (pp. 1–115) [Working Report]. Environmental Protection Service, Environment Canada, Ottawa.
- Prince, R. C., Owens, E. H., & Sergy, G. A. (2002). Weathering of an Arctic oil spill over 20 years: The BIOS experiment revisited. *Marine Pollution Bulletin*, 44(11), 1236–1242. [https://doi.org/10.1016/S0025-326X\(02\)00214-X](https://doi.org/10.1016/S0025-326X(02)00214-X)
- Sergy, G. A., & Blackall, P. J. (1987). Design and conclusions of the Baffin Island Oil Spill project. *ARCTIC*, 40(5), 1–9. <https://doi.org/10.14430/arctic1797>